Research Paper

GEOSPHERE

GEOSPHERE; v. 12, no. 3

doi:10.1130/GES01256.1

17 figures; 1 table

CORRESPONDENCE: c.magee@imperial.ac.uk

CITATION: Magee, C., Muirhead, J.D., Karvelas, A., Holford, S.P., Jackson, C.A.L., Bastow, I.D., Schofield, N., Stevenson, C.T.E., McLean, C., McCarthy, W., and Shtukert, O., 2016, Lateral magma flow in mafic sill complexes: Geosphere, v. 12, no. 3, p. 809–841, doi:10.1130/GES01256.1.

Received 26 August 2015
Revision received 29 January 2016
Accepted 10 March 2016
Published online 28 April 2016

Lateral magma flow in mafic sill complexes

Craig Magee[1], James D. Muirhead[2], Alex Karvelas[3], Simon P. Holford[4], Christopher A.L. Jackson[1], Ian D. Bastow[1], Nick Schofield[5], Carl T.E. Stevenson[6], Charlotte McLean[7], William McCarthy[8], and Olga Shtukert[3]

[1]Basins Research Group, Department of Earth Science and Engineering, Imperial College London, London SW7 2BP, UK
[2]Department of Geological Sciences, University of Idaho, 875 Perimeter Drive, Moscow, Idaho 83844, USA
[3]Schlumberger Multiclient, Schlumberger House, Buckingham Gate, West Sussex RH 6 0NZ, UK
[4]Australian School of Petroleum, University of Adelaide, North Terrace, Adelaide SA 5005, Australia
[5]Department of Geology and Petroleum Geology, School of Geosciences, University of Aberdeen, Meston Building, Old Aberdeen, Aberdeen AB24 3UE, UK
[6]School of Geography, Earth and Environmental Sciences, University of Birmingham, Edgbaston, Birmingham B15 2TT, UK
[7]School of Geographical and Earth Sciences, University of Glasgow, Gregory Building, Glasgow G12 8QQ, UK
[8]Department of Earth Sciences, University of St Andrews, Irvine Building, St Andrews KY16 9AL, UK

ABSTRACT

The structure of upper crustal magma plumbing systems controls the distribution of volcanism and influences tectonic processes. However, delineating the structure and volume of plumbing systems is difficult because (1) active intrusion networks cannot be directly accessed; (2) field outcrops are commonly limited; and (3) geophysical data imaging the subsurface are restricted in areal extent and resolution. This has led to models involving the vertical transfer of magma via dikes, extending from a melt source to overlying reservoirs and eruption sites, being favored in the volcanic literature. However, while there is a wealth of evidence to support the occurrence of dike-dominated systems, we synthesize field- and seismic reflection–based observations and highlight that extensive lateral magma transport (as much as 4100 km) may occur within mafic sill complexes. Most of these mafic sill complexes occur in sedimentary basins (e.g., the Karoo Basin, South Africa), although some intrude crystalline continental crust (e.g., the Yilgarn craton, Australia), and consist of interconnected sills and inclined sheets. Sill complex emplacement is largely controlled by host-rock lithology and structure and the state of stress. We argue that plumbing systems need not be dominated by dikes and that magma can be transported within widespread sill complexes, promoting the development of volcanoes that do not overlie the melt source. However, the extent to which active volcanic systems and rifted margins are underlain by sill complexes remains poorly constrained, despite important implications for elucidating magmatic processes, melt volumes, and melt sources.

INTRODUCTION

Interactions between tectonic and magmatic processes, as well as the lithology and preexisting structure of the host rock, control the geometry and connectivity of magma conduits and reservoirs (i.e., a magma plumbing system). Delineating plumbing system structure can therefore provide important insights into: (1) continental rifting (e.g., Ebinger and Casey, 2001; Kendall et al., 2005; White et al., 2008; Ebinger et al., 2010); (2) total melt volume estimates, which can be used to assess the thermomechanical state of the mantle (White et al., 2008; Ferguson et al., 2010); (3) the physiochemical evolution of magma (e.g., Holness and Humphreys, 2003; Cashman and Sparks, 2013); (4) host-rock deformation induced by magma intrusion, which may be expressed at the Earth's surface (e.g., Wright et al., 2006; Biggs et al., 2009; Pagli et al., 2012; Jackson et al., 2013; Magee et al., 2013a; Tibaldi, 2015); and (5) volcanic eruption locations and styles (e.g., Abebe et al., 2007; Gaffney et al., 2007; Mazzarini, 2007; Tibaldi, 2015; Muirhead et al. 2016). However, the inaccessibility of active plumbing systems and limitations in exposure at the Earth's surface makes reconstructing the geometry and connectivity of regionally extensive intrusion networks from field outcrops challenging.

In order to delimit plumbing systems, it is therefore important to integrate field observations with data and imaging techniques that probe magma pathways and storage in the subsurface (Tibaldi, 2015). Indirect analytical approaches commonly involve: (1) the examination of ground deformation patterns (e.g., using InSAR, interferometric synthetic aperture radar) inferred to relate to the emplacement of magma (e.g., Pedersen, 2004; Wright et al., 2006; Pagli et al., 2012; Sparks et al., 2012); (2) scrutiny of petrological and geochemical data to assess magma contamination, residence times, crystallization histories, and melt source conditions (Cashman and Sparks, 2013, and references therein); and/or (3) mapping the location and crude geometry of crystallized intrusions or present-day zones of melt using geophysical techniques such as potential field, magnetotellurics, and seismicity (e.g., Cornwell et al., 2006; Whaler and Hautot, 2006; Desissa et al., 2013). For example, the application and synthesis of these techniques in the East African Rift system and Iceland have greatly improved our understanding of magma-tectonic interactions and allowed processes controlling continental break-up, such as dike intrusion, to be analyzed in real time (e.g., Ebinger et al., 2010; Gudmundsson et al., 2014; Sigmundsson et al., 2015). It is, however, important to consider that these data poorly constrain intrusion geometries and are commonly interpreted within the classical framework of igneous geology; i.e., magma migration within the Earth's crust is generally facilitated by the vertical intrusion of dikes, extending

from a deep magma reservoir or melt source to overlying shallow-level intrusions and volcanoes (Fig. 1A; Tibaldi, 2015, and references therein).

While numerous studies document vertical magma transport in dike-dominated volcanic plumbing systems (e.g., Kendall et al., 2005; Keir et al., 2006; Wright et al., 2006; Corti, 2009; Bastow et al., 2010; Cashman and Sparks, 2013; Muirhead et al., 2015; Tibaldi, 2015), it is also widely accepted that lateral magma flow can occur either within individual plumbing systems where volcanoes may be laterally offset by as much as ~20 km from their magma reservoir (e.g., Fig. 1A; e.g., Curtis, 1968; Cartwright and Hansen, 2006; Gudmundsson, 2006; Aoki et al., 2013; Aizawa et al., 2014; Muirhead et al., 2014; Tibaldi, 2015) or giant radiating dike swarms, which can facilitate lateral magma flow over hundreds to thousands of kilometers (e.g., Ernst and Baragar, 1992; Ernst et al., 1995; Macdonald et al., 2010). Recent field-, seismic reflection–, and modeling-based research further indicate that plumbing systems at shallow levels (typically <3 km depth), particularly those hosted in sedimentary basins, may instead be characterized by extensive sill complexes (e.g., Chevallier and Woodford, 1999; Smallwood and Maresh, 2002; Thomson and Hutton, 2004; Planke et al., 2005; Cartwright and Hansen, 2006; Kavanagh et al., 2006, 2015; Lee et al., 2006; Leuthold et al., 2012; Leat, 2008; Menand, 2008; Polteau et al., 2008a; Cukur et al., 2010; Bunger and Cruden, 2011; Gudmundsson and Løtveit, 2012; Muirhead et al., 2012; Svensen et al., 2012, 2015; Jackson et al., 2013; Magee et al., 2014; Zhao et al., 2014; Button and Cawthorn, 2015; Schofield et al., 2015). Sill complexes imaged in seismic data and observed in the field extend laterally for tens to thousands of kilometers and are dominated by an interconnected network of mafic, relatively thin (typically <100 m thick) sills, which frequently exhibit saucer-shaped morphologies, and inclined sheets with only a small proportion of dikes (e.g., Fig. 1B; e.g., Cartwright and Hansen, 2006; Leat, 2008; Muirhead et al., 2014). In contrast, the structure of shallowly emplaced (<3 km), intermediate to felsic plumbing systems (e.g., the Henry Mountain laccoliths, Utah, USA, Johnson and Pollard, 1973; Torres del Paine laccolith, Chile, Michel et al., 2008), which commonly form single or composite, thick (typically >1 km) laccoliths and plutons with limited lateral extents (≲20 km), differs significantly from that of mafic sill complexes (e.g., Cruden and McCaffrey, 2001; Corazzato and Groppelli, 2004; Menand, 2008; Bunger and Cruden, 2011). Mapping of flow indicators within sill complexes reveals that interconnected networks of mafic sills and inclined sheets can facilitate magma transport over distances of as much as 12 km vertically and 4100 km laterally (Cartwright and Hansen, 2006; Leat, 2008) and could thus feed volcanic eruptions that are laterally offset considerable distances from the source of mantle or lower crustal melting (Fig. 1B; Magee et al., 2013b; Muirhead et al., 2014). The consideration that a plumbing system may be characterized by a laterally extensive sill complex, as opposed to a network of vertical dikes, could therefore have broad implications for the interpretation of geochemical, petrological, and geophysical data obtained from volcanic settings (e.g., Meade et al., 2009). For example, recent field- and seismic-based studies have suggested that surface deformation, generated by sill and sill complex emplacement, may not directly correlate to the location and volume of intruding magma if plastic deformation of the host rock occurs (Jackson et al., 2013; Magee et al., 2013a, 2013b; Schofield et al., 2014).

To emphasize the potential importance of lateral magma flow within sill complexes, the aim of this contribution is to synthesize new and published data from mafic sill complexes around the world (Fig. 2). We examine different tectonic settings, temporal variations in sill complex emplacement relative to tectonic activity (e.g., synrift and postrift intrusion), durations of sill complex emplacement, and various melt sources (e.g., mantle plumes and/or small-scale mantle convection; Fig. 2). We highlight that (1) sill complexes can facilitate lateral magma flow (e.g., Leat, 2008), with little or no accompanying surface deformation (Jackson et al., 2013; Magee et al., 2013a; Schofield

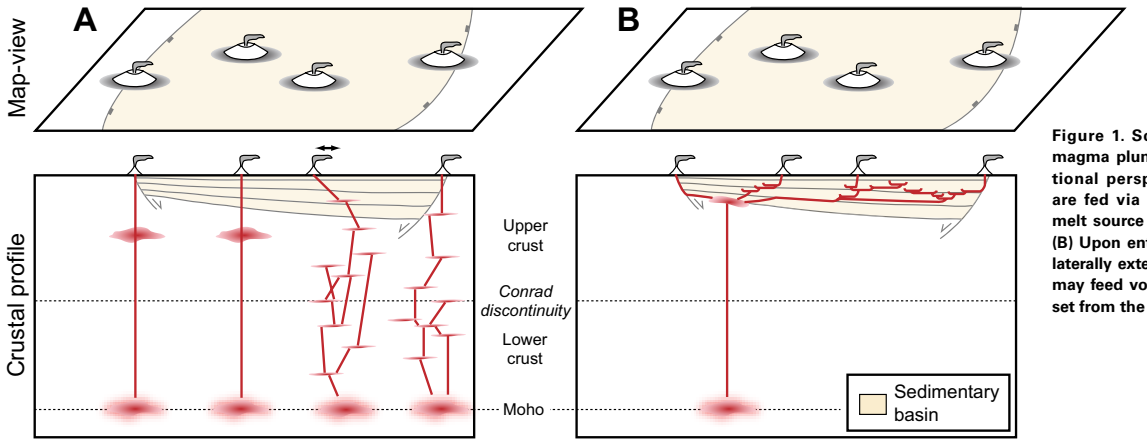

Figure 1. Schematic representation of magma plumbing systems. (A) The traditional perspective, whereby volcanoes are fed via dikes and directly over the melt source and shallow-level reservoirs. (B) Upon entering a sedimentary basin, a laterally extensive sill complex forms that may feed volcanoes that are laterally offset from the melt source.

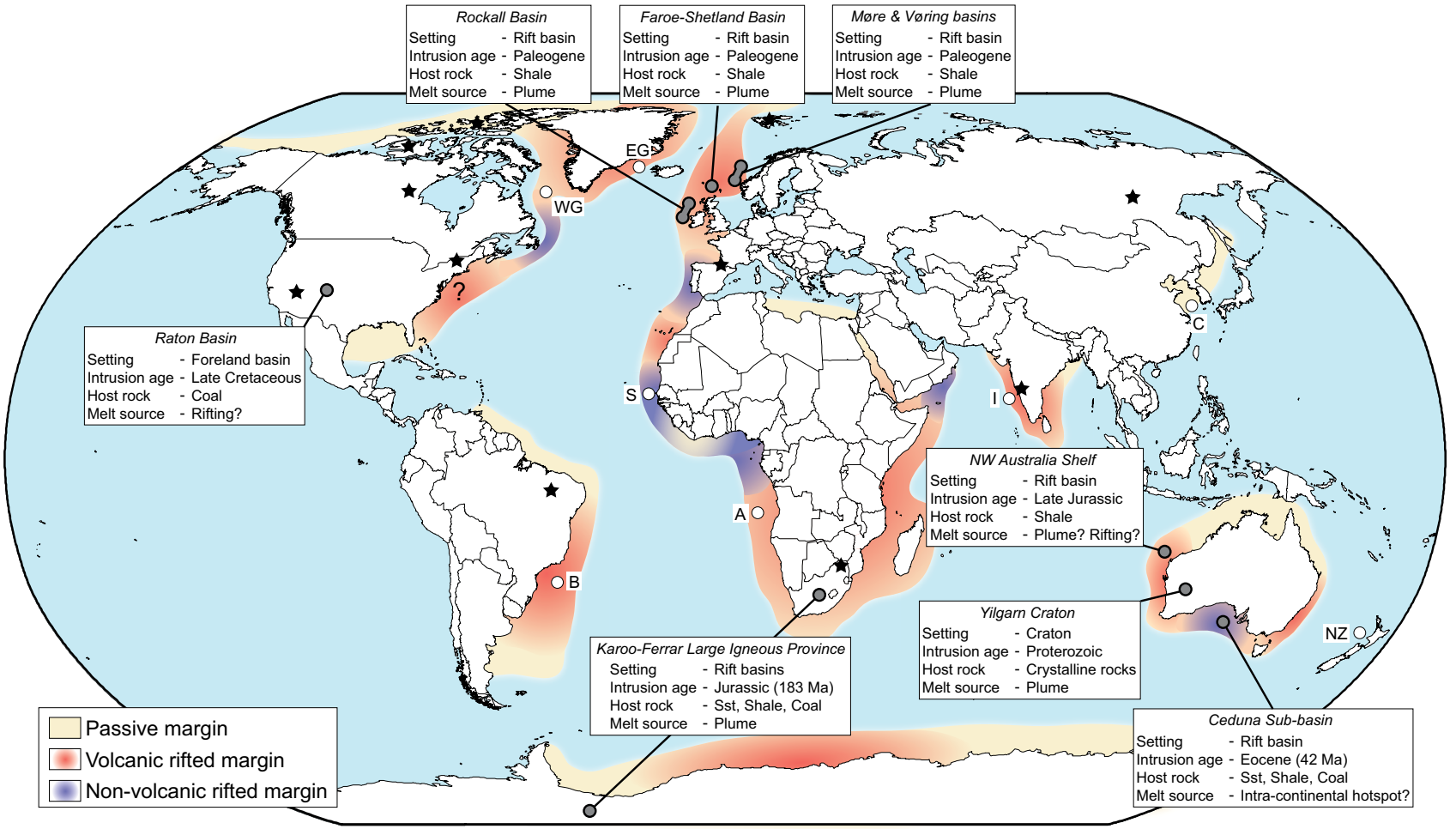

Figure 2. Map showing the global distribution of continental margin styles, the locations of the case studies reviewed here (gray circles), other offshore areas containing sill complexes (white circles), and onshore examples of sill complexes (stars) (Aspler et al., 2002; Svensen et al., 2004, 2012; Leat, 2008; Polteau et al., 2008a; Corti, 2009; Bedard et al., 2012; Schofield et al., 2012a, 2015; Duraiswami and Shaikh, 2013; Jackson et al., 2013; Magee et al., 2013a, 2014; Wyche et al., 2013; Agirrezabala, 2015; Button and Cawthorn, 2015; Evenchick et al., 2015). Highlighted offshore areas: EG—east Greenland; WG—west Greenland; B—Brazil; S—Senegal; A—Angola; I—India; C—China; NZ—New Zealand. Sst—sandstone.

et al., 2014); (2) the majority of sill complexes occur in sedimentary basins and their emplacement is primarily related to the intrusion of magma along mechanical discontinuities such as bedding planes and/or compliant lithologies (e.g., Mudge, 1968; Gretener, 1969; Einsele et al., 1980; Gudmundsson, 1986, 1990, 2011; Annen et al., 2006; Kavanagh et al., 2006; Menand, 2008; Thomson and Schofield, 2008; Schofield et al., 2010, 2012a; Magee et al., 2013a; Barnett and Gudmundsson, 2014; Button and Cawthorn, 2015; Kavanagh et al., 2015; Tibaldi, 2015); (3) faults can limit the lateral extent of sill complexes and provide important magma flow pathways (Delaney et al., 1986; Bedard et al., 2012; Magee et al., 2013c); (4) magma rheology and chemistry appear to influence intrusion network structure (Cruden and McCaffrey, 2001; Bunger and Cruden, 2011); and (5) eruption sites may be laterally offset from the melt source and shallow-level magma reservoirs (Magee et al., 2013b). In contrast to dike-fed volcanoes, the distributions of which are commonly used to map zones of

lower crustal and/or mantle melting or magma storage (e.g., Cashman and Sparks, 2013; Annen et al., 2015), the dispersal of eruption sites associated with a sill complex may not be a reliable indicator of magma generation zones.

APPLICATION OF SEISMIC REFLECTION DATA TO UNDERSTANDING PLUMBING SYSTEMS

High-quality marine seismic reflection data have revolutionized our understanding of sill complex emplacement because they allows subsurface intrusion networks to be imaged in three-dimensions (3D) at resolutions of tens of meters (e.g., Smallwood and Maresh, 2002; Thomson and Hutton, 2004; Cartwright and Hansen, 2006; Magee et al., 2014). Studies applying seismic techniques to analyzing plumbing systems have shown that (1) seismically imaged intrusions describe a range of morphologies that can be categorized, broadly, into strata concordant, saucer shaped (i.e., a flat inner sill that passes laterally into an encompassing, or partially encompassing, inclined limb; Thomson and Hutton, 2004; Magee et al., 2014), and inclined sheet geometries (Fig. 3; e.g., Thomson and Hutton, 2004; Planke et al., 2005; Magee et al., 2014); (2) different host-rock deformation mechanisms accommodating intrusion can be interpreted (e.g., Jackson et al., 2013; Magee et al., 2013a); and (3) magma flow pathways can be mapped across entire intrusion networks (e.g., Thomson and Hutton, 2004; Schofield et al., 2012b, 2015; Magee et al., 2014). Despite these advances, seismic interpretation is an underutilized tool in igneous-based research and remains an unfamiliar technique to many Earth scientists in the volcanic and magmatic community. It is therefore worth briefly considering the seismic interpretation methodology of igneous rocks, prior to the analysis of plumbing systems imaged in seismic data.

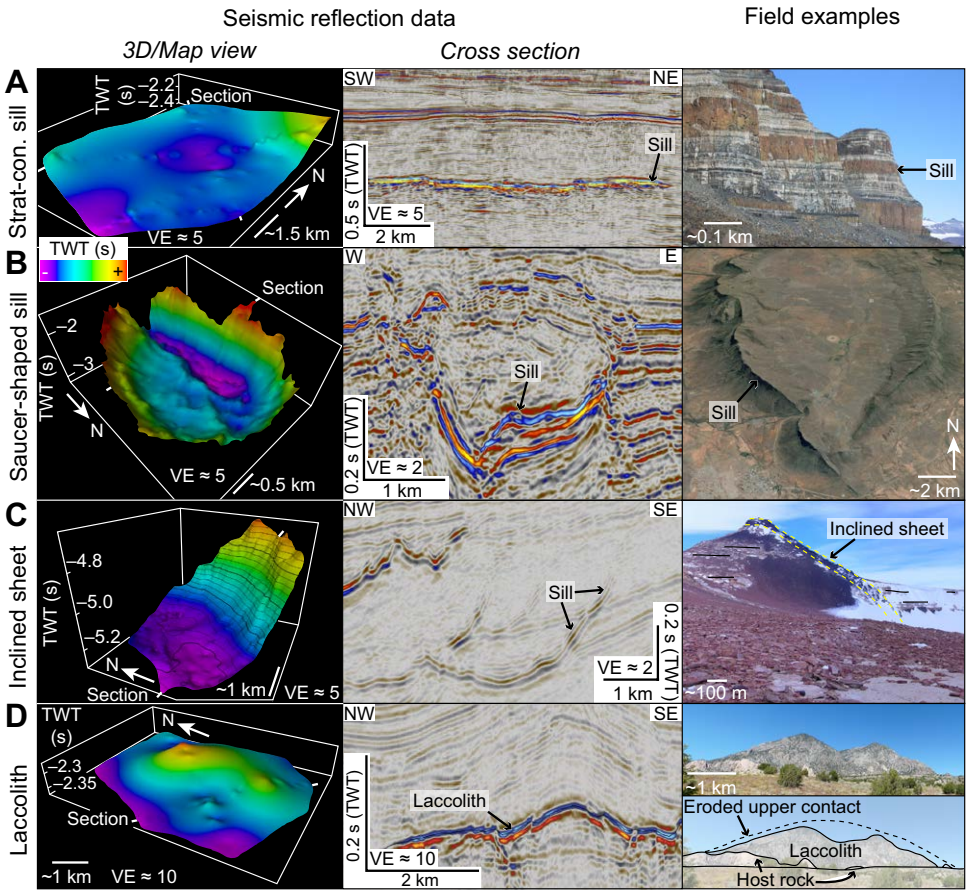

Figure 3. (A) Strata-concordant (Strat-con.) sills observed offshore southern Australia (see Jackson et al., 2013) and in the Theron Mountains, Antarctica (field photo courtesy of Donny Hutton). 3D—three dimensional. Vertical axes in seismic images are in two-way traveltime (TWT) and are vertically exaggerated (VE). (B) Saucer-shaped sills observed in seismic data from the Exmouth subbasin, northwest Australia (modified from Magee et al., 2013a) and the Golden Valley Sill in South Africa (Google Earth image). (C) Inclined sheets in the Rockall Basin (modified from Magee et al., 2014) and Antarctica. (D) Laccoliths observed offshore southern Australia (modified from Jackson et al., 2013) and in the Henry Mountains, Utah (USA).

Sill complexes are relatively well imaged in seismic data because igneous rocks commonly have greater densities and seismic velocities compared to the surrounding sedimentary strata. These physical differences at the intrusion–host rock contacts result in a high acoustic impedance contrast (Smallwood and Maresh, 2002), which reflects more seismic energy back to the surface than low impedance boundaries typically occurring between sedimentary rocks (Brown, 2004). In seismic data, igneous bodies are therefore commonly expressed as high-amplitude reflections (e.g., Symonds et al., 1998; Smallwood and Maresh, 2002; Planke et al., 2005; Magee et al., 2015). The geometry and seismic-stratigraphic relationships of high-amplitude reflections can be used to constrain whether they have an igneous origin or not (Symonds et al., 1998; Smallwood and Maresh, 2002; Planke et al., 2005; Magee et al., 2015). In particular, high-amplitude reflections attributed to igneous intrusions are commonly restricted in their lateral continuity and/or crosscut the host-rock strata (e.g., Mihut and Müller, 1998; Magee et al., 2013c, 2014). There are, however, two major problems with determining whether high-amplitude reflections correspond to and accurately define igneous intrusions: (1) it is often difficult to test the validity of seismic-based interpretations of subsurface structures because they are rarely intersected by boreholes; and (2) most intrusions are expressed in seismic data as tuned reflection packages (e.g., Figs. 3A, 3C), whereby reflections from the upper and lower intrusion contacts cannot be distinguished. Tuning occurs when the vertical intrusion thickness is between the limit of separability and the limit of visibility of the seismic data, causing reflections emanating from the upper and lower intrusion contact to interfere (Widess, 1973; Smallwood and Maresh, 2002; Brown, 2004; Hansen et al., 2008; Magee et al., 2015). This tuning response promotes uncertainty in the interpretation of the true intrusion geometry because it is difficult to determine the difference between real features and geophysical artifacts (Smallwood and Maresh, 2002; Magee et al., 2015). Several studies have, however, used borehole data to corroborate that interpreted magmatic and volcanic bodies are igneous (e.g., Smallwood and Maresh, 2002; Peron-Pinvidic et al., 2010; Grove, 2013; Rateau et al., 2013; Schofield et al., 2015). Synthetic seismic forward models, designed to test the seismic expression of igneous intrusion properties observed in the field, can also be utilized to assess the validity of seismic interpretations (Magee et al., 2015).

One limitation of seismic data is that subvertical dikes are rarely imaged (e.g., Thomson, 2007). The lack of dike imaging, which is attributed to the low amount of acoustic energy that reflects back to the surface off the subvertical wall of a dike, therefore biases seismic-based interpretations of plumbing systems. The role of dikes within sill complexes can, however, be investigated from (1) field analyses (e.g., Muirhead et al., 2014); (2) the interpretation of subvertical chaotic zones of reflection in seismic data as dikes (Thomson, 2007; Wall et al., 2010); and (3) the mapping of magma flow patterns in sills to identify potential dike feeders (see following). Through the careful application of these techniques and by comparison to field observations, seismic data can be used to delimit magma plumbing systems in more detail than field or other geophysical techniques.

Constraining Magma Flow Patterns in Outcrop and Seismic Data

Because this review assesses both field- and seismic-based observations pertaining to the role of lateral magma flow in sedimentary basins, it is important to describe how magma flow patterns can be mapped, particularly in seismic data. Within field-based studies there is a long history of using mineral and vesicle alignment and imbrication, measured using petrological or magnetic techniques, to delineate magma flow in sheet intrusions (e.g., Knight and Walker, 1988; Tarling and Hrouda, 1993; Launeau and Cruden, 1998; Tauxe et al., 1998; Gudmundsson and Marinoni, 1999; Archanjo and Launeau, 2004; Callot and Geoffroy, 2004; Cañón-Tapia, 2004; Cañón-Tapia and Chavez-Alvarez, 2004; Féménias et al., 2004; Liss et al., 2004; Philpotts and Philpotts, 2007; Cañón-Tapia and Herrero-Bervera, 2009; Magee et al., 2012a; Neres et al., 2014). Such mineral alignment analyses have shown that the long axes of intrusive steps, bridge structures, and magma fingers, which are commonly superimposed onto the larger scale sheet intrusion morphology, correlate to the primary magma flow axis (Fig. 4; e.g., Airoldi et al., 2012; Magee et al., 2012a; Schofield et al., 2012a; Hoyer and Watkeys, 2015). These flow indicators form because sheet intrusions typically do not initially intrude as continuous bodies of magma (Fig. 4; e.g., Rickwood, 1990; Hutton, 2009; Schofield et al., 2012a). Instead, the formation of a sheet intrusion is commonly preceded by the propagation of thin, laterally restricted magma segments, which may be vertically and/or laterally offset from each other (Fig. 4; e.g., Rickwood, 1990; Hutton, 2009; Schofield et al., 2012a). With sustained magma input, these segments inflate and coalesce to form a continuous sheet intrusion (Fig. 4; e.g., Rickwood, 1990; Hutton, 2009; Schofield et al., 2012a).

The magma flow indicators (e.g., intrusive steps) described here occur at scales ranging from centimeters to tens of meters and can be observed in outcrop and seismic data (Fig. 4; Schofield et al., 2012a, 2012b; Magee et al., 2013c, 2014; Rui et al., 2013). Synthetic seismic forward modeling suggests that intrusive steps, bridge structures, and magma fingers may manifest in seismic data as minor vertical offsets and corresponding amplitude variations in tuned reflection packages (Magee et al., 2015). Seismic- and field-based studies have also suggested that individual sills commonly consist of multiple magma lobes (e.g., Fig. 5A) that represent the incremental emplacement of discrete magma injections and may contain and/or be bound by intrusive step, bridge structures, or magma fingers (Thomson and Hutton, 2004; Hansen and Cartwright, 2006a; Schofield et al., 2010, 2012b; Magee et al., 2012b). Mapping the long axes of flow indicators, including lobe-lobe contacts, therefore provides insights into magma flow patterns within individual intrusions and allows magma input zones to be inferred (e.g., Fig. 5; Thomson and Hutton, 2004; Rui et al., 2013; Magee et al., 2014; Schofield et al., 2015). The style of flow indicator can also provide insights into mechanisms of emplacement; e.g., intrusive steps occur via brittle fracturing, whereas magma fingers form through the nonbrittle fluidization of the host rock (Fig. 4; Pollard et al., 1975; Rickwood, 1990; Hutton, 2009; Schofield et al., 2010, 2012a, 2012b).

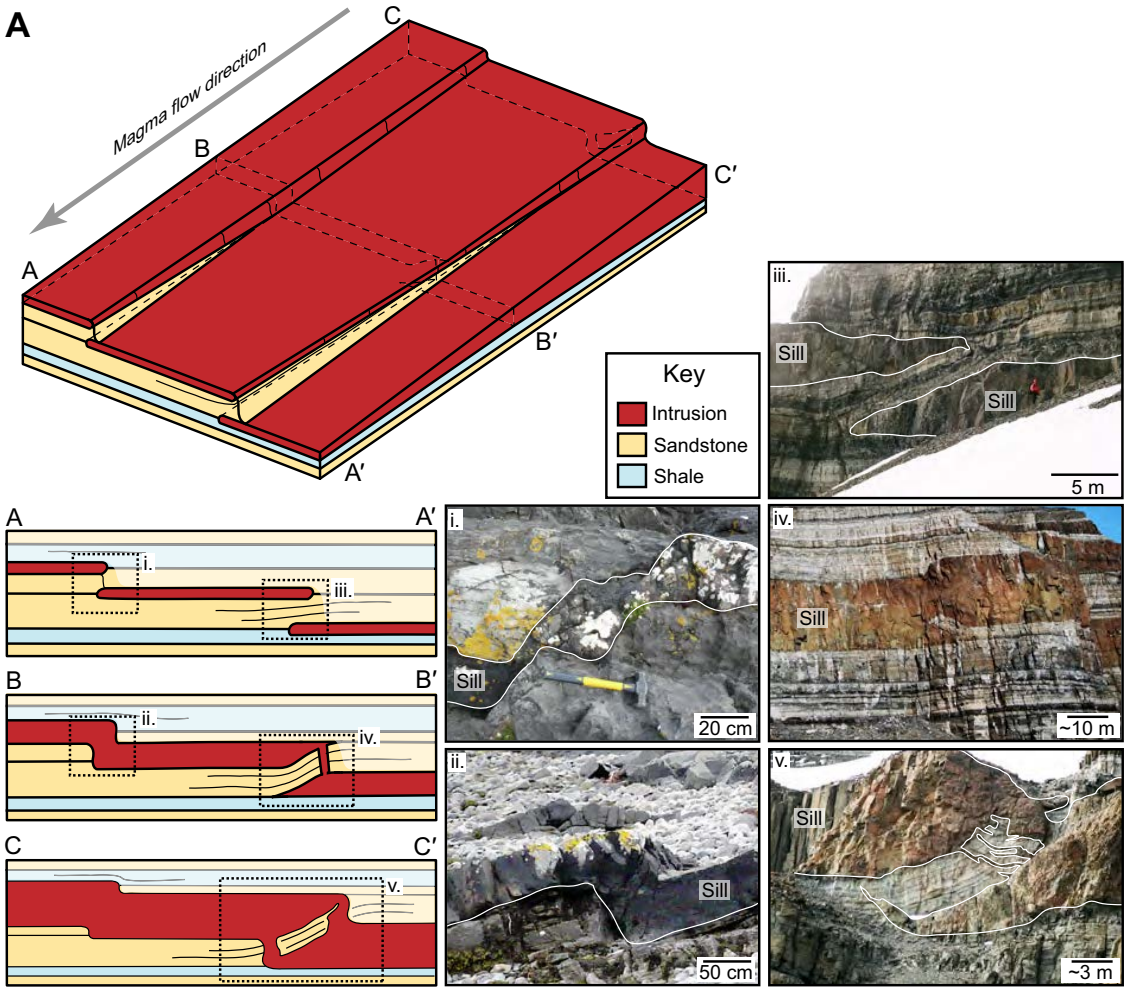

Figure 4 (*on this and following page*). (A) Magma flow indicators (i.e., intrusive steps and bridge structures) produced by brittle fracture processes. Field photos i. and ii. are of intrusive steps observed in inclined sheets and sills on Ardnamurchan, northwest Scotland. Field photos iii., iv., and v. from the Theron Mountains, Antarctica, document the growth of an intact sedimentary bridge between two magma segments (iii) into a broken bridge (iv) and a bridge xenolith (v) with increasing distance from the magma source (photos courtesy of Donny Hutton).

Magma flow patterns mapped across entire sill complexes commonly reveal that sills are fed by underlying sills or inclined sheets (e.g., Fig. 5B; Thomson and Hutton, 2004; Magee et al., 2014; Schofield et al., 2015). The extensive distribution of sill-sill junctions, which are a proxy for feeder relationships, implies that interconnected sills form efficient magma migration pathways (Cartwright and Hansen, 2006; Muirhead et al., 2012; Magee et al., 2014; Schofield et al., 2015). While sill-sill junctions may form via sill-sill abutment or crosscutting (Hansen et al., 2004; Galerne et al., 2011), as opposed to a feeding relationship, the mapping of flow patterns can help to constrain intrusion connectivity within sill complexes.

GEOLOGIC EXAMPLES OF SILL COMPLEXES

Having established how plumbing systems and magma flow patterns can be delimited in seismic data and in the field, we here present several field- and seismic-based case studies of sill complexes (Fig. 2; Table 1). Each case study provides important insights into the controls on and impacts of lateral magma flow in sill complexes. To provide context for the seismic-based analyses, we first review insights into tectonic-magmatic processes obtained from field studies focusing on the Raton Basin in Colorado and the Karoo-Ferrar large igneous province (LIP). We then examine plumbing systems imaged in seismic

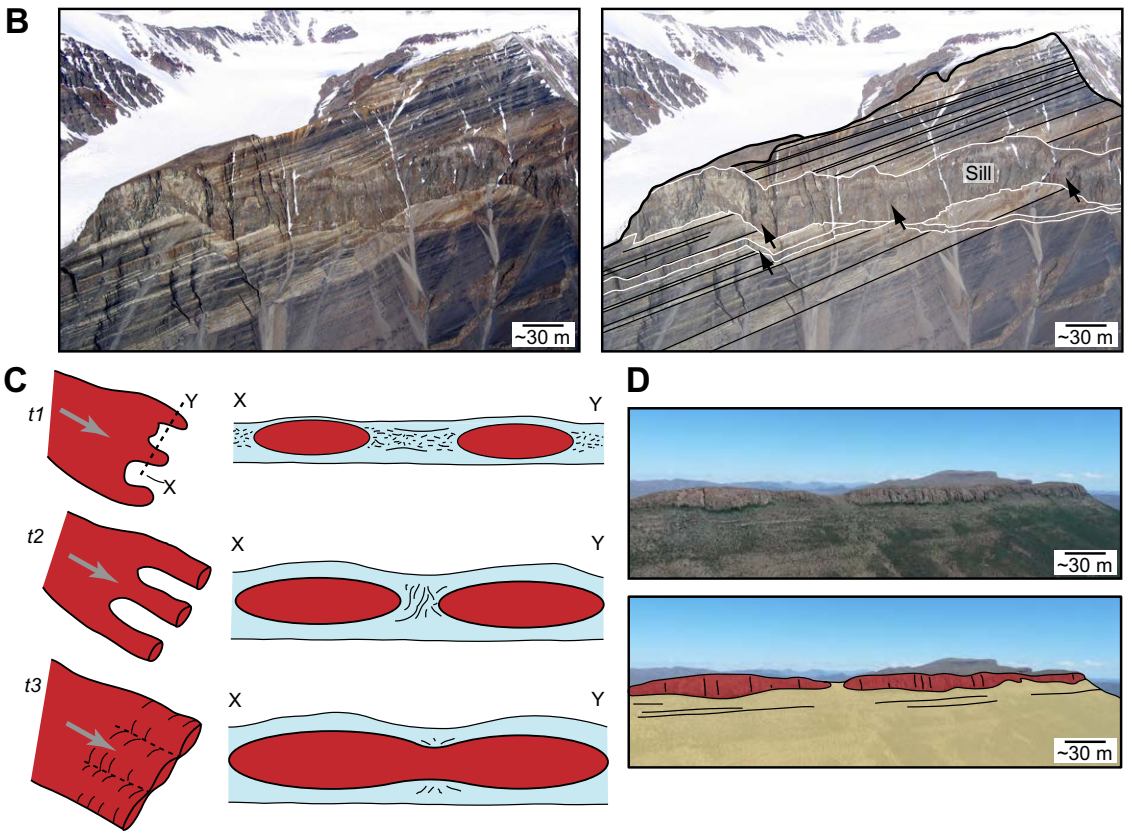

Figure 4 (*continued*). (B) Uninterpreted and interpreted field photo of a sill in Axel Heiburg, Canada, which displays intrusive steps (black arrows) at a seismically resolvable scale (courtesy of Martin Jackson). (C) Magma finger formation (modified from Schofield et al., 2012a). (D) Magma fingers in the Golden Valley Sill, South Africa: top—un-interpreted; bottom—interpreted.

data. In particular, we focus on sill complexes affiliated with the North Atlantic Igneous Province that are imaged in seismic data from the Rockall Basin, the Faroe-Shetland Basin, and the Møre and Vøring Basins (Fig. 2). We also review seismic-based studies of sill complexes from offshore and onshore Australia.

Raton Basin, Colorado, USA

The Raton Basin (Fig. 2) represents a foreland basin that formed during the Laramide orogeny. The basin hosts a series of Oligocene–Miocene basaltic sills emplaced within Late Cretaceous–early Paleogene medium-grade coal beds (Cooper et al., 2007). In cross section, the sills that intruded coal beds appear to consist of elliptical, finger-like magma segments that are as much as ~3 m thick, <5 m wide, and may be laterally separated by ≲5 m (Fig. 6A). The contacts between the coal and basalt are convoluted and lobate, with host-rock laminations within the coal becoming more chaotic toward the intrusion (e.g., Figs. 6A, 6B; Schofield et al., 2012a). Xenoliths of coal are incorporated into the sill margins, and clasts of basalt occurring within the coal are interpreted as a peperitic texture (Figs. 6A, 6B; Schofield et al., 2012a). Occasionally, adjacent magma segments are interconnected by thin (a few tens of centimeters) basalt sheets (e.g., Fig. 6A). Regardless of the variation in sill thickness observed across these segments, it is apparent that overlying and underlying sandstone beds remain undeformed (e.g., Fig. 6A; Jackson et al., 2013). This continuity in the strike and dip of sandstone beds implies that sill emplacement was not accommodated by roof uplift or floor subsidence (Jackson et al., 2013). Instead, the convoluted bedding within the coal, the lobate coal-sill margins, and the development of peperitic textures all suggest that emplacement occurred via fluidization of the host rock (Schofield et al., 2012a). The intruding basaltic magma is considered to have heated the coal until it behaved as a viscous fluid (Schofield et al., 2012a), the plastic deformation of which accommodated the intruded magma

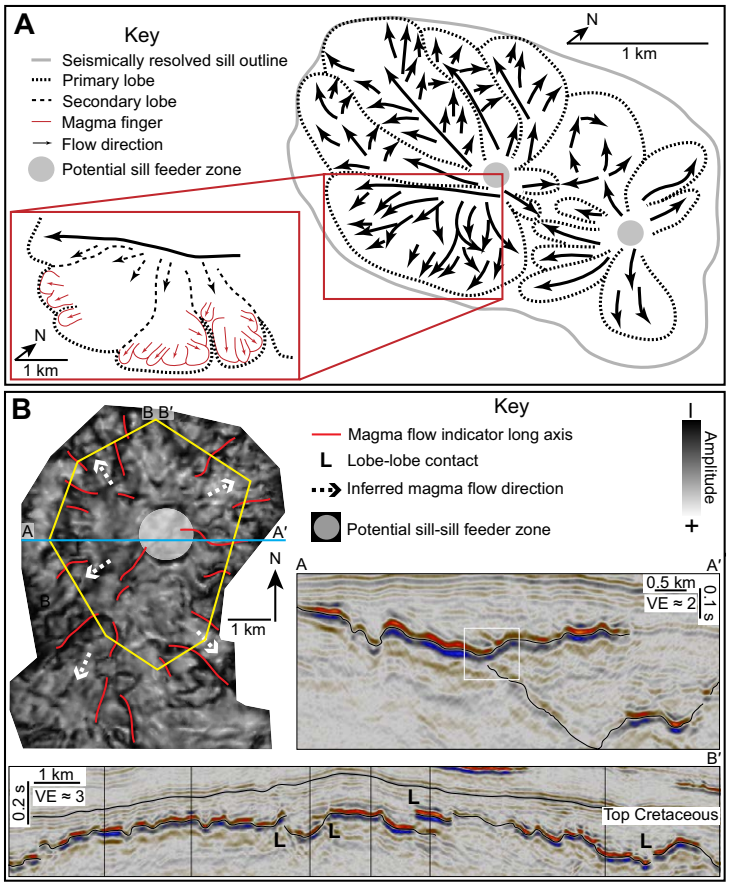

Figure 5. (A) Line drawing of magma lobes and fingers imaged in seismic data and used to delimit sill feeder locations (redrawn from Thomson and Hutton, 2004). (B) Magma flow patterns, derived from seismically resolved lobe-lobe contacts, consistent with a sill-sill feeding relationship (modified from Magee et al., 2014). VE—vertical exaggeration.

volume (Jackson et al., 2013). Because coal has a greater viscosity than basaltic magma (i.e., there is a high viscosity contrast), the fluid-fluid relationship between the two promoted the formation of magma fingers (Pollard et al., 1975; Schofield et al., 2012a), similar to what is observed during mafic-felsic magma interaction (e.g., Perugini and Poli, 2005). The magma fingers produced by intrusion into coal in the Raton Basin have an elongate geometry (Fig. 6C) and extend for kilometers to tens of kilometers. These observations highlight that nonbrittle emplacement along compliant horizons can facilitate lateral magma transport, without any roof uplift, over considerable distances (Fig. 6C).

Karoo-Ferrar LIP

Magmatic activity in the Karoo-Ferrar LIP initiated ca. 183 Ma (Encarnación et al., 1996), in response to plume and rift-related magmatism (Elliot and Fleming, 2000; Leat, 2008; Hole, 2015). The earliest stages of activity involved rapid emplacement (~1 m.y.) of significant magma volumes (>1 × 10^6 km^3) in the geochemically affiliated, yet geographically separated, sill complexes of the Karoo and Ferrar magmatic provinces (Heimann et al., 1994; Elliot and Fleming, 2000; Leat, 2008; Svensen et al., 2012). One of these sill complexes (>3 × 10^6 km^2) intruded into the Karoo Basin, a foreland basin currently exposed onshore South Africa (Figs. 2, 7A, and 7B; Chevallier and Woodford, 1999; Svensen et al., 2012; Scheiber-Enslin et al., 2014). Sills of the Ferrar magmatic province crop out in Antarctica, southeast Australia, and New Zealand (Figs. 2, 7B, and 7C; Leat, 2008). Despite the broad geographic distribution of the Ferrar magmatic province, the remarkably homogeneous compositions exhibited by intrusive and extrusive Ferrar rocks for thousands of kilometers is suggestive of a single magma source (Elliot et al., 1999). Ferrar intrusive rocks observed in Antarctica are found almost exclusively within the 2.5-km-thick Devonian–Jurassic Beacon Supergroup (e.g., Fig. 7C; Leat, 2008). Paleogeographic reconstructions suggest that the Ferrar sill complex extends for more than 4100 km from the proposed site of a plume head source (Fig. 7B; Elliot et al., 1999; Elliot and Fleming, 2000; Leat, 2008). Both the Karoo Basin and the basin-filling Beacon Supergroup rocks, which are relatively flat lying and unfaulted, are dominated by subhorizontal sandstone, shale, and coal beds (e.g., Fig. 7C; Barrett, 1981; Leat, 2008; Svensen et al., 2012).

Within the Karoo and Ferrar sill complexes, the abundance of dikes is limited and the absence of extensive (>10 km long) dike swarms suggests that magma transport primarily occurred and linked to the surface through interconnected sill complexes (e.g., Figs. 7A, 7B; Galerne et al., 2008; Leat, 2008; Polteau et al., 2008b; Airoldi et al., 2012; Muirhead et al., 2012, 2014; Svensen et al., 2012; Scheiber-Enslin et al., 2014). In the Ferrar magmatic province specifically, the role of sills in facilitating extensive lateral magma flow is supported by: (1) observed sill-sill feeding relationships (Muirhead et al., 2012, 2014); (2) decreasing Mg# and MgO contents along the length of the Ferrar magmatic province that are consistent with fractional crystallization during lateral magma flow as far as 4100 km from the Weddell Sea region (Elliot et al., 1999; Elliot and Fleming, 2000; Leat, 2008); and (3) the consistent orientation of bridge and/or broken bridge structure long axes and magnetic lineations within sills and interconnected sheets across Antarctica (e.g., in the Theron Mountains, Antarctica) (Dragoni et al., 1997; Hutton, 2009; Airoldi et al., 2012). Overall, these data imply that sills facilitated magma transport lengthwise across the East Antarctic margin within Beacon Supergroup rocks (Storey and Kyle, 1997; Leat, 2008). It is proposed that the development of a broad region of topographic uplift above the proposed plume head generated sufficient hydraulic head to promote the lateral emplacement of the Ferrar sills for ~4100 km (Leat, 2008). A similar plume-related mechanism was suggested to explain the lateral (250 km) emplacement of the 2.11 Ga Griffin gabbro sills in

TABLE 1. MAFIC SILL COMPLEXES: CHARACTERISTICS OF CASE STUDIES

Main sill complex location	Data source	Age	Host rock lithology	Faults play a key role	Transgressive height (km)	Area (km^2)	Volume (km^3)	Distance of lateral magma transport (km)	Likely melt source	Key references
Raton Basin, Colorado, USA	Field	Oligocene–Miocene	Coal	No	?	?	?	>10	Rift related?	Schofield et al. (2012a)
Karoo Basin, South Africa	Field	Early Jurassic	Sandstone, shale, and coal	No	3 (?)	~3,000,000	>340,000	>200	Plume	Svensen et al. (2012)
Antarctica (i.e., Ferrar sill complex)	Field	Early Jurassic	Sandstone, shale, and coal	No	?	~560,000	<125,000	<4100	Plume	Leat (2008); Airoldi et al. (2011); Muirhead et al. (2012, 2014)
Irish Rockall Basin, offshore west Ireland	Seismic	Paleocene–Eocene	Shale and volcaniclastic sandstones	No	~4	>748	?	>60	Plume	Magee et al. (2014)
North Rockall Basin, offshore northwest Scotland	Seismic	Paleocene–Eocene	Shale	Yes	>3	?	?	50–60	Plume	Thomson and Hutton (2004); this study
Faroe-Shetland Basin, offshore east Faroe Islands	Seismic	Paleocene–Eocene	Shale	Yes	>3	>22,500	?	20	Plume	Schofield et al. (2015)
Møre and Vøring Basins, offshore west Norway	Seismic	Paleocene–Eocene	Shale and crystalline basement	Yes	12	>80,000	?	?	Plume	Skogseid et al. (1992); Planke et al. (2005); Cartwright and Hansen, (2006)
Ceduna subbasin, offshore South Australia	Seismic	Eocene	Sandstone, shale, and coal	No	<1.5	<20,000	?	?	Hotspot?	Jackson et al. (2013); Magee et al. (2013b)
Northwest Australian Shelf, offshore northwest Australia	Seismic	Late Jurassic–Early Cretaceous	Shale	Yes	<15	?	?	?	Rift related?	Symonds et al. (1998); Magee et al. (2013a, 2013c); Rohrman (2013, 2015)
Yilgarn craton	Field	Proterozoic	Granite and granitic gneisses	Yes	<10	?	?	>300	Plume	Wingate et al. (2008); Ivanic et al. (2013)

?—parameters that are unknown and/or poorly constrained.

the Hurwitz Basin, Canada (Aspler et al., 2002). The scale of lateral transport in Ferrar sills (i.e., as much as 4100 km) rivals that of the ~2000-km-long, 1270 Ma Mackenzie dike swarm of Canada (Ernst and Baragar, 1992).

Sill Complexes in the North Atlantic Igneous Province

The North Atlantic Igneous Province formed ca. 62–53 Ma in response to the break-up of the North Atlantic and the impingement of a mantle plume at the base of the lithosphere (White and McKenzie, 1989; Saunders et al., 1997; Kent and Fitton, 2000; Emeleus and Bell, 2005; Storey et al., 2007; Hansen et al., 2009). Age relationships and radiometric dating suggest that the North Atlantic Igneous Province can be divided into two main phases of magmatic activity; one between ca. 62 and 58 Ma (e.g., west Greenland, Great Britain) and the other (e.g., east Greenland) spanning ca. 57–53 Ma (Saunders et al., 1997). Voluminous sill complexes, dike swarms, volcanic centers, and extrusive igneous rocks, primarily of basaltic composition, were emplaced during these phases (~6.6×10^6 km^2 in total) and are located along two volcanic rifted margins; the conjugate east Greenland–northwest European and the west Greenland–Baffin Bay margins (Fig. 2; Storey et al., 2007; Hansen et al., 2009).

Irish Rockall Basin, North Atlantic

A sill complex located along the northeastern margin of the Irish Rockall Basin consisted of 82 seismically resolved intrusions, and was analyzed in Magee et al. (2014) (Figs. 2 and 8). Individual intrusions predominantly displayed saucer-shaped and inclined sheet morphologies, which range in diameter from 0.3 to 7.1 km and transgress as much as 1.79 km of strata (Magee et al., 2014). The sills are vertically stacked (i.e., numerous sills separated by layers of host-rock strata occur within a vertical sequence) and commonly overlap laterally (Fig. 8B; Magee et al., 2014). The sill complex crosscuts an ~2-km-thick stratigraphic sequence of Cretaceous marine shale and Paleogene volcaniclastic sandstone, and extends across an area >748 km^2 (Figs. 8A, 8B; Magee et al., 2014). The main inclined portions of the intrusions primarily dip to the northwest and the sills appear to be interconnected; i.e., inclined sheets and sill limbs apparently feed stratigraphically saucer-shaped sills (Figs. 5B and 8A; Magee et al., 2014). Because acoustic energy is attenuated within igneous rocks, seismic imaging directly beneath sills is commonly poor and it is thus difficult to confirm whether inferred sill-sill junctions are physically connected (e.g., Fig. 5B; e.g., Smallwood and Maresh, 2002; Cartwright and Hansen, 2006). However, a comparison between the Irish Rockall Basin seismic data and synthetic seismic forward models, designed to test

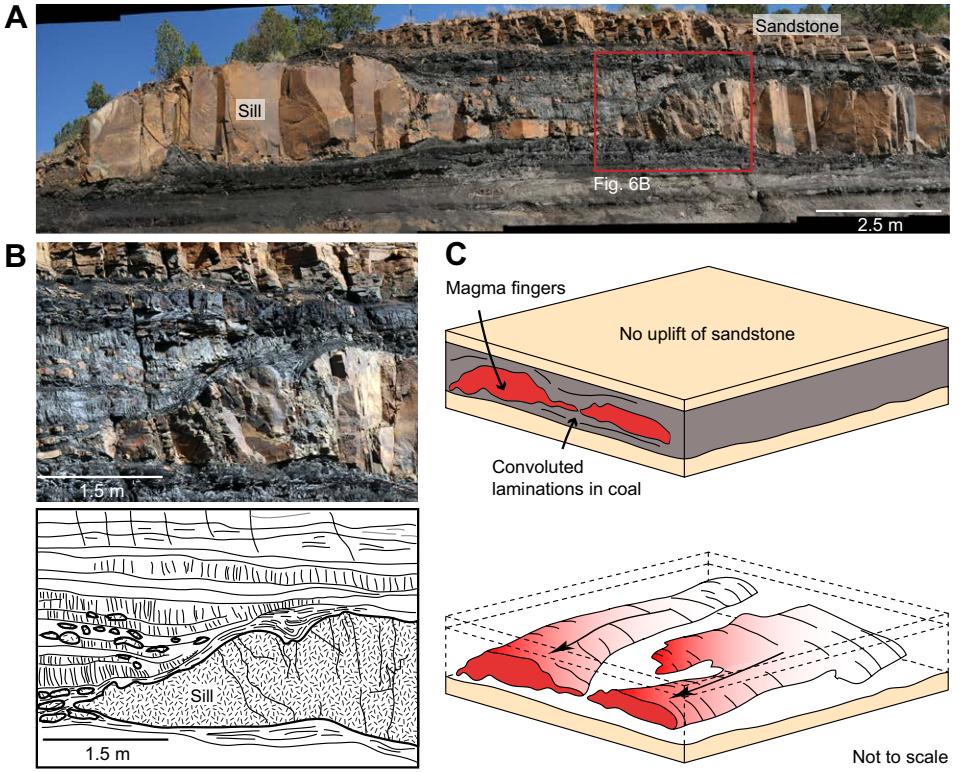

Figure 6. (A) Field photo of magma fingers developed within a coal layer in the Raton Basin, Colorado (USA). Note that the overlying sandstone bed displays no evidence of uplift above the thicker portions of the magma fingers. (B) Closeup highlighting the convoluted coal laminations close to the intrusion and the clasts of dolerite within the coal (A and B are modified from Schofield et al., 2012a). (C) Conceptual box model of magma fingers in the Raton Basin.

how sill connectivity affects reflection configurations, suggests that at least some sills are physically connected, with lower sills feeding overlying sills (Magee et al., 2015, Fig. 11 therein). Connectivity between individual sills is further supported by mapping of flow indicators, which commonly radiate outward from inferred sill-sill feeder zones (e.g., Fig. 5B; Magee et al., 2014). Observations related to sill connectivity are consistent with a regional southeast-directed lateral magma flow regime, perhaps indicative of a melt source associated with the Hebridean Terrace igneous complex located ~10 km to the northwest (Magee et al., 2014). Based on the position of the furthest sills from the Hebridean Terrace igneous complex, it is plausible that this sill complex documents at least 60 km of lateral magma flow.

In addition to delimiting plumbing systems and flow patterns within sedimentary basins, it is also important to constrain the time frame of magmatic activity. This is because the rate of intrusion and volume of melt can provide important insights into (1) the evolution of the melt source (White et al., 2008); (2) the longevity of potential volcanic activity; and (3) deformation of the host rock. Above the sill complex mapped by Magee et al. (2014), a series of dome-shaped folds are developed within the upper Cretaceous to top lower Eocene strata (Fig. 8A). The outline of these folds corresponds to the lateral termination of underlying sills and, particularly along the top Paleocene horizon, seismic reflections can be observed to onlap onto the folds (Fig. 8A). These seismic-stratigraphic relationships imply that fold growth was generated by and accommodated sill emplacement, resulting in the formation of bathymetric highs that were onlapped by synkinematic sediment (Fig. 8C; Trude et al., 2003; Hansen and Cartwright, 2006b; Jackson et al., 2013; Magee et al., 2013a, 2014). Because the sills are vertically stacked and laterally overlap each other, the folds display a complex compound fold morphology (Fig. 8A); i.e., during the growth of individual forced folds, continued magma intrusion promoted fold coalescence and formed folds as much as 244 km^2 and 296 km high (Fig. 8C; Magee et al., 2014). Onlap relationships are observed throughout the folded succession, between the top Cretaceous and top lower Eocene boundaries (Fig. 8A), suggesting that sill emplacement and fold growth occurred incrementally over 15 m.y. between ca. 65 and 54 Ma (Magee et al., 2014).

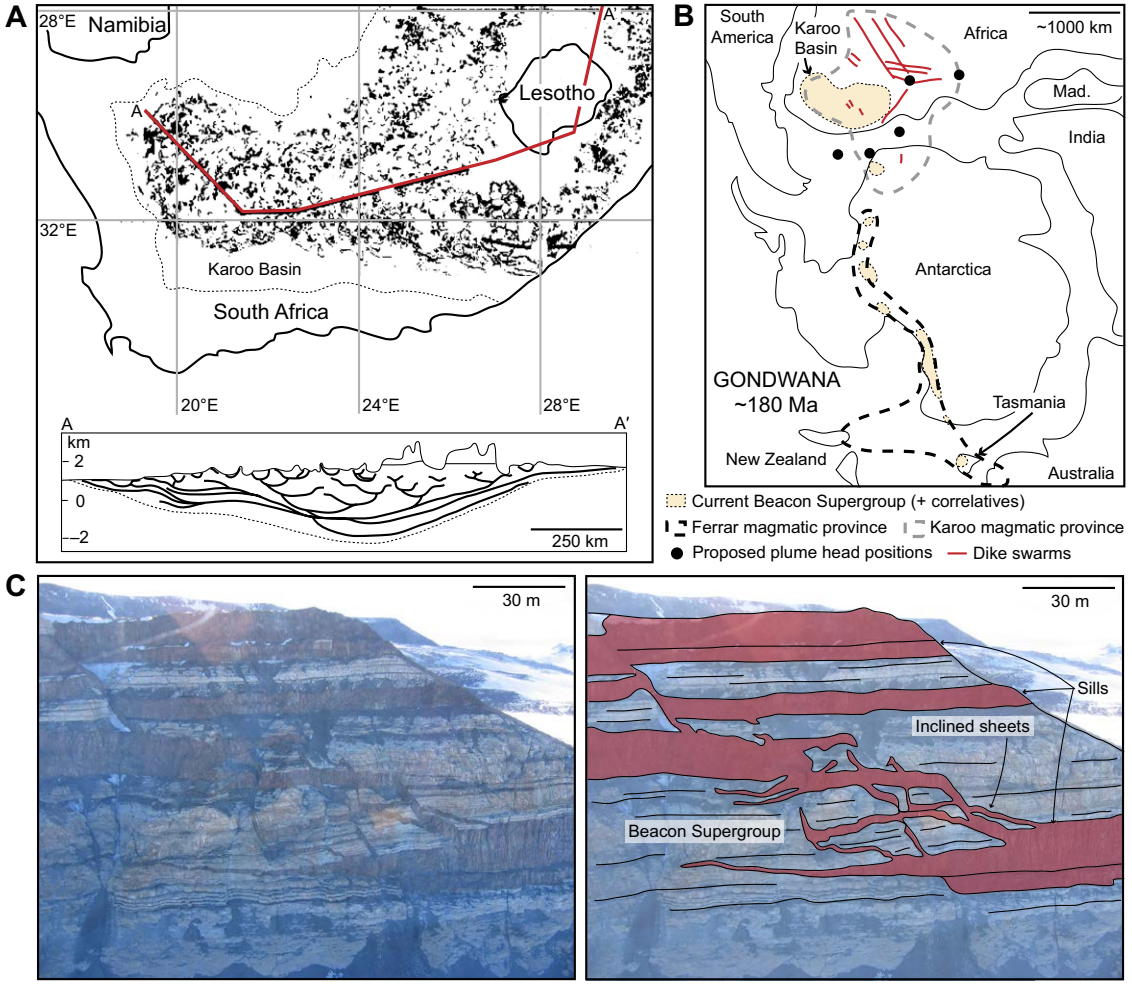

Figure 7. (A) Distribution of sills (black) within the Karoo Basin (dashed outline) and a schematic cross section (modified from Svensen et al., 2012). (B) Paleogeographic reconstruction (ca. 180 Ma) highlighting the current extent of the Karoo-Ferrar large igneous province and associated basin exposures (based on Mortimer et al., 1995; Leat, 2008; Hastie et al., 2014). Mad.—Madagascar. (C) Field photo and interpreted photo of interconnected Ferrar sills and inclined sheets intruded into the Beacon Supergroup in Antarctica (courtesy of James White).

Northeast Rockall Basin, North Atlantic

Similar to the Irish sector of the Rockall Basin, sill complexes within the northeast Rockall Basin were emplaced into upper Cretaceous marine shale during the Paleocene and Eocene (e.g., Fig. 9A; Thomson and Hutton, 2004; Archer et al., 2005; Hansen and Cartwright, 2006b). Associated with the sill complexes are series of large (~20 km diameter) igneous centers, which are interpreted to consist of broad volcanic edifices fed by underlying laccoliths and plutons (e.g., Figs. 9A, 9B; Archer et al., 2005). These igneous centers commonly occur in northwest-southeast– and east-northeast–west-southwest–trending chains and are situated along major crustal lineaments, which likely provided magma ascent pathways connecting the melt source to the Rockall Basin (Archer et al., 2005; Hansen and Cartwright, 2006b). Despite the spatial association between sill complexes and igneous centers in the northeast Rockall Basin (e.g., Figs. 9A, 9B), any genetic relationship between the two remains poorly constrained.

To test whether the sill complexes were fed from the igneous centers, we examine new observations of magma flow patterns exhibited by a sill complex located along the eastern margin of the northeast Rockall Basin (Fig. 9). The 2D seismic data reveal that the sill complex covers a broad area and extends toward the Darwin igneous center, which is located ~60 km to the northwest (Figs. 9A, 9B).

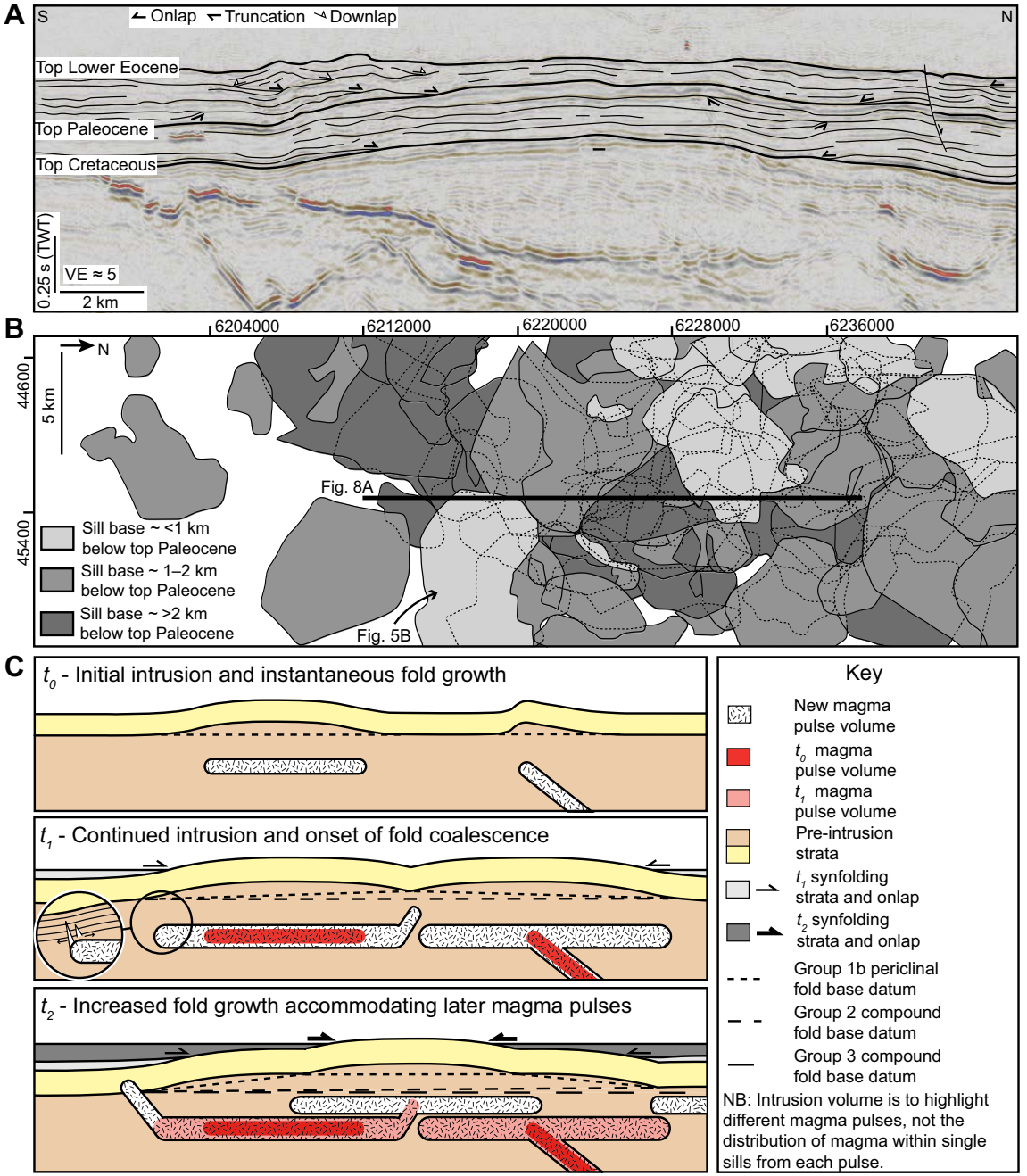

Figure 8. (A) Seismic section of forced folds and the underlying sill complex imaged along the eastern margin of the Irish Rockall Basin. Sills are primarily emplaced within the Cretaceous, shale-dominated succession. The Paleocene and Eocene strata are volcaniclastic- and shale-dominated, respectively. VE—vertical exaggeration. (B) Sill distribution map highlighting the overlapping nature of individual sills. (C) Conceptual model of fold growth and coalescence in response to the incremental injection of magma pulses (*t*—time) (A–C modified from Magee et al., 2014).

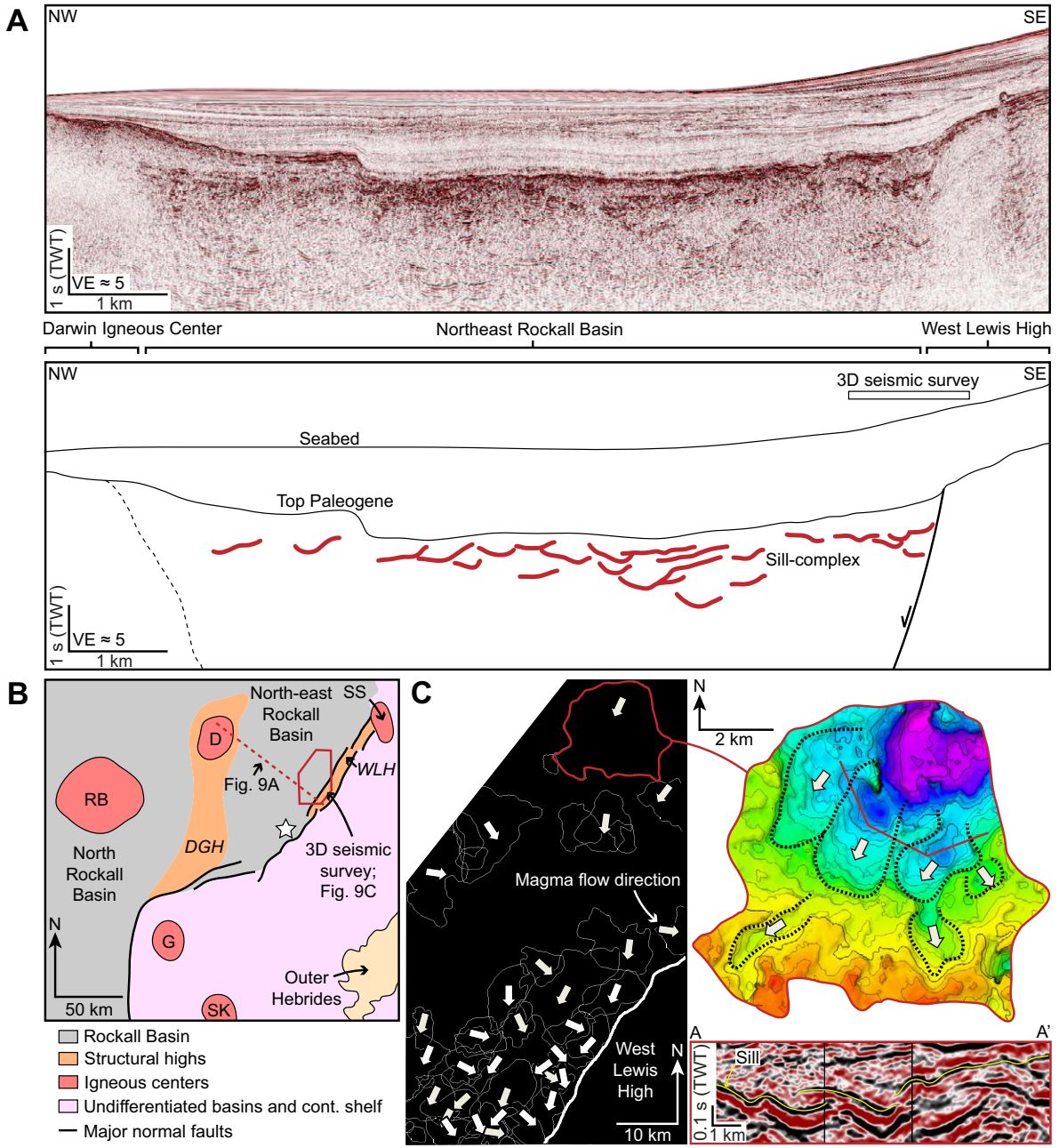

Figure 9. (A) Regional two-dimensional seismic line highlighting the distribution of sills within the northeast Rockall Basin. See Figure 10B for location. TWT—two-way traveltime; VE—vertical exaggeration; 3D—three dimensional. (B) Simplified geological map of the study area. Local igneous centers: RB—Rosebank; D—Darwin; SS—Sula Sgeir; G—Geikie; SK—Saint Kilda. The Darwin-Geikie High (DGH) and the West Lewis High (WLH) are also shown. The study of Thomson and Hutton (2004) examined magma flow patterns in sills located just to the southwest of the location of the 3D seismic data used here. (C) Sill outlines and mapped magma flow patterns. A map of an arbitrary seismic line through one sill is provided to demonstrate how magma lobes were used to delimit magma flow patterns.

Here we focus on a portion of the sill complex imaged within a 3D seismic data set that is located ~50 km southwest of the Sula Sgeir igneous center (Figs. 9A, 9B). Of 100 mapped intrusions, 72% have a saucer-shaped morphology and the remaining 18% are classified as inclined sheets. The sills appear to be interconnected, with inclined sheets and sill limbs predominantly dipping to the northwest. Mapping of magma lobes and other flow indicators within individual intrusions reveal that magma primarily propagated to the southwest or southeast, consistent with typical northwest-dipping orientation of transgressive intrusion portions (Figs. 9B, 9C). Similar magma flow patterns were recorded by Thomson and Hutton (2004) ~20 km to the southwest of the study area (Fig. 9B). Southwest-directed magma flow patterns are particularly well developed adjacent to and along strike of a northwest-dipping, basin-bounding fault, perhaps suggesting that sill propagation to the southeast was inhibited by the juxtaposition of sedimentary strata against crystalline basement in the fault footwall (Fig. 9B). These observations imply that the mapped sill complex could have been fed from the Darwin and/or Sula Sgeir igneous centers via lateral magma flow over ~50–60 km (Figs. 9A, 9B). Geochemical and further seismic analyses are required to test this hypothesis.

Faroe-Shetland Basin, North Atlantic

An extensive sill complex covering >22,500 km^2 and emplaced primarily within upper Cretaceous shale is imaged in seismic reflection data from the Faroe-Shetland Basin (Figs. 10A, 10B; Passey and Hitchen, 2011; Schofield et al., 2015). Radiometric dating of sills penetrated by boreholes and relative ages of sills determined from seismic-stratigraphic onlap relationships of overlying strata onto intrusion-induced forced folds suggests that intrusion occurred between ca. 61 and 52 Ma (Passey and Hitchen, 2011; Schofield et al., 2015). While >300 seismically resolved sills have been mapped in the basin (Fig. 10A), the actual number of intrusions that constitute the sill complex is likely much larger because:(1) imaging beneath the Paleogene flood basalt cover is poor, compromising mapping of underlying intrusions; and (2) borehole data suggest that a significant proportion (as much as ~80%) of intrusions have thicknesses below the limit of detectability of the seismic data (Schofield et al., 2015). The sills that are resolved display a wide variety of morphologies (e.g., saucer-shaped sills and inclined sheets) and have diameters of as much as tens of kilometers (e.g., Figs. 10A, 10B; Schofield et al., 2015). Individual intrusions may transgress as much as 2 km of the sedimentary succession and appear to connect to overlying sills, inclined sheets, and lava flows (e.g., Figs. 10A, 10B; Schofield et al., 2012b, 2015). Some inclined portions of intrusions coincide with and likely intruded along fault planes (Schofield et al., 2015). Connectivity between sills is supported by mapped flow indicators (Schofield et al., 2015). For example, the long axes of bridge and broken bridge structures, which bound magma lobes in the Flett Ridge Sill, radiate out from the inferred magma input zone at a sill-inclined sheet junction (Figs. 10C, 10D; Schofield et al., 2012b). The reconstruction of flow patterns within the Faroe-Shetland Basin sill complex implies that magma was fed into the basin via basement-involved faults, from which sills propagated laterally for as much as ~25 km into the hanging wall (Figs. 10A, 10B; Schofield et al., 2015).

Møre and Vøring Basins, North Atlantic

Sill complexes developed along the Norwegian margin (Fig. 11A) represent a continuation of the Late Cretaceous–Paleogene magmatic activity that generated networks of intrusions within the Rockall and Faroe-Shetland Basins to the southwest (Fig. 2; Skogseid et al., 1992; Planke et al., 2005; Cartwright and Hansen, 2006; Hansen, 2006). Sills were predominantly emplaced into Late Cretaceous and early Paleocene shale, although some sills intruded older sedimentary strata and crystalline basement (e.g., Cartwright and Hansen, 2006). A close spatial relationship between the lateral tips of sills and an overlying complex of 734 seismically resolved, genetically related hydrothermal vents suggests that (Fig. 11A) (1) the stratigraphic level of extrusion represents the paleoseabed contemporaneous to sill intrusion; and (2) emplacement occurred ca. 55 Ma (Svensen et al., 2004; Planke et al., 2005; Hansen, 2006). Overall, the sill complexes, which appear to be internally interconnected via sill-sill junctions, extend across >80,000 km^2 of the basin and, in places, transgress as much as 12 km of sedimentary strata and crystalline basement (e.g., Figs. 11A–11C; Svensen et al., 2004; Planke et al., 2005; Cartwright and Hansen, 2006). Some of the sills that extend into basement rocks may link to a high-velocity body inferred to represent the melt source (Fig. 11C; Cartwright and Hansen, 2006). Individually, the majority of sills display saucer-shaped and inclined sheet geometries (e.g., Fig. 11B), regardless of whether they intruded sedimentary or crystalline rocks (Planke et al., 2005; Cartwright and Hansen, 2006). Any major variations in sill geometry are primarily displayed by those intrusions emplaced at depths <1 km beneath the paleoseabed; these shallow-level sills are lobate in form and display prominent magma flow channels (Fig. 11D; Hansen and Cartwright, 2006a; Miles and Cartwright, 2010). Observations from the Møre and Vøring Basins are consistent with those gathered from the Rockall and Faroe-Shetland Basins; i.e., interconnected sill complexes within sedimentary basins are laterally extensive and also provide an efficient mechanism for magma ascent (e.g., Fig. 11B; Cartwright and Hansen, 2006).

Ceduna Subbasin, Offshore Southern Australia

An array of 46 intracontinental volcanoes and underlying sills and laccoliths are imaged in seismic data from the Ceduna subbasin (Fig. 12; Jackson, 2012; Magee et al., 2013b). Dredged samples from volcano summits exposed at the seabed in the west of the Ceduna subbasin suggest that the volcanoes have a basaltic composition (Fig. 12A; Clarke and Alley, 1993). The edifices range in height from 0.02 to 1 km, have diameters as much as ~18 km, and flank dips are <12°, indicative of a shield volcano morphology (e.g., Fig. 12;

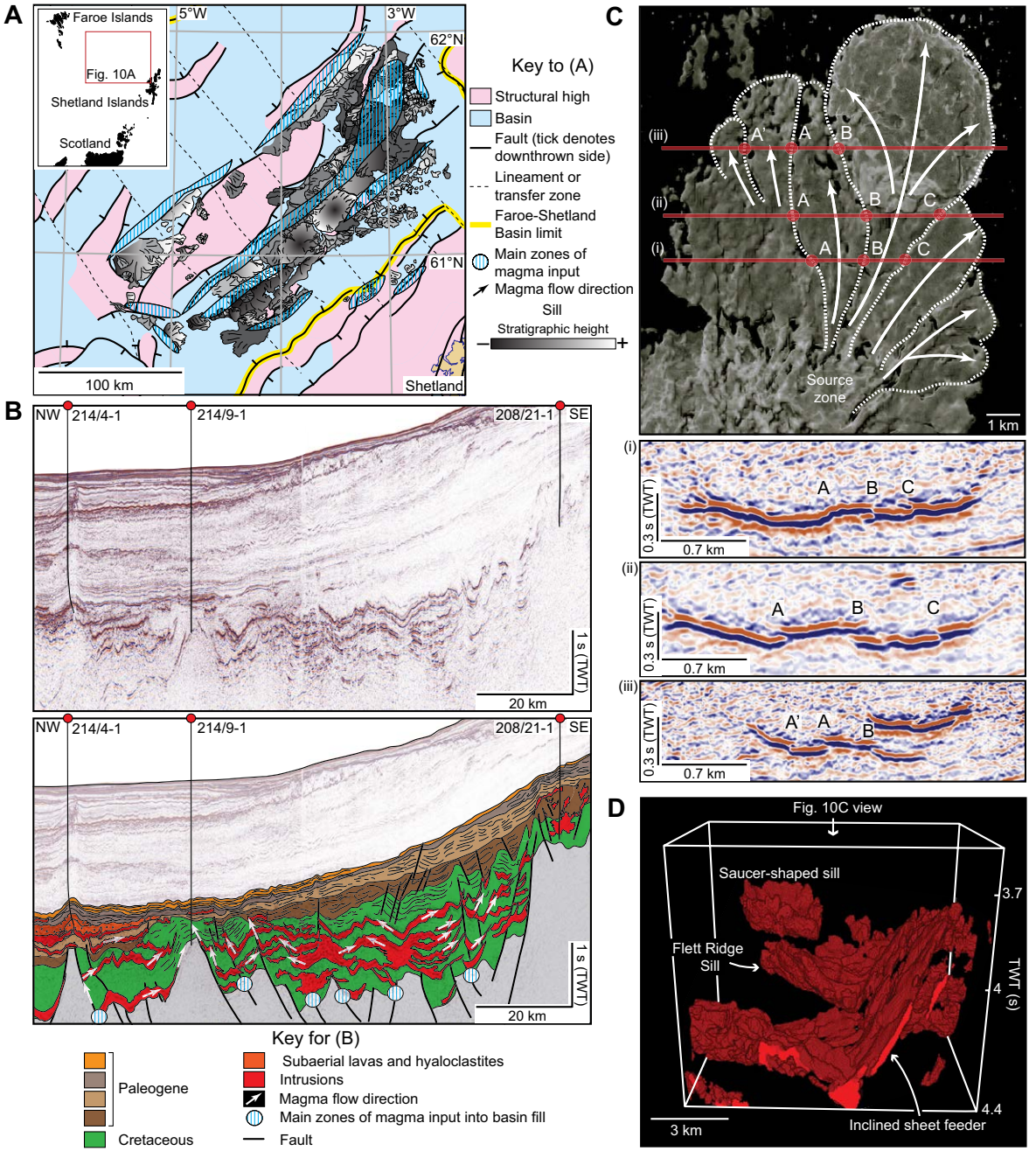

Figure 10. (A) Regional geology of the Faroe-Shetland Basin, including seismically mapped sills and magma flow directions. Magma flow patterns were used to infer magma input zones into the basin (modified from Schofield et al., 2015). (B) Representative seismic line (uninterpreted and interpreted) highlighting sill complex structure and association with faults (Schofield et al., 2015). TWT—two-way traveltime. (C) Opacity render of the Flett Basin Sill and corresponding seismic sections documenting intrusive step and broken bridge growth along lobe-lobe contacts (modified from Schofield et al., 2012b). A, A′, B, and C correspond to intrusive steps or bridge structures observed in profiles (i), (ii), and (iii). (D) Geobody interpretation of the Flett Basin Sill showing that the magma lobes imaged in C trace back to, and were likely fed from, a fault-hosted inclined sheet (modified from Schofield et al., 2012b).

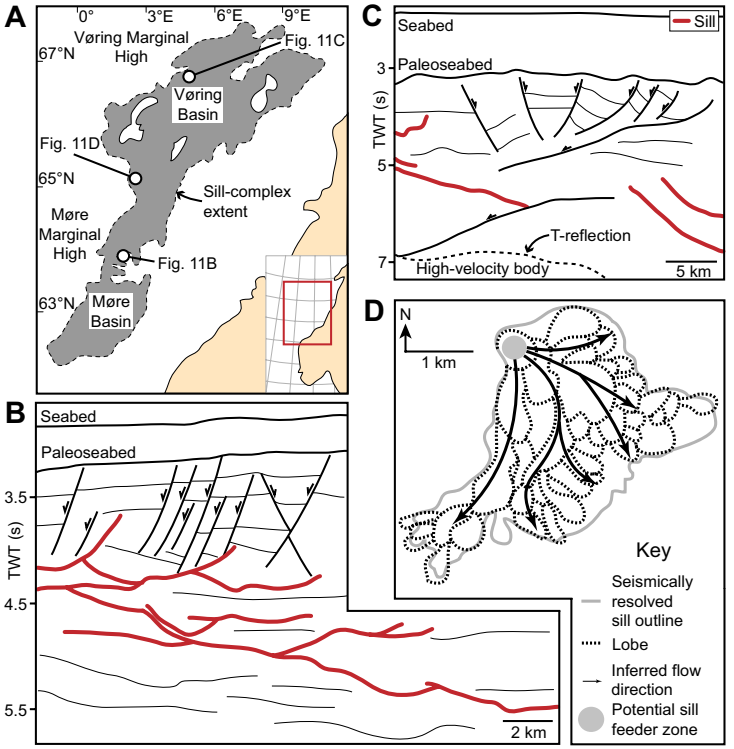

Figure 11. (A) Sill complex distribution (gray) within the Møre and Vøring Basins, offshore Norway (modified from Svensen et al., 2004). (B, C) Line drawings of two different seismic lines from Cartwright and Hansen (2006). The T-reflection corresponds to the top of the high-velocity body. TWT—two-way traveltime. (D) Mapped magma lobes and inferred flow directions for the Solsikke sill are shown (redrawn from Hansen and Cartwright, 2006a).

Magee et al., 2013b, their GP1 volcanogenic mounds). The volcanoes are on the top of the Pidinga Formation, are onlapped by the Nullarbor Limestone formation, and several are situated directly above the upper tips of normal faults (Fig. 12B; Jackson, 2012; Magee et al., 2013b). These seismic-stratigraphic observations and fault relationships are consistent with an emplacement age of 42 Ma (Jackson, 2012; Magee et al., 2013b). A series of intrusion-induced forced folds developed above sills and laccoliths are onlapped by the volcanoes and the Nullarbor Limestone (Fig. 12B; Jackson et al., 2013; Magee et al., 2013b). This implies that sill and volcano emplacement were contemporaneous and likely genetically related (Jackson, 2012; Magee et al., 2013b). Magmatic activity thus occurred immediately after the gravitational collapse of the southern Australian continental margin, ~40 m.y. after continental break-up between Australia and Antarctica (Schofield et al., 2008). Due to the lack of a temporal relationship between volcano emplacement and continental rifting, the origin of the magmatism in the Ceduna subbasin remains enigmatic. Recent studies, however, favor a model whereby melting was associated with a static, intracontinental hotspot located directly beneath the volcanic field (Schofield et al., 2008). Although magmatism was not linked to rifting, this case study presents a unique opportunity to examine the relationship between volcano growth and the subvolcanic plumbing system.

By analyzing the external morphology of the volcanoes and assessing the configuration of intravolcano seismic reflections, it was demonstrated (Magee et al., 2013b) that the basal diameter and summit height proportionally increased through progressive summit eruptions (Figs. 12C, 12D). Mapping of the volcanoes and associated intrusions reveals that 40% of the volcanoes overlie the lateral terminations of sills and/or laccoliths; 30% of the volcanoes are located directly above or close to upper fault tips, whereas the remaining 30% show no spatial relationship to underlying intrusions or faults (Figs. 12A, 12B; Magee et al., 2013b). The intrusions occur within the Potoroo Formation, which consists of interbedded fluvial sandstones and floodplain shales and coals, and were emplaced at depths of as much as 1.5 km beneath the paleosurface (i.e., the Pidinga Formation) (Jackson et al., 2013). It is difficult to assess the sill-sill and sill-volcano connectivity due to the ≥4 km spacing of the 2D seismic lines. However, if we assume that the sills and laccoliths are interconnected, similar to many sill complexes worldwide that display similar morphological characteristics (this study), a laterally extensive plumbing system within the Ceduna subbasin would imply that the melt source may not be located directly beneath the volcanoes (Magee et al., 2013b). Such an interpretation of a melt source laterally offset from the volcano array contrasts with the traditional assumption that intracontinental hotspot basaltic shield volcanoes are fed from an underlying zone of melting via dikes (Valentine and Gregg, 2008). Alternatively, dikes not imaged in these seismic data may feed the shallow-level intrusions. A role for dikes within the plumbing system of the Ceduna subbasin is supported by the observation that some volcanoes (30%) are not associated with underlying sills or faults (Figs. 12A, 12B; Magee et al., 2013b).

Analyses of intrusion thickness (i.e., where discrete upper and lower contact reflections are resolved) and forced fold amplitude allow mechanisms of sill emplacement to be assessed (Hansen and Cartwright, 2006b; Jackson et al., 2013; Magee et al., 2013a). If it is assumed that only roof uplift accommodates the intruded magma volume, then fold amplitude should equal the intrusion thickness (Hansen and Cartwright, 2006b). Discrete upper and lower contact reflections for individual intrusion can occasionally be mapped within the Ceduna subbasin, allowing the relationship between intrusion thickness and fold amplitude to be investigated (Jackson et al., 2013). Some of the sills and folds have a 1:1 relationship between intrusion thickness and fold amplitude, implying that roof uplift accommodated intrusion (Fig. 13; Jackson et al., 2013). However, the majority of the fold amplitudes measured are as much as 83% less than (average of 37%) the thickness of underlying intrusions (Fig. 13; Jackson et al., 2013). Similar discrepancies between sill thickness and fold amplitudes are observed elsewhere in other sedimentary basins (Fig. 13; Hansen and Cartwright, 2006b; Magee et al., 2013a).

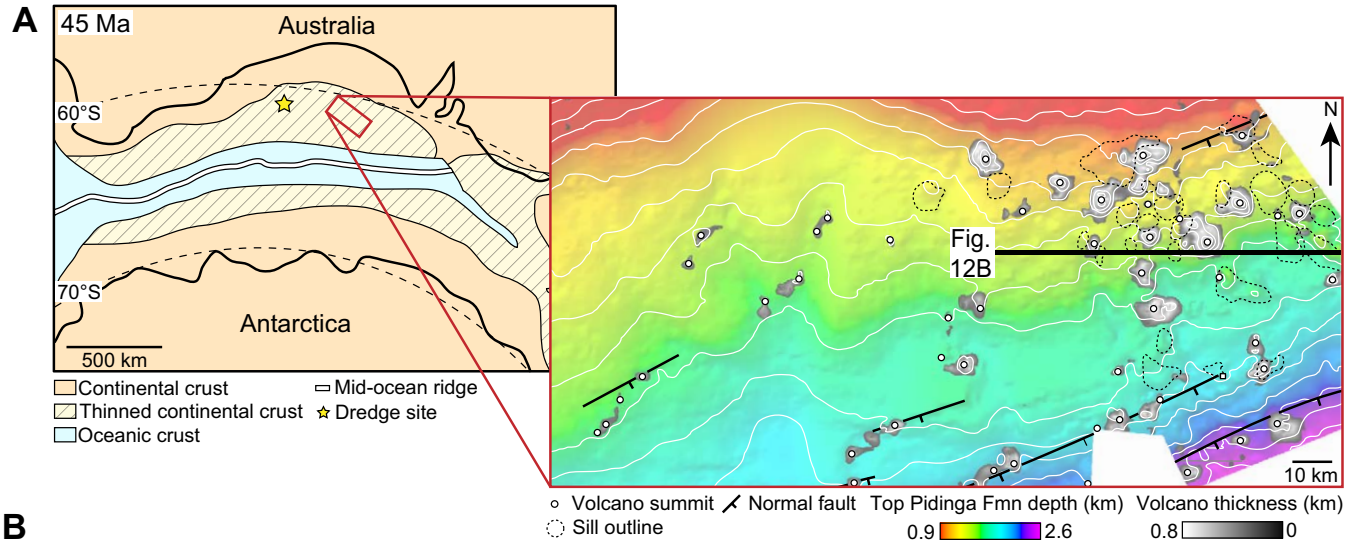

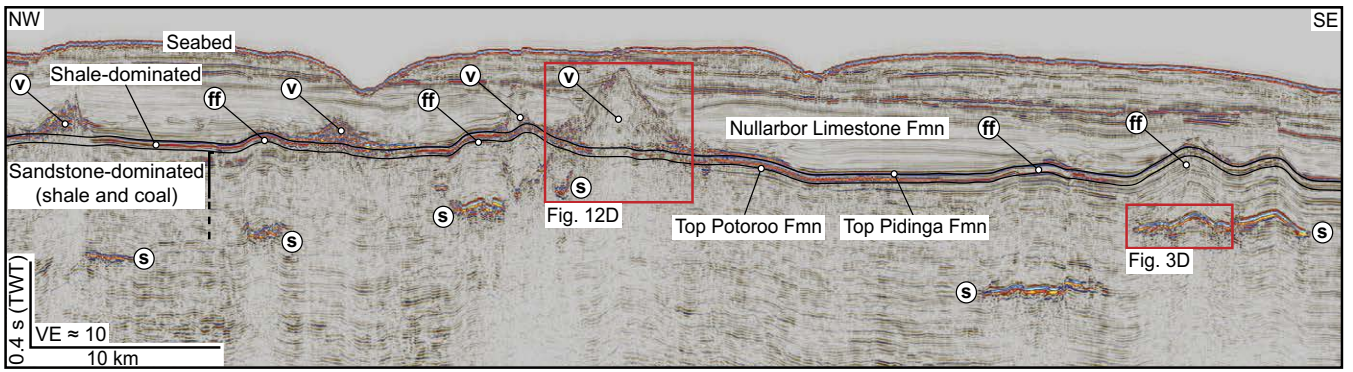

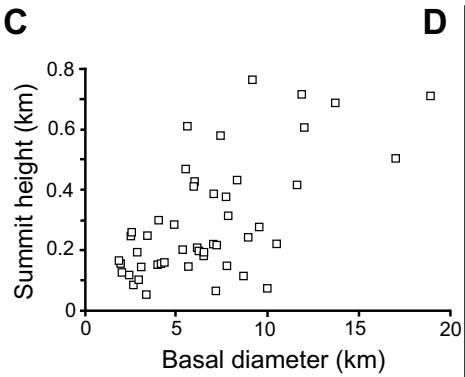

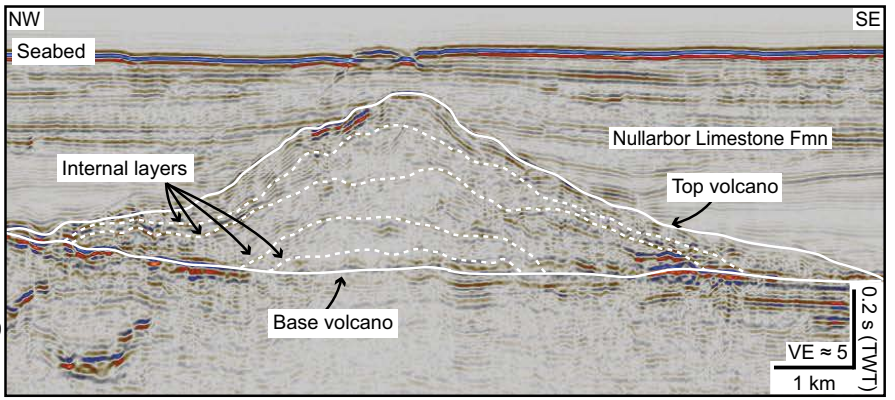

Figure 12. (A) Paleogeographic reconstruction (modified from Espurt et al., 2009) documenting the regional structure immediately prior to the emplacement of a suite of volcanoes mapped in the Ceduna subbasin (inset) (modified from Magee et al., 2013b). (B) Seismic section delimiting high-amplitude reflections (s—sills), forced folds (ff), and volcanoes (v) (modified from Jackson et al., 2013). Fmn—formation; TWT—two-way traveltime; VE—vertical exaggeration. (C) Plot of volcano basal diameter against summit height (Magee et al., 2013b). (D) Internal reflections within a volcano that are inferred to relate to discrete tuff layers and/or lava flows.

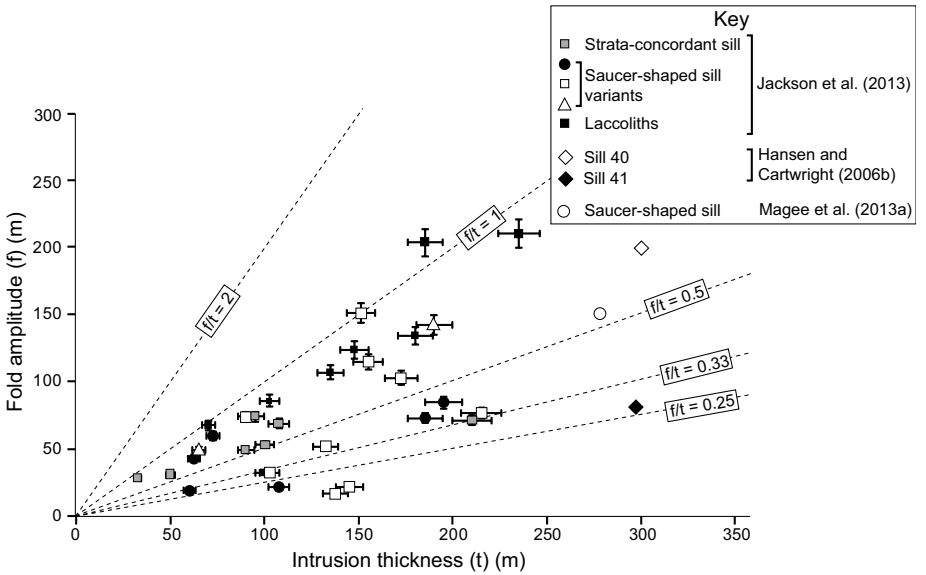

Figure 13. Plot of intrusion thickness (measured where upper and lower intrusive contacts can be distinguished) against the amplitude of overlying forced folds.

This discrepancy between sill thickness and fold amplitude could perhaps be attributed to measurement errors (e.g., incorrect depth conversion) or geologic processes that restrict the maximum fold amplitude (e.g., out-of-plane strain or strain interference between neighboring folds; Jackson et al., 2013). In Jackson et al. (2013) it was suggested that other space-making mechanisms may play a role during emplacement and thus control the intrusion thickness to fold amplitude ratio. This is supported by numerous field- and seismic-based observations (Schofield et al., 2010, 2012a; Jackson et al., 2013; Magee et al., 2013a). For example, sills intruded into coal in the Raton Basin were emplaced via the development of a viscous fluid-fluid contact between the magma and host rock; i.e., space for the magma was generated by plastic deformation and porosity reduction of the coal (e.g., Fig. 6; Schofield et al., 2012a). Space-making mechanisms that do not involve roof uplift may also occur during intrusion into siliciclastic sequences (e.g., sandstone compaction, Morgan et al., 2008; shale fluidization, Schofield et al., 2010). The likely occurrence of multiple processes accommodating intrusion implies that overburden uplift, and therefore the degree of surface deformation, may not directly correlate to the volume or location of magma emplaced (Magee et al., 2013a).

Northwest Australian Shelf

The Paleozoic–Holocene, ~535,000 km^2 North Carnarvon Basin, located offshore northwest Australia (Fig. 2), contains numerous Mesozoic depocenters (e.g., the Exmouth subbasin) that host sill complexes emplaced between the Kimmeridgian and Aptian (Symonds et al., 1998; Magee et al., 2013a, 2013c; McClay et al., 2013; Rohrman, 2013). These emplacement ages, constrained from onlap of strata onto intrusion-induced forced folds and the presence of lava flows emplaced along the top Aptian, indicate that magmatic activity occurred immediately prior to and during continental break-up (Magee et al., 2013a; McClay et al., 2013; Rohrman, 2015). A key observation is that inclined sheets and sill limbs commonly coincide with and likely intruded along fault planes for as much as 1 s two-way traveltime (e.g., ~300 m; Fig. 14A; Magee et al., 2013c; McClay et al., 2013). However, in Magee et al. (2013c) it was noted that only certain sill portions appear to intrude up fault planes, with other sections crosscutting faults (e.g., Fig. 14A). Field observations and mapping of flow indicators in seismic data suggest that the interaction style between magma and faults is primarily controlled by the fault-plane geometry and orientation (Valentine and Krogh, 2006; Bedard et al., 2012; Magee et al., 2013c). In particular, sills may only intrude up faults when they are hosted in the hanging wall and flowing toward or along the strike of the fault plane; i.e., uplift of the overburden reduces the normal stress across the fault, allowing magma to intrude (Fig. 14B; Magee et al., 2013c).

Northern Yilgarn Craton, Western Australia

The Yilgarn craton in Western Australia (Fig. 15A) consists of metavolcanic and metasedimentary rocks, granites, and granitic gneisses that formed principally between ca. 3.05 and ca. 2.62 Ga (Cassidy et al., 2006). The Yilgarn craton is subdivided into a series of terranes, including the Youanmi terrane, which contains substantial greenstone belts separated by granite and granitic

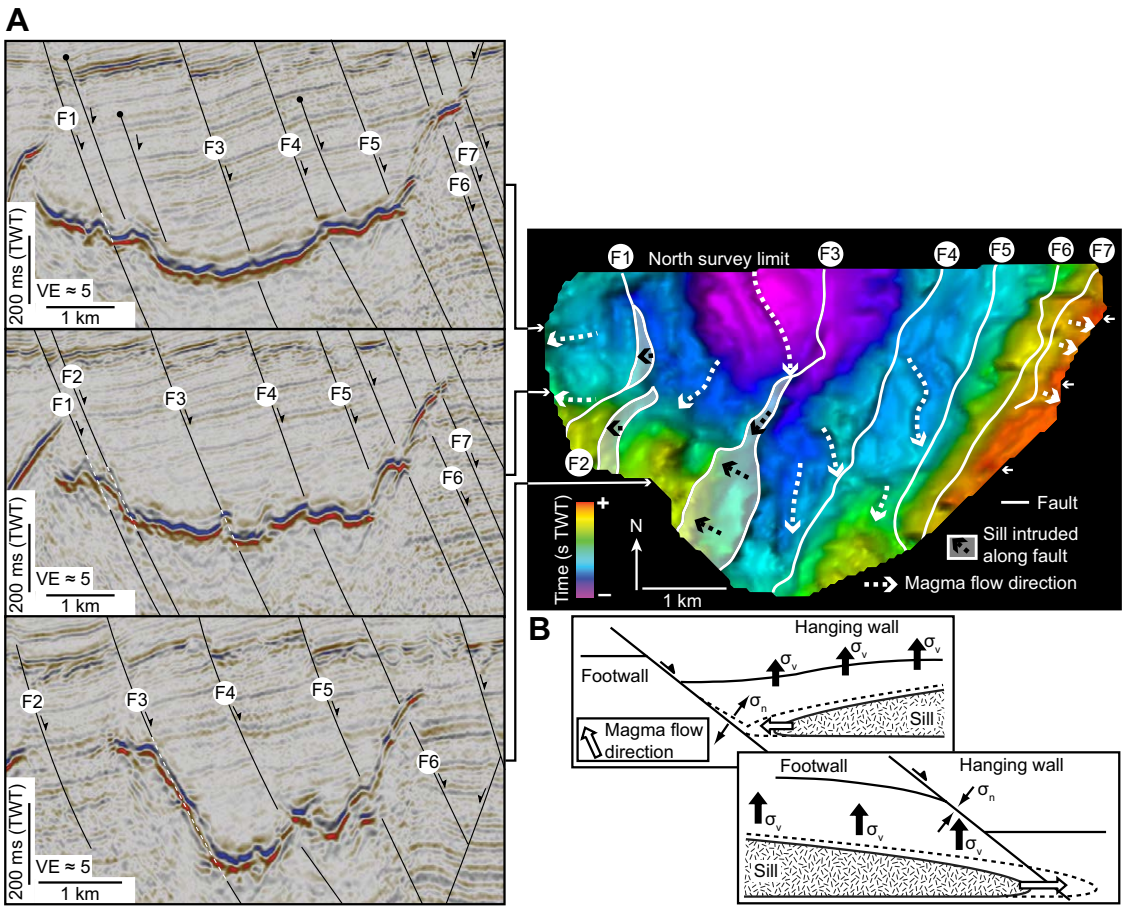

Figure 14. (A) Three seismic sections highlight different magma-fault interaction styles. In places the sill crosscuts the fault, in others it steps up the fault, and occasionally its inclined limb coincides with and likely intruded along the fault plane for ~300 ms two-way traveltime (TWT; VE—vertical exaggeration). The sills are emplaced into Late Jurassic mudstones (Magee et al., 2013c). The sill map shows that the sill extends up faults when its magma flow direction in the hanging wall is parallel to fault strike or toward the fault plane. (B) Schematic diagram demonstrating how uplift related to magma intruding toward a fault in the hanging wall may serve to open the fault (i.e., a decrease in σ_n) and vice versa (i.e., an increase in σ_n). Modified from Magee et al. (2013c).

gneiss (Fig. 15A; Wyche et al., 2013). In 2010, 3 deep seismic reflection profiles totaling 694 km in length were acquired to 20 s two-way traveltime in the northern Youanmi terrane (Fig. 15B; Costelloe and Jones, 2013). The interpretation of these profiles has led to the identification of an interconnected network of highly reflective, generally saucer-shaped sills that extend for several hundreds of kilometers (e.g., Figs. 15C, 15D; Ivanic et al., 2013). The sills mainly occur shallower than 3 s two-way traveltime, and typically dip at <10°–20° (Figs. 15C, 15D). Seismic modeling, assuming representative P-wave velocities and densities for dolerites and granites, indicates that the sills have a minimum thickness of 25 m, and some may be as much as 200 m thick (Ivanic et al., 2013). Some sills appear to have been intruded along shear zones, while others crosscut and truncate reflections associated with preexisting shear zones and listric faults (Figs. 15C, 15D; Ivanic et al., 2013).

The seismic data were acquired in a region transected by numerous Proterozoic mafic dikes and sills associated with the Widgiemooltha (ca. 2410 Ma), Marnda Moorn (ca. 1210 Ma), and Warakurna (ca. 1070 Ma) LIPs (Fig. 15B; Wyche et al., 2013). Dolerite dikes are typically 5–30 m wide, 50–300 km long, and trend mainly east to northeast, while sills recognized at the surface are as much as 50 m thick and 300 km in length (Ivanic et al., 2013). The Widgiemooltha and Marnda Moorn LIPs are generally characterized by dike suites that are not evident in the seismic data due to their steeper dips (Thomson, 2007), and thus the intrusions identified in the Youanmi seismic lines are interpreted to belong to the ca. 1070 Ma Warakurna LIP (Ivanic et al., 2013). The Warakurna LIP consists of mafic igneous rocks that were rapidly emplaced within an area of ~1.5 × 10^6 km^2 in central and Western Australia, and is interpreted to have been generated by a mantle plume (Wingate et al., 2004).

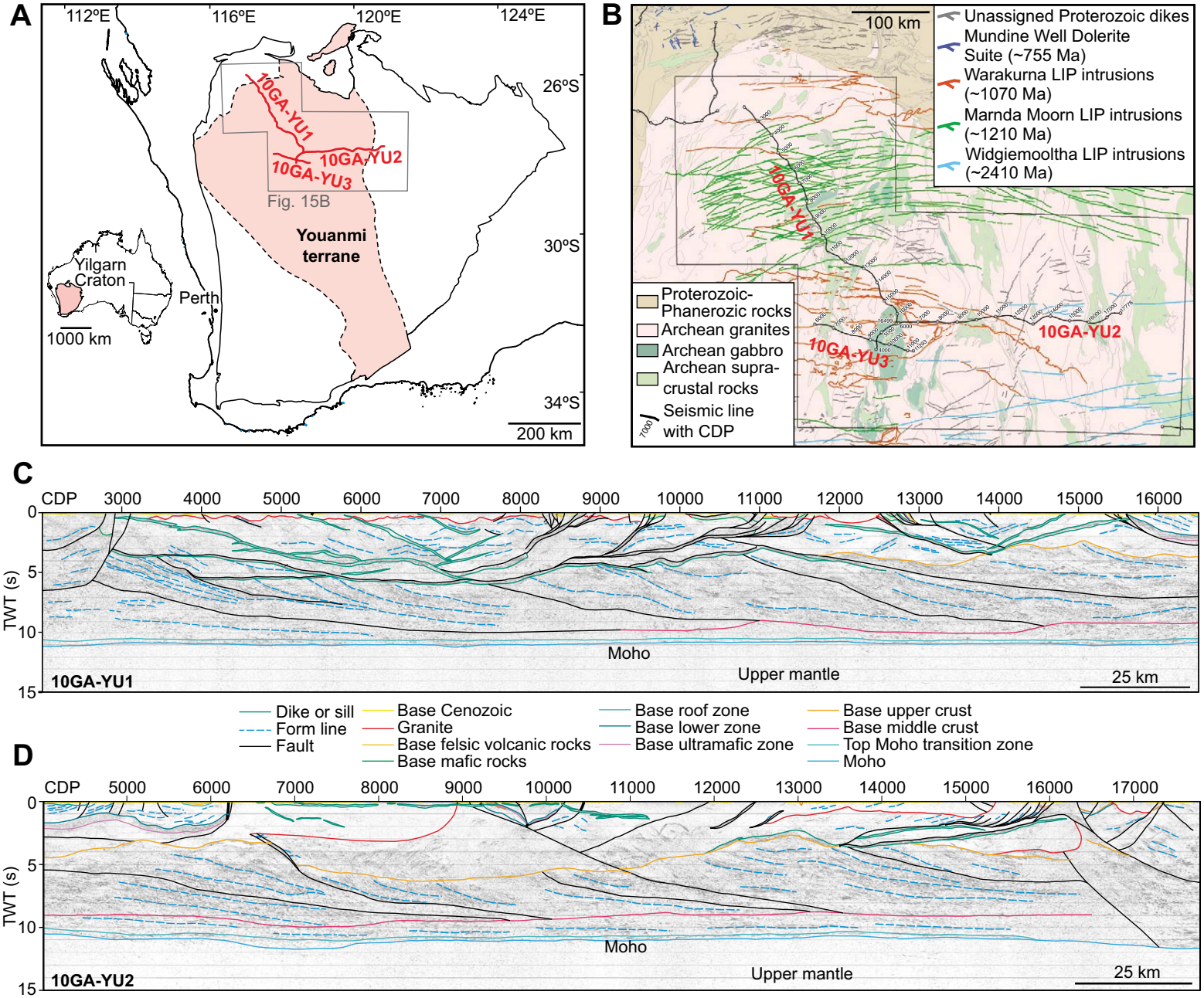

Figure 15. (A) Geology of the Yilgarn craton showing terrane boundaries and locations of Youanmi seismic lines (modified from Wyche et al., 2013). (B) Interpreted geological map of the northern Yilgarn craton showing suites of Proterozoic intrusions in the region of the Youanmi seismic lines (modified from Ivanic et al., 2013). LIP—large igneous province; CDP—common depth point; TWT—two-way traveltime. (C) Interpreted deep seismic reflection profile 10GA-YU1. Note abundant high-amplitude reflection packages interpreted to be saucer-shaped sills in the shallow parts (<5 s two-way traveltime, TWT) of the profile (modified from Ivanic et al., 2013). (D) Interpreted migrated deep seismic reflection profile 10GA-YU2 (modified from Ivanic et al., 2013).

The sill that extends from common depth point (CDP) 6500 to CDP 11000 on seismic profile 10GA-YU2 (Fig. 15D) is thought to be the Mount Homes Gabbro Sill, which crops out near the town of Sandstone and has a crystallization age of 1070 ± 18 Ma based on sensitive high-resolution ion microprobe U-Pb dating of baddeleyite (Wingate et al., 2008). The exposed portion of the Mount Homes Gabbro Sill, which is ascribed to the Warakurna LIP, consists of an ~5-m-thick medium- to coarse-grained gabbro, dips ~5° to the north, and intrudes metamorphosed Archean mafic and ultramafic rocks (Wingate et al., 2008). To the north of line 10GA-YU2, the sill is exposed again and has a thickness of ~30 m and margins containing abundant granitic xenoliths (Ivanic et al., 2013). Aeromagnetic data suggest that the strike length of the sill exceeds 400 km (Wingate et al., 2008). A minimum constraint on the depth of emplacement of these sills is provided by apatite fission track data, which indicate that the northern Yilgarn craton has been exhumed by at least ~3 km since the early Permian (Weber et al., 2005). The interconnected network of saucer-shaped sills interpreted from the Yilgarn craton seismic data share many characteristics with those documented in the other case studies presented herein. It is important that the Yilgarn craton data suggest that interconnected sill complexes facilitating long-distance lateral magma transport can also develop within crystalline continental crust.

DISCUSSION

Seismic reflection data and field observations suggest that upper crustal plumbing systems, particularly those emplaced within sedimentary basins, may be dominated by interconnected sills and inclined sheets (e.g., Figs. 6–15). Two recurring observations of shallow-level plumbing systems are apparent from the case studies presented here: (1) sill complexes can provide efficient magma flow pathways, transporting melt from source to surface over great vertical (tens of kilometers) and lateral distances (more than hundreds of kilometers) (Table 1; e.g., Cartwright and Hansen, 2006; Leat, 2008; Schofield et al., 2015); and (2) host-rock lithology and structure influence the stratigraphic level of emplacement and how an intruded magma volume is accommodated (e.g., Schofield et al., 2012a, 2014; Jackson et al., 2013). However, the influence of shallow-level, laterally extensive mafic sill complexes on volcanism and tectonic processes remains enigmatic. Here we summarize the key controls on sill complex emplacement and discuss their potential implications for future volcanological studies.

Sill Complex Formation

Mechanics of Sill Emplacement

Sill emplacement within sedimentary basins has been attributed to (see Menand, 2011, and references therein) (1) the deflection of dikes into sills at a depth where magma density equals that of the host rock (i.e., the level of neutral buoyancy) and the magma pressure overcomes the strength of the wall rock and lithostatic load (Gilbert, 1877; Francis, 1982); (2) mechanical contrasts in material toughness and Young's modulus across an interface, resulting in an elastic mismatch that promotes deflection of dikes or inclined sheets into sills (Gudmundsson, 2011, 2014; Barnett and Gudmundsson, 2014); (3) the local rotation of the minimum compressive principal stress axis to vertical, favoring sill intrusion (Anderson, 1951; Mudge, 1968; Gretener, 1969; Leaman, 1975; Kavanagh et al., 2006; Valentine and Krogh, 2006; Menand, 2008; Menand et al., 2010; Kavanagh and Pavier, 2014); and (4) the exploitation of compliant horizons via nonbrittle mechanisms (Pollard et al., 1975; Einsele et al., 1980; Schofield et al., 2010, 2012a). The broad depth range across which individual sill complexes extend (e.g., Figs. 6–15) suggests that the level of neutral buoyancy exerts little influence on sill emplacement (e.g., Johnson and Pollard, 1973; Cartwright and Hansen, 2006; Menand, 2011; Taisne et al., 2011; Gudmundsson, 2012). We therefore discuss the processes controlling sill emplacement along rock-rock interfaces (e.g., bedding planes) or compliant horizons and examine how space is generated for the intruded magma volume.

One important control on sill emplacement is elastic mismatch (e.g., Gudmundsson, 2011; Barnett and Gudmundsson, 2014). When a propagating vertical or inclined extension fracture approaches a subhorizontal interface between two layers, across which there is a significant difference in material toughness and Young's modulus, its continued propagation direction is dependent on (Fig. 16A; e.g., Gudmundsson, 2011; Barnett and Gudmundsson, 2014): (1) the ratio of the energy release rate required to penetrate the interface (G_p) or deflect along it (G_d), which is a function of the material toughness of the interface, the overlying layer, and the stress intensity factor for mode I and mode II cracks; relative to (2) Dundurs elastic mismatch parameter, which characterizes the difference in the Young's modulus between the two layers. Experimental investigations corroborate that elastic mismatch will typically favor deflection of a dike or an inclined sheet into a sill if the overlying layer is stiffer than the underlying layer (Fig. 16A; Kavanagh et al., 2006; Gudmundsson, 2011; Barnett and Gudmundsson, 2014). This effect is further enhanced when magma pressure exceeds the fracture toughness of the interface (Kavanagh and Pavier, 2014), or magma flux and temperature conditions, which control solidification, favor sill emplacement (Chanceaux and Menand, 2014). Heterogeneities in the strength, Young's modulus, and pore fluid pressure between rock units within layered strata can also instigate the rotation of the minimum compressive principal stress axis to vertical orientations, promoting the deflection of ascending dikes into strata-concordant sills (Anderson, 1951; Gretener, 1969; Kavanagh et al., 2006; Valentine and Krogh, 2006; Gressier et al., 2010; Gudmundsson, 2011; Barnett and Gudmundsson, 2014; Kavanagh and Pavier, 2014).

Magma emplacement facilitated by brittle failure of rock-rock interfaces or stiff rocks is commonly accommodated by (1) compaction of the overburden and/or underlying sedimentary strata (e.g., Morgan et al., 2008); (2) floor subsidence (e.g., Cruden and McCaffrey, 2001); and/or (3) overburden uplift when the magma pressure within a sill exceeds the lithostatic load (e.g., Pollard and Johnson, 1973; Koch et al., 1981; Jackson and Pollard, 1990; Bunger and Cruden,

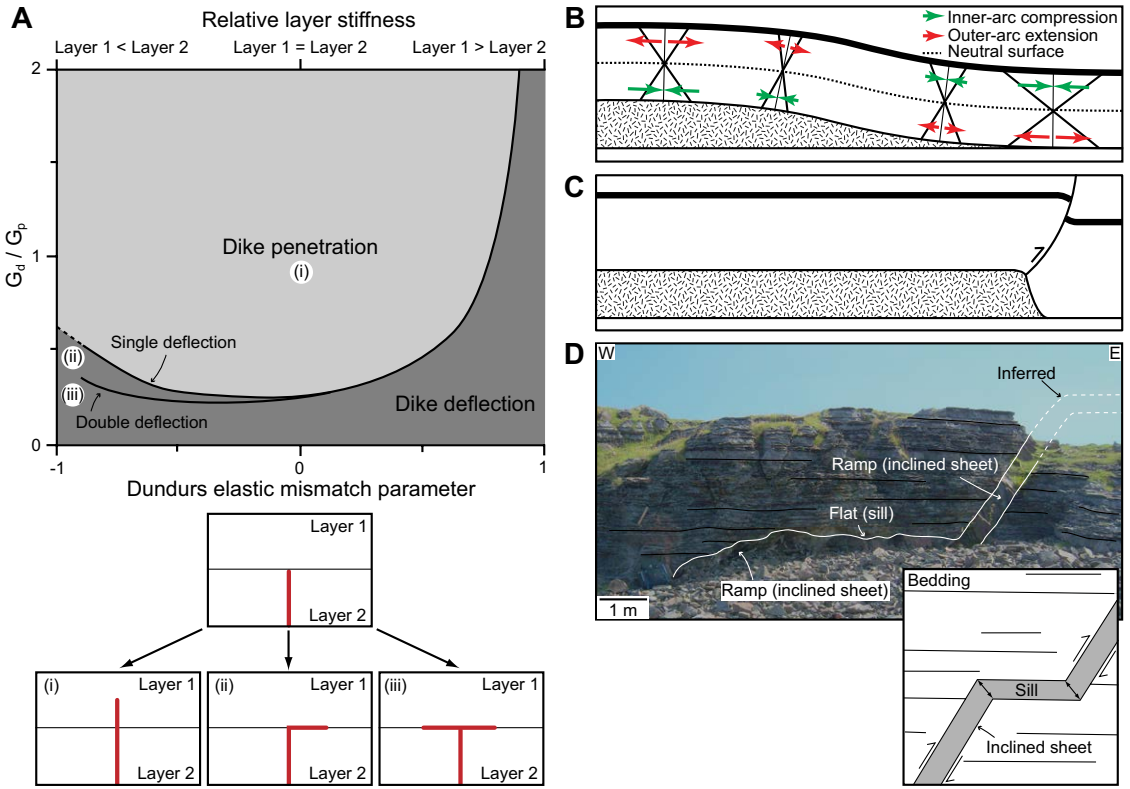

Figure 16. (A) A plot depicting how the relation between Dundurs elastic mismatch parameter, a quantitative measure of the difference in Young's modulus between two layers, and the ratio of the energy release rate (i.e., G_d/G_p) affects the geometry of a propagating dike upon reaching a contact between two layers (modified from Gudmundsson, 2011; Barnett and Gudmundsson, 2014). The parameters G_d and G_p correspond to the energy release rate required for a vertically propagating fracture in Layer 2 to either penetrate Layer 1 (i) or deflect along the Layer 1 and 2 interface (ii and iii), respectively (Gudmundsson, 2011). (B) Extensional and compressional strains generated during forced folding above intrusions with dome-shaped upper contacts (modified from Cosgrove and Hillier, 1999). (C) Formation of flat-topped forced folds and intrusions through concentrated strain along the intrusion periphery, which may result in reverse faulting. (D) Example of a transgressive sheet intrusion on Ardnamurchan, northwest Scotland, which consists of sill and inclined sheet segments and overall exhibits a ramp-flat morphology (see Magee et al., 2012a). A schematic diagram is inset that highlights the opening vectors (black double-headed arrows) of the intrusion (modified from Muirhead et al., 2014).

2011; Agirrezabala, 2015). Of these three space-making mechanisms, only evidence of roof uplift (i.e., forced folds above intrusions) is observed in seismic reflection data (e.g., Figs. 3B, 3D, 8A, 8B, and 12B; e.g., Hansen and Cartwright, 2006b; Jackson et al., 2013; Magee et al., 2013a; Sun et al., 2014); poor seismic imaging immediately beneath intrusions compromises our ability to discern floor subsidence. The geometry of these intrusion-induced forced folds, which broadly mirrors the morphology of the associated upper sill or laccolith contact (e.g., Figs. 3B, 3D, 8A, 8B, and 12B), can provide further information on brittle emplacement conditions and mechanisms (Pollard and Johnson, 1973; Koch et al., 1981; Jackson and Pollard, 1988, 1990; Galland, 2012; Galland and Scheibert, 2013; van Wyk de Vries et al., 2014; Agirrezabala, 2015). For example, dome-shaped forced folds developed above sills or laccoliths that taper toward their lateral tips (e.g., Figs. 3D, 12B, and 16B) require a homogeneous pressure distribution within the intrusion and layer-parallel slip to occur along the fold limbs (Pollard and Johnson, 1973; Koch et al., 1981; Jackson and Pollard, 1990; Galland and Scheibert, 2013). Outer arc extensional strains generated within the host rock during this type of forced folding may promote tensile failure and/or normal faulting at the crest or periphery of the fold (Fig. 16B; e.g., Magee et al., 2013a). In contrast to the formation of dome-shaped folds, numerical modeling suggests that flat-topped, steep-sided intrusions and associated forced folds (Fig. 16C) may form over time as a consequence of fluid mechanics (e.g., the weight of the magma) and/or a heterogeneous magma pressure distribution (Bunger and Cruden, 2011; Galland and Scheibert, 2013). The formation of flat-topped forced folds, which may also be promoted by intrusion beneath a sequence of rigid strata that resist folding and layer-parallel slip, is likely to concentrate shear stresses near the intrusion tips and possibly result in the nucleation of reverse faults that may be subsequently intruded (Fig. 16C; Thomson and Schofield, 2008; Bunger and Cruden, 2011; van Wyk de Vries et al., 2014). Because sill complexes comprise multiple intrusions that may overlap laterally, the growth of individual forced folds may be inhibited or modified due to the impingement of neighboring folds; this could result in fold coalescence and the formation of compound folds (Fig. 8C; Magee et al., 2014).

While the emplacement and accommodation of sheet intrusions is traditionally regarded as being controlled by linear elastic fracture mechanics (e.g., Pollard, 1973; Rubin, 1995; Malthe-Sørenssen et al., 2004; Kavanagh et al., 2006; Menand et al., 2010; Bunger and Cruden, 2011), field observations suggest that sills may intrude into shale, coal, or poorly consolidated beds via nonbrittle processes (e.g., Schofield et al., 2012a; Muirhead et al. 2016). For example, magmatic heating can cause coal or certain salts (e.g., carnallite) to behave as a viscous fluid during intrusion, inhibiting the propagation of brittle fractures and instead promoting the formation of magma finger instabilities along the fluidal magma–host rock contact (e.g., Figs. 2B and 6; McClintock and White, 2002; Schofield et al., 2012a, 2014). Similar pseudoviscous fluid-fluid interfaces may be generated by the intrusion of magma into wet, poorly consolidated host rocks at emplacement depths typically ≲500 m (Einsele et al., 1980; Miles and Cartwright, 2010; Airoldi et al., 2011; Schofield et al., 2012a). The fluidization of intact rocks by the expansion and volatization of pore fluids or vapor decreases the cohesion between grains, and can also promote the development of viscous fluid-fluid contacts between the magma and the host rock (Schofield et al., 2010, 2012a; Magee et al., 2014). Fluidization may be triggered by magmatic heating and/or depressurization during rapid, intrusion-induced failure of the host rock (Schofield et al., 2010, 2012a). These nonbrittle mechanisms of host-rock deformation can accommodate some, if not all, of the related magma volume through porosity reduction and plastic deformation (e.g., Fig. 6A). The occurrence of multiple brittle and/or nonbrittle space-making processes during emplacement may explain why forced fold amplitudes measured in seismic data are commonly less than the intrusion thickness (Fig. 13).

Inclined Sheet Formation

Seismic data reveal that strata-concordant sills may transition laterally into transgressive inclined sheets, potentially forming saucer-shaped sills if the inclined sheets encompass the intrusion (Figs. 8–12 and 14; Thomson and Hutton, 2004). These inclined sheets transfer magma from deeper sills to shallower stratigraphic levels and are thus integral to facilitating magma ascent in sedimentary basins (Thomson and Hutton, 2004; Cartwright and Hansen, 2006; Holford et al., 2012; Muirhead et al., 2012; Magee et al., 2013c, 2014). Within the volcanological literature, studies of inclined sheet emplacement have primarily focused on the formation of cone sheets, i.e., swarms of concentric, inwardly inclined sheet intrusions that dip toward and are inferred to emanate from a central magma chamber (e.g., Anderson, 1937; Gautneb et al., 1989; Schirnick et al., 1999; Klausen, 2004; Geshi, 2005; Bistacchi et al., 2012; Burchardt et al., 2013). Field observations reveal that the majority of these cone sheets occur in extension fractures and thereby intruded when σ_1 was radially inclined inward, parallel to the inclined sheet plane, while σ_3 was orthogonal to the intrusion plane (e.g., Anderson, 1937; Gautneb et al., 1989; Gudmundsson, 2002, 2006; Klausen, 2004; Geshi, 2005; Siler and Karson, 2009; Magee et al., 2012a; Muirhead et al., 2012). Stress fields favoring classical cone sheet formation (e.g., Anderson, 1937) have been reproduced numerically during inflation of circular or oblate-shaped magma chambers (e.g., Gudmundsson, 2002, 2006; Bistacchi et al., 2012). Similarly, within sill complexes, numerical modeling has demonstrated that toward the lateral tips of a sill, during intrusion and/or inflation, σ_1 is radially inclined inward and can thereby promote the transgression of an inclined sheet (e.g., Gudmundsson, 2002, 2006; Malthe-Sørenssen et al., 2004; Gudmundsson and Løtveit, 2012; Barnett and Gudmundsson, 2014). It may therefore be expected that inclined sheets within sill complexes commonly occur within extension fractures.

However, field kinematic studies indicate that some cone sheets (e.g., the Tejeda Complex, Canary Islands, Schirnick et al., 1999; Ardnamurchan, Scotland, Magee et al., 2012a) and sill-fed inclined sheet swarms (e.g., the Ferrar sill complex, Antarctica, Muirhead et al., 2012, 2014) emplaced as mixed-mode fractures. Although the initial stages of these inclined sheets were probably characterized by mode-I fracture propagation (i.e., Gudmundsson, 2002), field observations reveal that these intrusions transgress via a series of small interconnected sill and inclined sheet segments (i.e., they have a ramp-flat morphology; Fig. 16D; Airoldi et al., 2011; Magee et al., 2012a; Muirhead et al., 2012). The intrusions thus exhibit two different components of opening, dilation normal to the inclined sheet plane and subvertical opening of the sill segments (Airoldi et al., 2011; Magee et al., 2012a; Muirhead et al., 2012). The combination of these modes of opening results in intrusion propagation and growth under mixed-mode I-II fracturing, and produces a component of reverse shear along the intrusion plane (Fig. 16D; Muirhead et al., 2012, 2014; Mathieu et al., 2015). Because entire sill complexes, which consist of interconnected sills and inclined sheets, are comparable to the smaller scale ramp-flat sheets described here (cf. Figs. 7C, 11B, and 16D), it may be expected that mixed-mode fracturing is prevalent in sill complex emplacement.

There are several other mechanisms that may aid or promote the development of inclined sheets: (1) the generation of tensile strains and fractures at the tips of sills in response to overburden bending (Figs. 8C and 16B; Jackson and Pollard, 1990; Malthe-Sørenssen et al., 2004; Goulty and Schofield, 2008; Thomson and Schofield, 2008; Muirhead et al., 2012; Galland and Scheibert, 2013; Magee et al., 2013a, 2014); (2) the emplacement of magma along reverse faults that nucleated during the growth of flat-topped forced folds (Fig. 16C; Thomson and Schofield, 2008; Bunger and Cruden, 2011); (3) intrusion along preexisting faults (e.g., Fig. 14A; Bedard et al., 2012; Magee et al., 2013c; McClay et al., 2013); (4) the intrusion of magma along inclined unconformity surfaces (C. McLean, personal observations); or (5) the upward deflection, along a curved trajectory, of a propagating fracture beyond the lateral tip of a sill in response to the asymmetrical emplacement of magma above the initial level of the extension fracture (Hansen, 2015). In summary, magma ascent along inclined sheets in sill complexes is likely facilitated by multiple processes, and therefore resolving the key controls on transgression is challenging.

Role of Dikes

An important consideration when examining sill complex emplacement concerns the role of dikes in facilitating magma transport between individual sills, inclined sheets, and the surface. It is, however, difficult to assess the role of dikes within sill complexes using seismic data because the technique is biased toward imaging subhorizontal to moderately inclined sheet intrusions (Smallwood and Maresh, 2002; Thomson, 2007). Field observations indicate that dikes are volumetrically minor components of sill complexes (Fig. 7; e.g., the Karoo-Ferrar LIP; Leat, 2008; Hastie et al., 2014; Muirhead et al., 2014). Recent analogue experiments conducted by Kavanagh et al. (2015) may provide an alternative explanation for the apparent lack of dikes in sill complexes. The analogue models showed that magma pressure within underlying feeder dikes decreased upon the inception and propagation of a sill, promoting dike contraction (Kavanagh et al., 2015). Although there is currently little field evidence to support feeder dike contraction during sill emplacement, it may be considered that the complete or partial closure of dikes could serve to reduce their apparent volumetric importance in sill complexes. The role of dikes in sedimentary basins may therefore be underestimated. However, it is important to note that the majority of sills within a sill complex likely have thicknesses below the limit of detectability in seismic data, implying that the volume of sills may be underestimated (Button and Cawthorn, 2015; Schofield et al., 2015).

Influence of Magma Rheology and the Growth of Sill Complexes

Field and borehole data indicate that laterally extensive sill complexes commonly have mafic compositions (e.g., Chevallier and Woodford, 1999; Smallwood and Maresh, 2002; Leat, 2008; Wingate et al., 2008; Schofield et al., 2015). In contrast, field observations reveal that the incremental injection of more viscous magmas with evolved, intermediate to felsic compositions and emplaced at shallow levels will tend to form laccoliths instead of sills (e.g., Johnson and Pollard, 1973; John and Blundy, 1993; Cruden and Launeau, 1994; Stevenson et al., 2007; Michel et al., 2008; Bunger and Cruden, 2011). Experimental and numerical modeling, coupled with field observations, indicate that the emplacement of mafic sills and felsic laccoliths are both initially characterized by the intrusion and lateral propagation of a thin sill (e.g., Johnson and Pollard, 1973; Cruden and McCaffrey, 2001; Leuthold et al., 2012; Kavanagh et al., 2006, 2015; Currier and Marsh, 2015). While these thin, mafic and intermediate to felsic sills will both subsequently undergo a phase of inflation, their final growth stage varies (e.g., Johnson and Pollard, 1973; Kavanagh et al., 2006, 2015; Currier and Marsh, 2015). For example, observations presented here indicate that mafic sills commonly transition into inclined sheets at their lateral tips (e.g., Malthe-Sørenssen et al., 2004; Thomson and Hutton, 2004; Polteau et al., 2008b; Magee et al., 2013c; Hansen, 2015). In contrast, laccoliths form through sill thickening in response to continued magma injection and overburden bending (Johnson and Pollard, 1973; Cruden and McCaffrey, 2001; Menand, 2011), suggesting that inclined sheet intrusion at the lateral sill tips is largely inhibited (Pollard and Johnson, 1973). Given that the host rock–magma interactions facilitating mafic sill transgression (e.g., stress rotation) occur at the lateral tips of intermediate to felsic sills (e.g., Pollard and Johnson, 1973; Gudmundsson, 2012), it is likely that magma rheology is an important control on whether a sill complex or laccolith develops (Johnson and Pollard, 1973; McLeod and Tait, 1999; Currier and Marsh, 2015); i.e., it appears easier for mafic magma, which typically has a higher temperature and lower viscosity than intermediate to felsic magma, to form inclined sheets at sill tips. Because the rheology of a magma is a function of its chemistry, dissolved and exsolved volatile content, crystal content, ascent/emplacement rate, and temperature (Pistone et al., 2012, 2013), the incremental development of a sill complex or laccolith through the injection of distinct magma pulses will therefore be influenced by the magma input rate and its solidification dynamics (Johnson and Pollard, 1973; Glazner et al., 2004; Currier and Marsh, 2015). While numerous studies have examined how magma rheology may affect the growth of an individual intrusion (e.g., Johnson and Pollard, 1973; Taisne and Tait, 2011; Currier and Marsh, 2015), our understanding of the influence of magma rheology on the development of entire shallow-level plumbing systems is limited and represents an important aspect that requires further research.

Lateral Magma Flow

Field- and seismic-based observations suggest that plumbing systems within sedimentary basins are typically dominated by interconnected sill complexes that transgress as much as 12 km of strata and extend across lateral distances of as much as 4100 km (e.g., Figs. 6–12, 14, and 15; Table 1; e.g., Aspler et al., 2002; Cartwright and Hansen, 2006; Leat, 2008; Svensen et al., 2012; Jackson et al., 2013; Magee et al., 2014; Muirhead et al., 2014; Neres et al., 2014; Schofield et al., 2015). While the source of numerous sill complexes remains poorly constrained, commonly due a paucity of seismic and/or borehole data in relevant areas, several studies have proposed that sill complexes may (1) originate from underlying melt zones (high-velocity bodies in seismic data) via dikes, fault-hosted intrusions, or transgressive sills (e.g., Figs. 10A, 10B, and 11C; e.g., Cartwright and Hansen, 2006; Galerne et al., 2011; Rohrman, 2013; Schofield et al., 2015); (2) be fed by laterally propagating dike swarms that emanate from volcanic centers or mantle plume heads (e.g., Hyndman and Alt, 1987; Ernst et al., 1995); (3) propagate directly away from volcanic centers (Magee et al., 2014; Neres et al., 2014); or (4) be sourced directly from a plume head, with lateral movement promoted by emplacement into an area of topographic uplift above the plume head and the generation of a hydraulic gradient sufficient enough to allow sills (<10 m thick) to flow laterally for thousands of kilometers without freezing (Fialko and Rubin, 1999; Aspler et al., 2002; Leat, 2008).

The distribution of sill complexes is also influenced by the structure and stratigraphy of the basin (Schofield et al., 2012a; Magee et al., 2013c). In particular, the presence of fault arrays in sedimentary basins can limit the areal extent of sill complexes by (1) providing suitable magma ascent pathways to the

Earth's surface or shallower stratigraphic levels where cooler host rocks facilitate solidification (e.g., Fig. 14A) or (2) deflecting sill propagation, particularly if footwall basement rocks are juxtaposed against hanging-wall sedimentary strata (e.g., Fig. 9C). Sill complexes emplaced within relatively unstructured basins (e.g., the Karoo Basin), however, cover areas that are orders of magnitude larger than those intruded into faulted basins; e.g., the Karoo sill complex covers ~3 × 10^6 km^2 (Fig. 7A), whereas sill complexes across the Møre and Vøring Basins only cover ~8 × 10^4 km^2 (Fig. 11A; cf. Planke et al., 2005; Leat, 2008; Svensen et al., 2012; Magee et al., 2014; Schofield et al., 2015).

Duration of Sill Complex Emplacement

Sill complexes represent tortuous magma ascent pathways compared to swarms of dikes. It may therefore be expected that magma migration, from melt source to the Earth's surface, will take longer if facilitated by sill, as opposed to dike, emplacement. The duration of sill complex development may thus prolong magma residence times, affecting geochemical and petrological processes. For sill complexes where absolute age data are available or relative dating techniques can be employed, studies suggest that magma injection occurs rapidly over a few million years (Skogseid et al., 1992; Archer et al., 2005; Planke et al., 2005; Cartwright and Hansen, 2006; Hansen and Cartwright, 2006b; Hansen, 2006; Svensen et al., 2012; Schofield and Jolley, 2013). For example, radiometric dating suggests that sills within the Karoo magmatic province were emplaced over 0.47 m.y. at a rate of 0.78 km^3/yr (Svensen et al., 2012). However, in Magee et al. (2014), multiple onlap relationships in forced folded successions above a sill complex in the Rockall Basin were shown, suggesting that fold growth, and thereby sill emplacement, occurred incrementally over ~15 m.y. through the periodic injection of small magma batches (Figs. 8A, 8B). Evidence for the prolonged development of a sill complex in the Rockall Basin therefore implies that seismic-stratigraphic or radiometric dates obtained from only one or several intrusions in a sill complex, which most previous studies relied upon, cannot reliably be applied to the entire magmatic network (Magee et al., 2014; Evenchick et al., 2015).

Numerous studies have documented that individual sills and laccoliths, as well as entire intrusion networks, may develop through the emplacement of distinct magma pulses, the duration between which is highly variable (e.g., Coleman et al., 2004; Glazner et al., 2004; Michel et al., 2008; Miller et al., 2011; Magee et al., 2014; Annen et al., 2015; Broderick et al., 2015; Currier and Marsh, 2015). If some sill complexes are emplaced incrementally but over time frames in which magma solidification should theoretically occur, how then does magma rheology vary and how do magma migration pathways remain operational within these systems? Consider a scenario whereby new distinct magma pulses may intrude along the contact, which likely represents a strong mechanical discontinuity, between fully or partially solidified intrusions and the host rock (i.e., underaccretion or overaccretion; Fig. 17A; see Annen et al., 2015, and references therein). This stacking and amalgamation of sills through repeated magma injection along sill–host rock contacts can influence its thermal and chemical evolution (see Annen et al., 2015, and references therein). If the duration between distinct pulses is too long, allowing the preexisting intrusion to cool and potentially solidify, any new batch of magma is effectively intruded into a relatively low-temperature environment (Annen, 2011). The accretion of new magma above or below a preexisting sill or stack of sills within a relatively low-temperature environment will therefore simply serve to thicken the igneous body, potentially forming laccoliths, without significant lateral propagation (e.g., John and Blundy, 1993; Menand, 2008; Annen, 2011; Broderick et al., 2015). This thickening and stacking of sills (i.e., little or no lateral growth) may be aided by the contraction of preexisting intrusion components during solidification, generating space for new, distinct magma batches (John and Blundy, 1993). If, however, the duration between the injection of distinct magma pulses is short and/or there is sufficient latent heat of crystallization, the maintenance of locally elevated temperatures may allow later magma pulses to remain hotter for longer, facilitating intrusion further up into the stratigraphic sequence (Fig. 17A; e.g., Glazner et al., 2004; Annen, 2011; Annen et al., 2015). The accretion of sills would result in an increase in the apparent total thickness of intruded material (Fig. 17A), possibly producing discernable top and basal seismic reflections. However, the vast majority of sills imaged in seismic data are expressed as tuned reflection packages and it is thus difficult to determine if mapped reflectors correspond to one or multiple intrusions (e.g., Figs. 6–12 and 14).

An alternative explanation concerns the development and prolonged longevity of discrete magma flow pathways within individual intrusions (Fig. 17B). Numerous studies have shown that sills commonly form through the coalescence of magma segments or fingers and, on a larger scale, magma lobes (e.g., Figs. 4 and 5; e.g., Pollard et al., 1975; Thomson and Hutton, 2004; Schofield et al., 2010, 2012a, 2012b). The channelization of magma into one or several of these zones can increase the segment thickness, allowing magma flow to be sustained while neighboring portions of the intrusion crystallize (Fig. 17B; Holness and Humphreys, 2003). If these channelized segments remain partially molten, through the continued injection of small magma batches and/or insulation by adjacent lobes, subsequent magma pulses may preferentially reactivate the channels (Fig. 17B; Currier and Marsh, 2015). Flow of magma through thin channels, which then bud off to form larger sills, is supported by mapped magma flow patterns that suggest that sills are intruded from a point-like source (e.g., Fig. 5; Thomson and Hutton, 2004; Magee et al., 2013c, 2014; Schofield et al., 2015).

Implications for Volcano Monitoring

Understanding volcano histories and tracking real-time magma movement within the subsurface is crucial to the appraisal and mitigation of volcanic hazards (Sparks, 2003; Sparks et al., 2012; Cashman and Sparks, 2013). Traditionally, volcano data (e.g., geochemistry, petrology, geophysics) are generally interpreted within the framework of a vertically stacked magma plumbing system where the eruption site overlies the melt source (e.g., Fig. 1A; Cashman

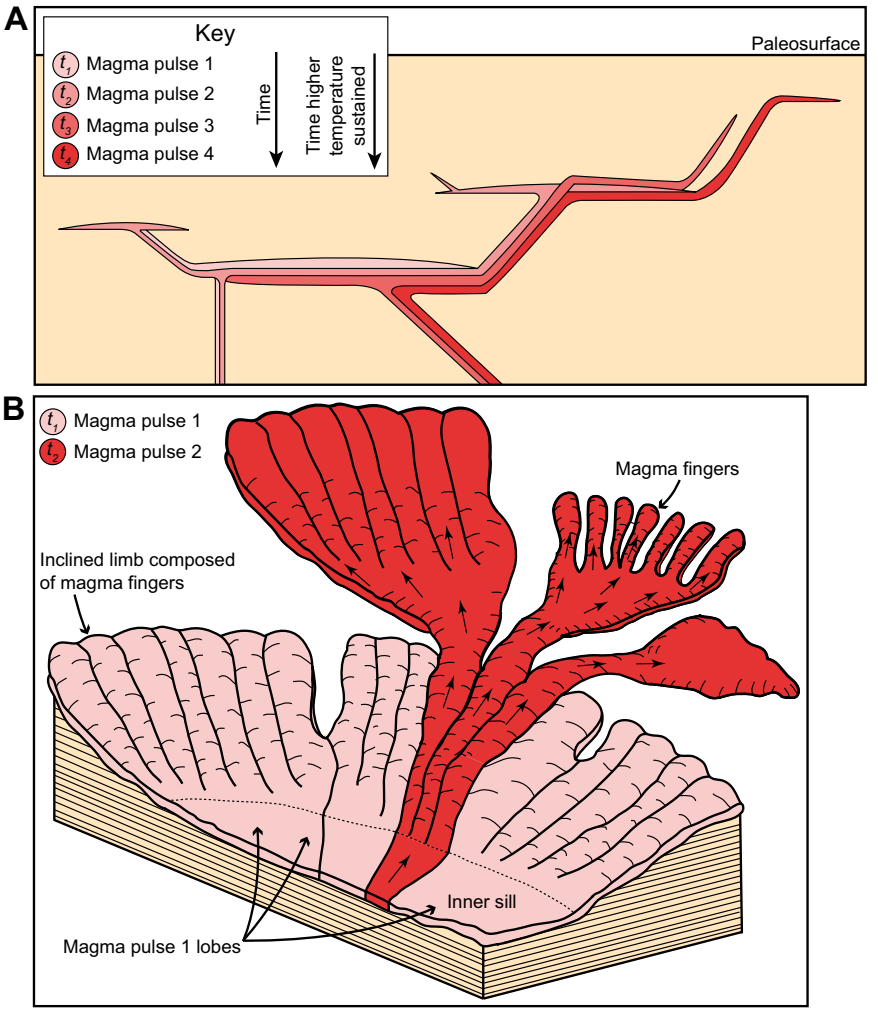

Figure 17. (A) Schematic diagram demonstrating how the emplacement of one magma pulse may facilitate the intrusion of later pulses further up into the sedimentary sequence if accretion allows sills to remain hotter for longer (Annen et al., 2015). (B) Sketch depicting how discrete magma segments and/or lobes may preferentially remain open as magma channels (magma pulse 2), feeding stratigraphically higher intrusions, when adjacent portions of the sill have crystallized (magma pulse 1).

and Sparks, 2013; Tibaldi, 2015). However, this review documents that sill complexes, consisting of interconnected sills and inclined sheets, can cover broad areas and feed volumetrically important eruptions (e.g., Fig. 1B; e.g., Planke et al., 2005; Leat, 2008; Svensen et al., 2012; Magee et al., 2014; Muirhead et al., 2014; Schofield et al., 2015). Furthermore, observations from offshore Norway and onshore Australia suggest that sill complexes may develop in crystalline continental crust (Figs. 11C and 15; Cartwright and Hansen, 2006). These observations of lateral magma flow within sill complexes, which extend as much as 4100 km from the melt source and intrude a variety of host rocks, imply that melt processes cannot be mapped from the distribution of eruption sites. The possibility that some volcanoes and volcano fields, regardless of the tectonic setting, are the product of a laterally extensive and interconnected magma plumbing system therefore needs to be incorporated into volcanological studies.

To emphasize how the consideration of a laterally arranged magma plumbing system is integral to volcanic hazard assessment, we briefly discuss how sill complex development may affect ground deformation patterns. The analysis of ground deformation patterns, recorded using InSAR and tilt meters, is commonly applied to tracking the migration and volume of magma in volcanic systems (e.g., Sparks, 2003; Wright et al., 2006; Biggs et al., 2009, 2011; Sparks

et al., 2012). Seismic-based studies highlight that eruption sites may be offset from shallow-level magma reservoirs and that magma migration through a sill complex follows a convoluted route (e.g., Fig. 12; e.g., Jackson, 2012; Magee et al., 2013b). Uplift and subsidence patterns expressed at the Earth's surface and associated with magma movement within a sill complex may therefore occur away from volcanoes. For example, geodetic and seismicity studies indicate that the magma reservoir for recent eruptions at Asama Volcano (Japan) was located 8 km to the west of the summit (Aoki et al., 2013). Perhaps the most important implication to studies of ground deformation, however, is that magma intrusion is not necessarily accommodated by roof uplift (e.g., Fig. 13; Schofield et al., 2012a; Magee et al., 2013a). Instead, multiple space-making processes can accommodate magma emplacement, some of which may produce no discernible ground deformation (e.g., porosity reduction). We suggest that ground deformation inversions are therefore likely to underestimate magma volumes (Galland, 2012). In extreme circumstances where magma emplacement occurs via nonbrittle fluidization of the host rock and no overburden deformation occurs (e.g., Fig. 6A; Schofield et al., 2012a, 2014), the intruded magma volume would be hidden from ground deformation, and potentially seismicity, monitoring techniques.

Implications for Continental Break-Up

Continental rifting and break-up are commonly associated with the formation of sedimentary basins and the generation of large, mafic melt volumes. Ethiopia is an ideal natural laboratory to study magmatic plumbing system structure during continental break-up because ongoing earthquakes and volcanic eruptions associated with the East African Rift system mean that the interaction between tectonic and magmatic processes can be observed and constrained (e.g., Ebinger and Casey, 2001; Keir et al., 2006; Wright et al., 2006; Corti, 2009; Ebinger et al., 2010). Based on a variety of disciplines, a consensus has emerged that Quaternary magmatism in Ethiopia is almost entirely dominated by diking, which accommodates extension (e.g., Ebinger and Casey, 2001; Keir et al., 2006; Wright et al., 2006, 2012; Corti, 2009; Ebinger et al., 2010). The importance of dike intrusion in Ethiopia is supported by (1) recording of 14 individual dike intrusions during the 2005–2010 Dabbahu-Manda-Harraro rifting event (Ebinger et al., 2010; Wright et al., 2012); (2) measurements of seismic anisotropy from the Main Ethiopia Rift that suggest the presence of aligned melt bodies, interpreted as swarms of dikes (Keir et al., 2005; Kendall et al., 2005; Bastow et al., 2010); and (3) volcanic cones in the Main Ethiopia Rift that are aligned along underlying dikes (Korme et al., 1997; Keir et al., 2015; Muirhead et al., 2015) and exhibit geochemical variations consistent with variable and heterogeneous mantle sources (e.g., Rooney et al., 2011, 2012). Farther north of the Main Ethiopian Rift, however, where the Red Sea Rift descends toward and below sea level in the Danakil Depression (i.e., a sedimentary basin), the style of volcanism changes; i.e., Quaternary–Holocene volumes of fissure basalt flows are significantly greater than to the south (e.g., Barberi and Varet, 1970). On the strength of this evidence, and the observation of abrupt crustal thinning into the Danakil Depression, Bastow and Keir (2011) proposed that the final stages of continent-ocean transition in Ethiopia are being characterized not by a shift to magma intrusion-dominated extension, but by a late stage of plate stretching and sedimentary basin formation. For dikes to reach the surface in the Danakil Depression, or in other sedimentary basins developed along the East African Rift system, they are likely to interact with subhorizontal strata and may be expected to deflect into sills (e.g., Schofield et al., 2014). To date, InSAR studies have recorded the emplacement of individual sill-like intrusions within rift basins, such as the Danakil Depression, along the East African Rift system (Biggs et al., 2009, 2011, 2013; Pagli et al., 2012). It is therefore worth investigating whether these observed sill emplacement events correspond to the growth of a sill complex, particularly when considering that sill complexes can host significant volumes of magma and facilitate long-distance magma transport (Leat, 2008; Svensen et al., 2012).

CONCLUSIONS

The structure of magma plumbing systems influences tectonic and volcanic processes, and is traditionally considered to be dominated by the vertical intrusion of dikes. Delimiting the true structure of plumbing systems is, however, challenging due to the accessibility of active systems and limitations in exposure at the Earth's surface. Seismic reflection data have arguably revolutionized our understanding of plumbing systems and, in conjunction with field observations, have revealed that interconnected sills and inclined sheets (i.e., a sill complex) can facilitate the magma transport over vertical distances of ≲12 km and for as much as ~4100 km laterally. Volcanoes fed by sill complexes may thus be laterally offset from the melt source. These sill complexes preferentially form in sedimentary basins, although they may also occur within crystalline continental crust. In particular, mechanical contrasts across rock-rock interfaces (e.g., elastic mismatch) and the presence of compliant rock units, which may be intruded in a nonbrittle fashion (e.g., fluidization of shale), promote sill emplacement and control the structure of sill complexes. Magma is accommodated via a combination of roof uplift, which may produce discernible ground deformation, and other space-making processes such as porosity reduction. The occurrence of multiple accommodation mechanisms implies that ground deformation may not correlate to the entire magma volume emplaced and, in extreme circumstances, no uplift may be associated with shallow-level sill intrusion. These space-making processes compromise our ability to estimate magma volumes and locations using ground deformation analyses. The presence of a sill complex emplaced into continental crystalline crust in the Yilgarn craton highlights that extensive lateral magma transport in sills could feasibly occur in any host rock and tectonic setting. Furthermore, the extent to which active volcanic systems and rifted margins are underlain by networks of sills remains unknown. We conclude that it is crucial to consider that plumbing systems may be characterized by sill complexes when constraining magmatic processes, melt volumes, and melt sources.

ACKNOWLEDGMENTS

We benefitted from discussions with many Earth scientists in different disciplines over the years; we particularly thank Ken Thomson, Donny Hutton, Brian O'Driscoll, Mike Petronis, Ken McDermott, Derek Keir, Ben van Wyk de Vries, and Davie Brown for their insights. We thank Schlumberger for software and data provision, and Department of Communications, Energy, and Natural Resources (Petroleum Affairs Division) in Ireland, Geoscience Australia, and PGS (Petroleum Geo-Services) for provision of seismic data. This work was completed as part of Magee's Junior Research Fellowship funded by Imperial College London. Muirhead acknowledges support from Fulbright New Zealand and the Ministry of Science and Innovation. We thank Shan de Silva for his editorial handling of the manuscript and Tyrone Rooney, Agust Gudmundsson, and Mattia Pistone for the time and effort they put in to their constructive reviews.

REFERENCES CITED

Abebe, B., Acocella, V., Korme, T., and Ayalew, D., 2007, Quaternary faulting and volcanism in the Main Ethiopian Rift: Journal of African Earth Sciences, v. 48, p. 115–124, doi:10.1016/j.jafrearsci.2006.10.005.

Agirrezabala, L.M., 2015, Syndepositional forced folding and related fluid plumbing above a magmatic laccolith: Insights from outcrop (Lower Cretaceous, Basque-Cantabrian Basin, western Pyrenees): Geological Society of America Bulletin, doi:10.1130/B31192.1.

Airoldi, G., Muirhead, J.D., White, J.D., and Rowland, J., 2011, Emplacement of magma at shallow depth: Insights from field relationships at Allan Hills, south Victoria Land: East Antarctica: Antarctic Science-Institutional Subscription, v. 23, no. 3, p. 281, doi:10.1017/S0954102011000095.

Airoldi, G., Muirhead, J.D., Zanella, E., and White, J.D., 2012, Emplacement process of Ferrar Dolerite sheets at Allan Hills (South Victoria Land, Antarctica) inferred from magnetic fabric: Geophysical Journal International, v. 188, p. 1046–1060, doi:10.1111/j.1365-246X.2011.05334.x.

Aizawa, K., et al., 2014, Three-dimensional resistivity structure and magma plumbing system of the Kirishima Volcanoes as inferred from broadband magnetotelluric data: Journal of Geophysical Research, v. 119, p. 198–215, doi:10.1002/2013JB010682.

Anderson, E.M., 1937, Cone-sheets and ring-dykes: The dynamical explanation: Bulletin Volcanologique, v. 1, p. 35–40, doi:10.1007/BF03028041.

Anderson, E.M., 1951, The dynamics of faulting and dyke formation with applications to Britain (second edition): Edinburgh, Oliver and Boyd, 206 p.

Annen, C., 2011, Implications of incremental emplacement of magma bodies for magma differentiation, thermal aureole dimensions and plutonism-volcanism relationships: Tectonophysics, v. 500, p. 3–10, doi:10.1016/j.tecto.2009.04.010.

Annen, C., Blundy, J., and Sparks, R., 2006, The genesis of intermediate and silicic magmas in deep crustal hot zones: Journal of Petrology, v. 47, no. 3, p. 505–539, doi:10.1093/petrology/egi084.

Annen, C., Blundy, J.D., Leuthold, J., and Sparks, R.S.J., 2015, Construction and evolution of igneous bodies: Towards an integrated perspective of crustal magmatism: Lithos, v. 230, p. 206–221, doi:10.1016/j.lithos.2015.05.008.

Aoki, Y., Takeo, M., Ohminato, T., Nagaoka, Y., and Nishida, K., 2013, Magma pathway and its structural controls of Asama Volcano, Japan, *in* Pyle, D.M., et al., eds., Remote sensing of volcanoes and volcanic processes: Integrating observation and modelling: Geological Society of London Special Publication 380, p. 67–84, doi:10.1144/SP380.6.

Archanjo, C.J., and Launeau, P., 2004, Magma flow inferred from preferred orientations of plagioclase of the Rio Ceara–Mirim dyke swarm (NE Brazil) and its AMS significance, *in* Martín-Hernandez, M., et al., eds., Magnetic fabric: Methods and application: Geological Society of London Special Publication 238, p. 285–298, doi:10.1144/GSL.SP.2004.238.01.17.

Archer, S.G., Bergman, S.C., Iliffe, J., Murphy, C.M., and Thornton, M., 2005, Palaeogene igneous rocks reveal new insights into the geodynamic evolution and petroleum potential of the Rockall Trough, NE Atlantic Margin: Basin Research, v. 17, p. 171–201, doi:10.1111/j.1365-2117.2005.00260.x.

Aspler, L.B., Cousens, B.L., and Chiarenzelli, J.R., 2002, Griffin gabbro sills (2.11 Ga), Hurwitz Basin, Nunavut, Canada: Long-distance lateral transport of magmas in western Churchill Province crust: Precambrian Research, v. 117, p. 269–294, doi:10.1016/S0301-9268(02)00090-6.

Barberi, F., and Varet, J., 1970, The Erta Ale volcanic range (Danakil depression, northern Afar, Ethiopia): Bulletin Volcanologique, v. 34, p. 848–917, doi:10.1007/BF02596805.

Barnett, Z.A., and Gudmundsson, A., 2014, Numerical modelling of dykes deflected into sills to form a magma chamber: Journal of Volcanology and Geothermal Research, v. 281, p. 1–11, doi:10.1016/j.jvolgeores.2014.05.018.

Barrett, P., 1981, History of the Ross Sea region during the deposition of the Beacon Supergroup 400–180 million years ago: Royal Society of New Zealand Journal, v. 11, p. 447–458, doi:10.1080/03036758.1981.10423334.

Bastow, I.D., and Keir, D., 2011, The protracted development of the continent-ocean transition in Afar: Nature Geoscience, v. 4, p. 248–250, doi:10.1038/ngeo1095.

Bastow, I., Pilidou, S., Kendall, J.M., and Stuart, G., 2010, Melt-induced seismic anisotropy and magma assisted rifting in Ethiopia: Evidence from surface waves: Geochemistry, Geophysics, Geosystems, v. 11, Q0AB05, doi:10.1029/2010GC003036.

Bedard, J.H., et al., 2012, Fault-mediated melt ascent in a Neoproterozoic continental flood basalt province, the Franklin sills, Victoria Island, Canada: Geological Society of America Bulletin, v. 124, p. 723–736, doi:10.1130/B30450.1.

Biggs, J., Anthony, E., and Ebinger, C., 2009, Multiple inflation and deflation events at Kenyan volcanoes, East African Rift: Geology, v. 37, p. 979–982, doi:10.1130/G30133A.1.

Biggs, J., Bastow, I.D., Keir, D., and Lewi, E., 2011, Pulses of deformation reveal frequently recurring shallow magmatic activity beneath the Main Ethiopian Rift: Geochemistry, Geophysics, Geosystems, v. 12, Q0AB10, doi:10.1029/2011GC003662.

Biggs, J., Chivers, M., and Hutchinson, M.C., 2013, Surface deformation and stress interactions during the 2007–2010 sequence of earthquake, dyke intrusion and eruption in northern Tanzania: Geophysical Journal International, v. 195, p. 16–26, doi:10.1093/gji/ggt226.

Bistacchi, A., Tibaldi, A., Pasquarè, F.A., and Rust, D., 2012, The association of cone-sheets and radial dykes: Data from the Isle of Skye (UK), numerical modelling, and implications for shallow magma chambers: Earth and Planetary Science Letters, v. 339–340, p. 46–56, doi:10.1016/j.epsl.2012.05.020.

Broderick, C., Wotzlaw, J., Frick, D., Gerdes, A., Ulianov, A., Günther, D., and Schaltegger, U., 2015, Linking the thermal evolution and emplacement history of an upper-crustal pluton to its lower-crustal roots using zircon geochronology and geochemistry (southern Adamello batholith, N. Italy): Contributions to Mineralogy and Petrology, v. 170, doi:10.1007/s00410-015-1184-x.

Brown, A.R., 2004, Interpretation of three-dimensional seismic data (sixth edition): American Association of Petroleum Geologists Memoir 42, Society of Exploration Geophysicists Investigations in Geophysics 9, 560 p.

Bunger, A.P., and Cruden, A.R., 2011, Modeling the growth of laccoliths and large mafic sills: Role of magma body forces: Journal of Geophysical Research, v. 116, no. B2, B02203, doi:10.1029/2010JB007648.

Burchardt, S., Troll, V.R., Mathieu, L., Emeleus, H.C., and Donaldson, C.H., 2013, Ardnamurchan 3D cone-sheet architecture explained by a single elongate magma chamber: Scientific Reports, v. 3, 2891, doi:10.1038/srep02891.

Button, A., and Cawthorn, R., 2015, Distribution of mafic sills in the Transvaal Supergroup, northeastern South Africa: Journal of the Geological Society [London], v. 172, p. 357–367, doi:10.1144/jgs2014-101.

Callot, J.-P., and Geoffroy, L., 2004, Magma flow in the East Greenland dyke swarm inferred from study of anisotropy of magnetic susceptibility: Magmatic growth of a volcanic margin: Geophysical Journal International, v. 159, p. 816–830, doi:10.1111/j.1365-246X.2004.02426.x.

Cañón-Tapia, E., 2004, Anisotropy of magnetic susceptibility of lava flows and dykes: A historical account, *in* Martín-Hernandez, M., et al., eds., Magnetic fabric: Methods and application: Geological Society of London Special Publication 238, p. 205–225, doi:10.1144/GSL.SP.2004.238.01.14.

Cañón-Tapia, E., and Chavez-Alvarez, J., 2004, Theoretical aspects of particle movement in flowing magma: Implications for the anisotropy of magnetic susceptibility of dykes, *in* Martín-Hernandez, M., et al., eds., Magnetic fabric: Methods and application: Geological Society of London Special Publication 238, p. 227–249, doi:10.1144/GSL.SP.2004.238.01.15.

Cañón-Tapia, E., and Herrero-Bervera, E., 2009, Sampling strategies and the anisotropy of magnetic susceptibility of dykes: Tectonophysics, v. 466, p. 3–17, doi:10.1016/j.tecto.2008.11.012.

Cartwright, J., and Hansen, D.M., 2006, Magma transport through the crust via interconnected sill complexes: Geology, v. 34, p. 929–932, doi:10.1130/G22758A.1.

Cashman, K.V., and Sparks, R.S.J., 2013, How volcanoes work: A 25 year perspective: Geological Society of America Bulletin, v. 125, p. 664–690, doi:10.1130/B30720.1.

Cassidy, K.F., Champion, D.C., Krapez, B.B., Brown, S.J., Blewett, R.S., Groenewald, P.B., and Tyler, I.M., eds., 2006, A revised geological framework for the Yilgarn Craton, Western Australia: Geological Survey of Western Australia Record 2006/8, 8 p.

Chanceaux, L., and Menand, T., 2014, Solidification effects on sill formation: An experimental approach: Earth and Planetary Science Letters, v. 403, p. 79–88, doi:10.1016/j.epsl.2014.06.018.

Chevallier, L., and Woodford, A., 1999, Morpho-tectonics and mechanism of emplacement of the dolerite rings and sills of the western Karoo, South Africa: South African Journal of Geology, v. 102, p. 43–54.
Clarke, J.D., and Alley, N.F., 1993, Petrologic data on the evolution of the Great Australian Bight, *in* Findlay, R.H., et al., eds., Proceedings of the Gondwana Eight Symposium: Rotterdam, A.A. Balkema, p. 585–596.
Coleman, D.S., Gray, W., and Glazner, A.F., 2004, Rethinking the emplacement and evolution of zoned plutons: Geochronologic evidence for incremental assembly of the Tuolumne Intrusive Suite, California: Geology, v. 32, p. 433–436, doi:10.1130/G20220.1.
Cooper, J.R., Crelling, J.C., Rimmer, S.M., and Whittington, A.G., 2007, Coal metamorphism by igneous intrusion in the Raton Basin, CO and NM: Implications for generation of volatiles: International Journal of Coal Geology, v. 71, p. 15–27, doi:10.1016/j.coal.2006.05.007.
Corazzato, C., and Groppelli, G., 2004, Depth, geometry and emplacement of sills to laccoliths and their host-rock relationships: Montecampione group, Southern Alps, Italy, *in* Breitkreuz, C., and Petford, N., eds., Physical geology of high-level magmatic systems: Geological Society of London Special Publication 234, p. 175–194, doi:10.1144/GSL.SP.2004.234.01.11.
Cornwell, D., Mackenzie, G., England, R., and Maguire, P., 2006, Northern Main Ethiopian Rift crustal structure from new high-precision gravity data, *in* Yirgu, G., et al., eds., The Afar Volcanic Province within the East African Rift System: Geological Society of London Special Publication 259, p. 307–321, doi:10.1144/GSL.SP.2006.259.01.23.
Corti, G., 2009, Continental rift evolution: From rift initiation to incipient break-up in the Main Ethiopian Rift, East Africa: Earth-Science Reviews, v. 96, p. 1–53, doi:10.1016/j.earscirev.2009.06.005.
Cosgrove, J.W., and Hillier, R.D., 1999, Forced-fold development within Tertiary sediments of the Alba Field, UKCS evidence of differential compaction and post-depositional sandstone remobilization, *in* Cosgrove, J.W., and Ameen, M.S., eds., Forced folds and fractures: Geological Society of London Special Publication 169, p. 61–71, doi:10.1144/GSL.SP.2000.169.01.05.
Costelloe, R., and Jones, L., 2013, 2010 Youanmi seismic survey—Acquisition and processing, *in* Wyche, S., et al., compilers, Proceedings, Youanmi and Southern Carnarvon Seismic and Magnetotelluric (MT) Workshop: Geological Survey of Western Australia Record 2013/6, p. 1–7.
Cruden, A.R., and Launeau, P., 1994, Structure, magnetic fabric and emplacement of the Archean Lebel Stock, SW Abitibi greenstone belt: Journal of Structural Geology, v. 16, p. 677–691, doi:10.1016/0191-8141(94)90118-X.
Cruden, A., and McCaffrey, K., 2001, Growth of plutons by floor subsidence: Implications for rates of emplacement, intrusion spacing and melt-extraction mechanisms: Physics and Chemistry of the Earth, v. 26, p. 303–315, doi:10.1016/S1464-1895(01)00060-6.
Cukur, D., Horozal, S., Kim, D.C., Lee, G.H., Han, H.C., and Kang, M.H., 2010, The distribution and characteristics of the igneous complexes in the northern East China Sea Shelf Basin and their implications for hydrocarbon potential: Marine Geophysical Researches, v. 31, p. 299–313, doi:10.1007/s11001-010-9112-y.
Currier, R.M., and Marsh, B.D., 2015, Mapping real time growth of experimental laccoliths: The effect of solidification on the mechanics of magmatic intrusion: Journal of Volcanology and Geothermal Research, v. 302, p. 211–224, doi:10.1016/j.jvolgeores.2015.07.009.
Curtis, G., 1968, The stratigraphy of the ejecta from the 1912 eruption of Mount Katmai and Novarupta, Alaska, *in* Coats, R.R., et al., eds., Studies in Volcanology: Geological Society of America Memoir 116, p. 153–210, doi:10.1130/MEM116-p153.
Delaney, P.T., Pollard, D.D., Ziony, J.I., and McKee, E.H., 1986, Field relations between dikes and joints: Emplacement processes and paleostress analysis: Journal of Geophysical Research, v. 91, no. B5, p. 4920–4938, doi:10.1029/JB091iB05p04920.
Desissa, M., Johnson, N., Whaler, K., Hautot, S., Fisseha, S., and Dawes, G., 2013, A mantle magma reservoir beneath an incipient mid-ocean ridge in Afar, Ethiopia: Nature Geoscience, v. 6, p. 861–865, doi:10.1038/ngeo1925.
Dragoni, M., Lanza, R., and Tallarico, A., 1997, Magnetic anisotropy produced by magma flow: Theoretical model and experimental data from Ferrar dolerite sills (Antarctica): Geophysical Journal International, v. 128, p. 230–240, doi:10.1111/j.1365-246X.1997.tb04083.x.
Duraiswami, R., and Shaikh, T., 2013, Geology of the saucer-shaped sill near Mahad, western Deccan Traps, India, and its significance to the flood basalt model: Bulletin of Volcanology, v. 75, p. 1–18, doi:10.1007/s00445-013-0731-4.
Ebinger, C.J., and Casey, M., 2001, Continental breakup in magmatic provinces: An Ethiopian example: Geology, v. 29, p. 527–530, doi:10.1130/0091-7613(2001)029<0527:CBIMPA>2.0.CO;2.
Ebinger, C., Ayele, A., Keir, D., Rowland, J., Yirgu, G., Wright, T., Belachew, M., and Hamling, I., 2010, Length and timescales of rift faulting and magma intrusion: The Afar rifting cycle from 2005 to present: Annual Review of Earth and Planetary Sciences, v. 38, p. 439–466, doi:10.1146/annurev-earth-040809-152333.
Einsele, G., et al., 1980, Intrusion of basaltic sills into highly porous sediments, and resulting hydrothermal activity: Nature, v. 283, p. 441–445, doi:10.1038/283441a0.
Elliot, D., and Fleming, T., 2000, Weddell triple junction: The principal focus of Ferrar and Karoo magmatism during initial breakup of Gondwana: Geology, v. 28, p. 539–542, doi:10.1130/0091-7613(2000)28<539:WTJTPF>2.0.CO;2.
Elliot, D.H., Fleming, T.H., Kyle, P.R., and Foland, K.A., 1999, Long-distance transport of magmas in the Jurassic Ferrar large igneous province, Antarctica: Earth and Planetary Science Letters, v. 167, p. 89–104, doi:10.1016/S0012-821X(99)00023-0.
Emeleus, C.H., and Bell, B., 2005, The Palaeogene volcanic districts of Scotland (fourth edition): Keyworth, Nottingham: British Geological Survey, 214 p., doi:10.1017/S0016756806213050.
Encarnación, J., Fleming, T.H., Elliot, D.H., and Eales, H.V., 1996, Synchronous emplacement of Ferrar and Karoo dolerites and the early breakup of Gondwana: Geology, v. 24, p. 535–538, doi:10.1130/0091-7613(1996)024<0535:SEOFAK>2.3.CO;2.
Ernst, R.E., and Baragar, W.R.A., 1992, Evidence from magnetic fabric for the flow pattern of magma in the Mackenzie giant radiating dyke swarm: Nature, v. 356, no. 6369, p. 511–513, doi:10.1038/356511a0.
Ernst, R., Head, J., Parfitt, E., Grosfils, E., and Wilson, L., 1995, Giant radiating dyke swarms on Earth and Venus: Earth-Science Reviews, v. 39, p. 1–58, doi:10.1016/0012-8252(95)00017-5.
Espurt, N., Callot, J.P., Totterdell, J., Struckmeyer, H., and Vially, R., 2009, Interactions between continental breakup dynamics and large-scale delta system evolution: Insights from the Cretaceous Ceduna delta system, Bight Basin, Southern Australian margin: Tectonics, v. 28, TC6002, doi:10.1029/2009TC002447.
Evenchick, C.A., Davis, W.J., Bédard, J.H., Hayward, N., and Friedman, R.M., 2015, Evidence for protracted High Arctic large igneous province magmatism in the central Sverdrup Basin from stratigraphy, geochronology, and paleodepths of saucer-shaped sills: Geological Society of America Bulletin, v. 127, p. 1366–1390, doi:10.1130/B31190.1.
Féménias, O., Diot, H., Berza, T., Gauffriau, A., and Demaiffe, D., 2004, Asymmetrical to symmetrical magnetic fabric of dikes: Paleo-flow orientations and paleo-stresses recorded on feeder-bodies from the Motru Dike Swarm (Romania): Journal of Structural Geology, v. 26, p. 1401–1418, doi:10.1016/j.jsg.2003.12.003.
Ferguson, D.J., Barnie, T.D., Pyle, D.M., Oppenheimer, C., Yirgu, G., Lewi, E., Kidane, T., Carn, S., and Hamling, I., 2010, Recent rift-related volcanism in Afar, Ethiopia: Earth and Planetary Science Letters, v. 292, p. 409–418, doi:10.1016/j.epsl.2010.02.010.
Fialko, Y.A., and Rubin, A.M., 1999, Thermal and mechanical aspects of magma emplacement in giant dike swarms: Journal of Geophysical Research, v. 104, no. B10, p. 23,033–23,049, doi:10.1029/1999JB900213.
Francis, E., 1982, Magma and sediment-I Emplacement mechanism of late Carboniferous tholeiite sills in northern Britain President's anniversary address 1981: Journal of the Geological Society [London], v. 139, p. 1–20, doi:10.1144/gsjgs.139.1.0001.
Gaffney, E.S., Damjanac, B., and Valentine, G.A., 2007, Localization of volcanic activity: 2. Effects of pre-existing structure: Earth and Planetary Science Letters, v. 263, p. 323–338, doi:10.1016/j.epsl.2007.09.002.
Galerne, C.Y., Neumann, E.-R., and Planke, S., 2008, Emplacement mechanisms of sill complexes: Information from the geochemical architecture of the Golden Valley Sill Complex, South Africa: Journal of Volcanology and Geothermal Research, v. 177, p. 425–440, doi:10.1016/j.jvolgeores.2008.06.004.
Galerne, C.Y., Galland, O., Neumann, E.-R., and Planke, S., 2011, 3D relationships between sills and their feeders: Evidence from the Golden Valley Sill Complex (Karoo Basin) and experimental modelling: Journal of Volcanology and Geothermal Research, v. 202, p. 189–199, doi:10.1016/j.jvolgeores.2011.02.006.
Galland, O., 2012, Experimental modelling of ground deformation associated with shallow magma intrusions: Earth and Planetary Science Letters, v. 317, p. 145–156, doi:10.1016/j.epsl.2011.10.017.
Galland, O., and Scheibert, J., 2013, Analytical model of surface uplift above axisymmetric flat-lying magma intrusions: Implications for sill emplacement and geodesy: Journal of Volcanology and Geothermal Research, v. 253, p. 114–130, doi:10.1016/j.jvolgeores.2012.12.006.
Gautneb, H., Gudmundsson, A., and Oskarsson, N., 1989, Structure, petrochemistry and evolution of a sheet swarm in an Icelandic central volcano: Geological Magazine, v. 126, p. 659-673, doi:10.1017/S0016756800006956.

Geshi, N., 2005, Structural development of dike swarms controlled by the change of magma supply rate: The cone sheets and parallel dike swarms of the Miocene Otoge igneous complex, central Japan: Journal of Volcanology and Geothermal Research, v. 141, p. 267–281, doi:10.1016/j.jvolgeores.2004.11.002.

Gilbert, G.K., 1877, Report on the geology of the Henry Mountains: U.S. Geological Survey Monograph, 160 p.

Glazner, A.F., Bartley, J.M., Coleman, D.S., Gray, W., and Taylor, R.Z., 2004, Are plutons assembled over millions of years by amalgamation from small magma chambers?: GSA Today, v. 14, p. 4–12, doi:10.1130/1052-5173(2004)014<0004:APAOMO>2.0.CO;2.

Goulty, N.R., and Schofield, N., 2008, Implications of simple flexure theory for the formation of saucer-shaped sills: Journal of Structural Geology, v. 30, p. 812–817, doi:10.1016/j.jsg.2008.04.002.

Gressier, J.-B., Mourgues, R., Bodet, L., Matthieu, J.-Y., Galland, O., and Cobbold, P., 2010, Control of pore fluid pressure on depth of emplacement of magmatic sills: An experimental approach: Tectonophysics, v. 489, p. 1–13, doi:10.1016/j.tecto.2010.03.004.

Gretener, P., 1969, On the mechanics of the intrusion of sills: Canadian Journal of Earth Sciences, v. 6, p. 1415–1419.

Grove, C., 2013, Submarine hydrothermal vent complexes in the Paleocene of the Faroe-Shetland Basin: Insights from three-dimensional seismic and petrographical data: Geology, v. 41, p. 71–74, doi:10.1130/G33559.1.

Gudmundsson, Å., 1986, Formation of crystal magma chambers in Iceland: Geology, v. 14, p. 164–166, doi:10.1130/0091-7613(1986)14<164:FOCMCI>2.0.CO;2.

Gudmundsson, A., 1990, Emplacement of dikes, sills and crustal magma chambers at divergent plate boundaries: Tectonophysics, v. 176, p. 257–275, doi:10.1016/0040-1951(90)90073-H.

Gudmundsson, A., 2002, Emplacement and arrest of sheets and dykes in central volcanoes: Journal of Volcanology and Geothermal Research, v. 116, p. 279–298, doi:10.1016/S0377-0273(02)00226-3.

Gudmundsson, A., 2006, How local stresses control magma-chamber ruptures, dyke injections, and eruptions in composite volcanoes: Earth-Science Reviews, v. 79, p. 1–31, doi:10.1016/j.earscirev.2006.06.006.

Gudmundsson, A., 2011, Deflection of dykes into sills at discontinuities and magma-chamber formation: Tectonophysics, v. 500, p. 50–64, doi:10.1016/j.tecto.2009.10.015.

Gudmundsson, A., 2012, Magma chambers: Formation, local stresses, excess pressures, and compartments: Journal of Volcanology and Geothermal Research, v. 237–238, p. 19–41, doi:10.1016/j.jvolgeores.2012.05.015.

Gudmundsson, A., and Løtveit, I.F., 2012, Sills as fractured hydrocarbon reservoirs: Examples and models, *in* Spence, G.H., et al., eds., Advances in the study of fractured reservoirs: Geological Society of London Special Publication 374, p. 251–271, doi:10.1144/SP374.5.

Gudmundsson, A., and Marinoni, L., 1999, Geometry, emplacement, and arrest of dykes: Annals of Tectonics, v. 13, p. 71–92.

Gudmundsson, A., Lecoeur, N., Mohajeri, N., and Thordarson, T., 2014, Dike emplacement at Bardarbunga, Iceland, induces unusual stress changes, caldera deformation, and earthquakes: Bulletin of Volcanology, v. 76, p. 869–870, doi:10.1007/s00445-014-0869-8.

Hansen, D.M., 2006, The morphology of intrusion-related vent structures and their implications for constraining the timing of intrusive events along the NE Atlantic margin: Journal of the Geological Society [London], v. 163, p. 789–800, doi:10.1144/0016-76492004-167.

Hansen, D.M., and Cartwright, J., 2006a, Saucer-shaped sill with lobate morphology revealed by 3D seismic data: Implications for resolving a shallow-level sill emplacement mechanism: Journal of the Geological Society [London], v. 163, p. 509–523, doi:10.1144/0016-764905-073.

Hansen, D.M., and Cartwright, J., 2006b, The three-dimensional geometry and growth of forced folds above saucer-shaped igneous sills: Journal of Structural Geology, v. 28, p. 1520–1535, doi:10.1016/j.jsg.2006.04.004.

Hansen, D.M., Cartwright, J.A., and Thomas, D., 2004, 3D seismic analysis of the geometry of igneous sills and sill junction relationships, *in* Davies, R.J., et al., eds., 3D seismic technology: Application to the exploration of sedimentary basins: Geological Society of London Memoir 29, p. 199–208, doi:10.1144/GSL.MEM.2004.029.01.19.

Hansen, D.M., Redfern, J., Federici, F., di Biase, D., and Bertozzi, G., 2008, Miocene igneous activity in the northern subbasin, offshore Senegal, NW Africa: Marine and Petroleum Geology, v. 25, p. 1–15, doi:10.1016/j.marpetgeo.2007.04.007.

Hansen, J., 2015, A numerical approach to sill emplacement in isotropic media: Do saucer-shaped sills represent 'natural' intrusive tendencies in the shallow crust?: Tectonophysics, v. 664, p. 125–138, doi:10.1016/j.tecto.2015.09.006.

Hansen, J., Jerram, D.A., McCaffrey, K., and Passey, S.R., 2009, The onset of the North Atlantic Igneous Province in a rifting perspective: Geological Magazine, v. 146, p. 309–325, doi:10.1017/S0016756809006347.

Hastie, W.W., Watkeys, M.K., and Aubourg, C., 2014, Magma flow in dyke swarms of the Karoo LIP: Implications for the mantle plume hypothesis: Gondwana Research, v. 25, p. 736–755, doi:10.1016/j.gr.2013.08.010.

Heimann, A., Fleming, T., Elliot, D., and Foland, K., 1994, A short interval of Jurassic continental flood basalt volcanism in Antarctica as demonstrated by $^{40}Ar/^{39}Ar$ geochronology: Earth and Planetary Science Letters, v. 121, p. 19–41, doi:10.1016/0012-821X(94)90029-9.

Hole, M.J., 2015, The generation of continental flood basalts by decompression melting of internally heated mantle: Geology, v. 43, p. 311–314, doi:10.1130/G36442.1.

Holford, S.P., Schofield, N., MacDonald, J.D., Duddy, I.R., and Green, P.F., 2012, Seismic analysis of igneous systems in sedimentary basins and their impacts on hydrocarbon prospectivity: Examples from the southern Australian margin: APPEA Journal, v. 52, p. 229–252.

Holness, M., and Humphreys, M., 2003, The Traigh Bhàn na Sgùrra sill, Isle of Mull: Flow localization in a major magma conduit: Journal of Petrology, v. 44, p. 1961–1976, doi:10.1093/petrology/egg066.

Hoyer, L., and Watkeys, M.K., 2015, Assessing SPO techniques to constrain magma flow: Examples from sills of the Karoo Igneous Province, South Africa: Tectonophysics, v. 656, p. 61–73, doi:10.1016/j.tecto.2015.06.006, doi:10.1016/j.tecto.2015.06.006.

Hutton, D.H.W., 2009, Insights into magmatism in volcanic margins: Bridge structures and a new mechanism of basic sill emplacement—Theron Mountains, Antarctica: Petroleum Geoscience, v. 15, p. 269–278, doi:10.1144/1354-079309-841.

Hyndman, D.W., and Alt, D., 1987, Radial dikes, laccoliths, and gelatin models: Journal of Geology, v. 95, p. 763–774, doi:10.1086/629176.

Ivanic, T., et al., 2013, Preliminary interpretation of the 2010 Youanmi deep seismic reflection lines and magnetotelluric data for the Windimurra Igneous Complex, *in* Wyche, S., et al., compilers, Proceedings, Youanmi and Southern Carnarvon seismic and magnetotelluric (MT) workshop: Geological Survey of Western Australia Record 2013/6, p. 93–107.

Jackson, C.A.L., 2012, Seismic reflection imaging and controls on the preservation of ancient sill-fed magmatic vents: Journal of the Geological Society [London], v. 169, p. 503–506, doi:10.1144/0016-76492011-147.

Jackson, C.A.L., Schofield, N., and Golenkov, B., 2013, Geometry and controls on the development of igneous sill–related forced folds: A 2-D seismic reflection case study from offshore southern Australia: Geological Society of America Bulletin, v. 125, p. 1874–1890, doi:10.1130/B30833.1.

Jackson, M.D., and Pollard, D.D., 1988, The laccolith-stock controversy: New results from the southern Henry Mountains, Utah: Geological Society of America Bulletin, v. 100, p. 117–139, doi:10.1130/0016-7606(1988)100<0117:TLSCNR>2.3.CO;2.

Jackson, M.D., and Pollard, D.D., 1990, Flexure and faulting of sedimentary host rocks during growth of igneous domes, Henry Mountains, Utah: Journal of Structural Geology, v. 12, p. 185–206, doi:10.1016/0191-8141(90)90004-I.

John, B.E., and Blundy, J.D., 1993, Emplacement-related deformation of granitoid magmas, southern Adamello Massif, Italy: Geological Society of America Bulletin, v. 105, p. 1517–1541, doi:10.1130/0016-7606(1993)105<1517:ERDOGM>2.3.CO;2.

Johnson, A.M., and Pollard, D.D., 1973, Mechanics of growth of some laccolithic intrusions in the Henry Mountains, Utah, I: Field observations, Gilbert's model, physical properties and flow of the magma: Tectonophysics, v. 18, p. 261–309, doi:10.1016/0040-1951(73)90050-4.

Kavanagh, J.L., and Pavier, M.J., 2014, Rock interface strength influences fluid-filled fracture propagation pathways in the crust: Journal of Structural Geology, v. 63, p. 68–75, doi:10.1016/j.jsg.2014.03.001.

Kavanagh, J.L., Menand, T., and Sparks, R.S.J., 2006, An experimental investigation of sill formation and propagation in layered elastic media: Earth and Planetary Science Letters, v. 245, p. 799–813, doi:10.1016/j.epsl.2006.03.025.

Kavanagh, J., Boutelier, D., and Cruden, A., 2015, The mechanics of sill inception, propagation and growth: Experimental evidence for rapid reduction in magmatic overpressure: Earth and Planetary Science Letters, v. 421, p. 117–128, doi:10.1016/j.epsl.2015.03.038.

Keir, D., Kendall, J.M., Ebinger, C., and Stuart, G., 2005, Variations in late syn-rift melt alignment inferred from shear-wave splitting in crustal earthquakes beneath the Ethiopian rift: Geophysical Research Letters, v. 32, L23308, doi:10.1029/2005GL024150.

Keir, D., Ebinger, C.J., Stuart, G.W., Daly, E., and Ayele, A., 2006, Strain accommodation by magmatism and faulting as rifting proceeds to breakup: Seismicity of the northern Ethiopian rift: Journal of Geophysical Research, v. 111, B05314, doi:10.1029/2005JB003748.

Keir, D., Bastow, I.D., Corti, G., Mazzarini, F., and Rooney, T.O., 2015, The origin of along-rift variations in faulting and magmatism in the Ethiopian Rift: Tectonics, v. 34, p. 464–477, doi:10.1002/2014TC003698.

Kendall, J.-M., Stuart, G., Ebinger, C., Bastow, I., and Keir, D., 2005, Magma-assisted rifting in Ethiopia: Nature, v. 433, no. 7022, p. 146–148, doi:10.1038/nature03161.

Kent, R., and Fitton, J., 2000, Mantle sources and melting dynamics in the British Palaeogene Igneous Province: Journal of Petrology, v. 41, p. 1023–1040, doi:10.1093/petrology/41.7.1023.

Klausen, M.B., 2004, Geometry and mode of emplacement of the Thverartindur cone sheet swarm, SE Iceland: Journal of Volcanology and Geothermal Research, v. 138, p. 185–204, doi:10.1016/j.jvolgeores.2004.05.022.

Knight, M.D., and Walker, G.P., 1988, Magma flow directions in dikes of the Koolau Complex, Oahu, determined from magnetic fabric studies: Journal of Geophysical Research, v. 93, no. B5, p. 4301–4319, doi:10.1029/JB093iB05p04301.

Koch, F., Johnson, A., and Pollard, D., 1981, Monoclinal bending of strata over laccolithic intrusions: Tectonophysics, v. 74, p.T21–T31, doi:10.1016/0040-1951(81)90189-X.

Korme, T., Chorowicz, J., Collet, B., and Bonavia, F.F., 1997, Volcanic vents rooted on extension fractures and their geodynamic implications in the Ethiopian Rift: Journal of Volcanology and Geothermal Research, v. 79, p. 205–222, doi:10.1016/S0377-0273(97)00034-6.

Launeau, P., and Cruden, A., 1998, Magmatic fabric acquisition mechanisms in a syenite: Results of a combined anisotropy of magnetic susceptibility and image analysis study: Journal of Geophysical Research, v. 103, no. B3, p. 5067–5089, doi:10.1029/97JB02670.

Leaman, D.E., 1975, Form, mechanism, and control of dolerite intrusion near Hobart, Tasmania: Geological Society of Australia Journal, v. 22, p. 175–186, doi:10.1080/00167617508728886.

Leat, P.T., 2008, On the long-distance transport of Ferrar magmas, *in* Thomson, K., and Petford, N., eds., Structure and emplacement of high-level magmatic systems: Geological Society of London Special Publication 302, p. 45–61, doi:10.1144/SP302.4.

Lee, G.H., Kwon, Y.I., Yoon, C.S., Kim, H.J., and Yoo, H.S., 2006, Igneous complexes in the eastern Northern South Yellow Sea Basin and their implications for hydrocarbon systems: Marine and Petroleum Geology, v. 23, p. 631–645, doi:10.1016/j.marpetgeo.2006.06.001.

Liss, D., Owens, W.H., and Hutton, D.H.W., 2004, New palaeomagnetic results from the Whin Sill complex: Evidence for a multiple intrusion event and revised virtual geomagnetic poles for the late Carboniferous for the British Isles: Journal of the Geological Society [London], v. 161, p. 927–938, doi:10.1144/0016-764903-156.

Leuthold, J., Müntener, O., Baumgartner, L.P., Putlitz, B., Ovtcharova, M., and Schaltegger, U., 2012, Time resolved construction of a bimodal laccolith (Torres del Paine, Patagonia): Earth and Planetary Science Letters, v. 325–326, p. 85–92, doi:10.1016/j.epsl.2012.01.032.

Macdonald, R., Bagiński, B., Upton, B.G.J., Pinkerton, H., MacInnes, D.A., and MacGillivray, J.C., 2010, The Mull Palaeogene dyke swarm: Insights into the evolution of the Mull igneous centre and dyke-emplacement mechanisms: Mineralogical Magazine, v. 74, p. 601–622, doi:10.1180/minmag.2010.074.4.601.

Magee, C., Stevenson, C.T.E., O'Driscoll, B., and Petronis, M.S., 2012a, Local and regional controls on the lateral emplacement of the Ben Hiant Dolerite intrusion, Ardnamurchan (NW Scotland): Journal of Structural Geology, v. 39, p. 66–82, doi:10.1016/j.jsg.2012.03.005.

Magee, C., Stevenson, C., O'Driscoll, B., Schofield, N., and McDermott, K., 2012b, An alternative emplacement model for the classic Ardnamurchan cone sheet swarm, NW Scotland, involving lateral magma supply via regional dykes: Journal of Structural Geology, v. 43, p. 73–91, doi:10.1016/j.jsg.2012.08.004.

Magee, C., Briggs, F., and Jackson, C.A.L., 2013a, Lithological controls on igneous intrusion-induced ground deformation: Journal of the Geological Society [London], v. 170, p. 853–856, doi:10.1144/jgs2013-029.

Magee, C., Hunt-Stewart, E., and Jackson, C.A.L., 2013b, Volcano growth mechanisms and the role of sub-volcanic intrusions: Insights from 2D seismic reflection data: Earth and Planetary Science Letters, v. 373, p. 41–53, doi:10.1016/j.epsl.2013.04.041.

Magee, C., Jackson, C.A.L., and Schofield, N., 2013c, The influence of normal fault geometry on igneous sill emplacement and morphology: Geology, v. 41, p. 407–410, doi:10.1130/G33824.1.

Magee, C., Jackson, C.L., and Schofield, N., 2014, Diachronous sub-volcanic intrusion along deep-water margins: Insights from the Irish Rockall Basin: Basin Research, v. 26, p. 85–105, doi:10.1111/bre.12044.

Magee, C., Maharaj, S.M., Wrona, T., and Jackson, C.A.L., 2015, Controls on the expression of igneous intrusions in seismic reflection data: Geosphere, v. 11, p. 1024–1041, doi:10.1130/GES01150.1.

Malthe-Sørenssen, A., Planke, S., Svensen, H., and Jamtveit, B., 2004, Formation of saucer-shaped sills, *in* Breitkreuz, C., and Petford, N., eds., Physical geology of high-level magmatic systems: Geological Society of London Special Publication 234, p. 215–227, doi:10.1144/GSL.SP2004.234.01.13.

Mathieu, L., Burchardt, S., Troll, V.R., Krumbholz, M., and Delcamp, A., 2015, Geological constraints on the dynamic emplacement of cone-sheets—The Ardnamurchan cone-sheet swarm, NW Scotland: Journal of Structural Geology, v. 80, p. 133–141, doi:10.1016/j.jsg.2015.08.012.

Mazzarini, F., 2007, Vent distribution and crustal thickness in stretched continental crust: The case of the Afar Depression (Ethiopia): Geosphere, v. 3, p. 152–162, doi:10.1130/GES00070.1.

McClay, K., Scarselli, N., and Jitmahantakul, S., 2013, Igneous intrusions in the Carnarvon Basin, NW Shelf, Australia, *in* Keep, M., and Moss, S.J., eds., The sedimentary basins of Western Australia IV: Proceedings of the Petroleum Exploration Society of Australia Symposium: Perth, Petroleum Exploration Society of Western Australia, p. 1–20.

McClintock, M., and White, J., 2002, Granulation of weak rock as a precursor to peperite formation: Coal peperite, Coombs Hills, Antarctica: Journal of Volcanology and Geothermal Research, v. 114, p. 205–217, doi:10.1016/S0377-0273(01)00292-X.

McLeod, P., and Tait, S., 1999, The growth of dykes from magma chambers: Journal of Volcanology and Geothermal Research, v. 92, p. 231–245, doi:10.1016/S0377-0273(99)00053-0.

Meade, F.C., Chew, D.M., Troll, V.R., Ellam, R.M., and Page, L., 2009, Magma ascent along a major terrane boundary: Crustal contamination and magma mixing at the Drumadoon Intrusive complex, Isle of Arran, Scotland: Journal of Petrology, v. 50, p. 2345–2374, doi:10.1093/petrology/egp081.

Menand, T., 2008, The mechanics and dynamics of sills in layered elastic rocks and their implications for the growth of laccoliths and other igneous complexes: Earth and Planetary Science Letters, v. 267, p. 93–99, doi:10.1016/j.epsl.2007.11.043.

Menand, T., 2011, Physical controls and depth of emplacement of igneous bodies: A review: Tectonophysics, v. 500, p. 11–19, doi:10.1016/j.tecto.2009.10.016.

Menand, T., Daniels, K., and Benghiat, P., 2010, Dyke propagation and sill formation in a compressive tectonic environment: Journal of Geophysical Research, v. 115, B08201, doi:10.1029/2009JB006791.

Michel, J., Baumgartner, L., Putlitz, B., Schaltegger, U., and Ovtcharova, M., 2008, Incremental growth of the Patagonian Torres del Paine laccolith over 90 k.y.: Geology, v. 36, p. 459–462, doi:10.1130/G24546A.1.

Mihut, D., and Müller, R.D., 1998, Volcanic margin formation and Mesozoic rift propagators in the Cuvier Abyssal Plain off Western Australia: Journal of Geophysical Research, v. 103, p. 27,135–27,149, doi:10.1029/97JB02672.

Miles, A., and Cartwright, J., 2010, Hybrid flow sills: A new mode of igneous sheet intrusion: Geology, v. 38, p. 343–346, doi:10.1130/G30414.1.

Miller, C.F., Furbish, D.J., Walker, B.A., Claiborne, L.L., Koteas, G.C., Bleick, H.A., and Miller, J.S., 2011, Growth of plutons by incremental emplacement of sheets in crystal-rich host: Evidence from Miocene intrusions of the Colorado River region, Nevada, USA: Tectonophysics, v. 500, p. 65–77, doi:10.1016/j.tecto.2009.07.011.

Morgan, S., Stanik, A., Horsman, E., Tikoff, B., de Saint Blanquat, M., and Habert, G., 2008, Emplacement of multiple magma sheets and wall rock deformation: Trachyte Mesa intrusion, Henry Mountains, Utah: Journal of Structural Geology, v. 30, p. 491–512, doi:10.1016/j.jsg.2008.01.005.

Mortimer, N., Parkinson, D., Raine, J.I., Adams, C.J., Graham, I.J., Oliver, P.J., and Palmer, K., 1995, Ferrar magmatic province rocks discovered in New Zealand: Implications for Mesozoic Gondwana geology: Geology, v. 23, p. 185–188, doi:10.1130/0091-7613(1995)023<0185:FMPRDI>2.3.CO;2.

Mudge, M.R., 1968, Depth control of some concordant intrusions: Geological Society of America Bulletin, v. 79, p. 315–332, doi:10.1130/0016-7606(1968)79[315:DCOSCI]2.0.CO;2.

Muirhead, J.D., Airoldi, G., Rowland, J.V., and White, J.D., 2012, Interconnected sills and inclined sheet intrusions control shallow magma transport in the Ferrar large igneous province, Antarctica: Geological Society of America Bulletin, v. 124, p. 162–180, doi:10.1130/B30455.1.

Muirhead, J.D., Airoldi, G., White, J.D., and Rowland, J.V., 2014, Cracking the lid: Sill-fed dikes are the likely feeders of flood basalt eruptions: Earth and Planetary Science Letters, v. 406, p. 187–197, doi:10.1016/j.epsl.2014.08.036.

Muirhead, J.D., Kattenhorn, S.A., and Le Corvec, N., 2015, Varying styles of magmatic strain accommodation across the East African Rift: Geochemistry, Geophysics, Geosystems, v. 16, p. 2775–2795, doi:10.1002/2015GC005918.

Muirhead, J.D., Van Eaton, A.R., Re, G., White, J.D.L., and Ort, M.H., 2016, Monogenetic volcanoes fed by interconnected dikes and sills in the Hopi Buttes volcanic field, Navajo Nation, USA: Bulletin of Volcanology, v. 78, doi:10.1007/s00445-016-1005-8.

Neres, M., Bouchez, J., Terrinha, P., Font, E., Moreira, M., Miranda, R., Launeau, P., and Carvallo, C., 2014, Magnetic fabric in a Cretaceous sill (Foz da Fonte, Portugal): Flow model and implications for regional magmatism: Geophysical Journal International, v. 199, p. 78–101, doi:10.1093/gji/ggu250.

Pagli, C., Wright, T.J., Ebinger, C.J., Yun, S.-H., Cann, J.R., Barnie, T., and Ayele, A., 2012, Shallow axial magma chamber at the slow-spreading Erta Ale Ridge: Nature Geoscience, v. 5, p. 284–288, doi:10.1038/ngeo1414.

Passey, S., and Hitchen, K., 2011, Cenozoic (igneous), *in* Ritchie, J.D., et al., eds., Geology of the Faroe-Shetland Basin and adjacent areas: British Geological Survey Research Report RR/11/01, p. 209–228.

Pedersen, R., 2004, InSAR based sill model links spatially offset areas of deformation and seismicity for the 1994 unrest episode at Eyjafjallajökull volcano, Iceland: Geophysical Research Letters, v. 31, L14610, doi:10.1029/2004GL020368.

Peron-Pinvidic, G., Shillington, D.J., and Tucholke, B.E., 2010, Characterization of sills associated with the U reflection on the Newfoundland margin: Evidence for widespread early post-rift magmatism on a magma-poor rifted margin: Geophysical Journal International, v. 182, p. 113–136, doi:10.1111/j.1365-246X.2010.04635.x.

Perugini, D., and Poli, G., 2005, Viscous fingering during replenishment of felsic magma chambers by continuous inputs of mafic magmas: Field evidence and fluid-mechanics experiments: Geology, v. 33, p. 5, doi:10.1130/G21075.1.

Philpotts, A.R., and Philpotts, D.E., 2007, Upward and downward flow in a camptonite dike as recorded by deformed vesicles and the anisotropy of magnetic susceptibility (AMS): Journal of Volcanology and Geothermal Research, v. 161, p. 81–94, doi:10.1016/j.jvolgeores.2006.11.006.

Pistone, M., Caricchi, L., Ulmer, P., Burlini, L., Ardia, P., Reusser, E., Marone, F., and Arbaret, L., 2012, Deformation experiments of bubble-and crystal-bearing magmas: Rheological and microstructural analysis: Journal of Geophysical Research: Solid Earth, v. 117, B05208, doi:10.1029/2011JB008986.

Pistone, M., Caricchi, L., Ulmer, P., Reusser, E., and Ardia, P., 2013, Rheology of volatile-bearing crystal mushes: mobilization vs. viscous death: Chemical Geology, v. 345, p. 16–39, doi:10.1016/j.chemgeo.2013.02.007.

Planke, S., Rasmussen, T., Rey, S.S., and Myklebust, R., 2005, Seismic characteristics and distribution of volcanic intrusions and hydrothermal vent complexes in the Vøring and Møre basins, *in* Doré, A.G., ed., Petroleum geology: North-West Europe and global perspectives: Proceedings of the 6th Petroleum Geology Conference: Geological Society of London Petroleum Geology Conference Series Volume 6, p. 833–844, doi:10.1144/0060833.

Pollard, D.D., 1973, Derivation and evaluation of a mechanical model for sheet intrusions: Tectonophysics, v. 19, p. 233–269, doi:10.1016/0040-1951(73)90021-8.

Pollard, D.D., and Johnson, A.M., 1973, Mechanics of growth of some laccolithic intrusions in the Henry Mountains, Utah, II: Bending and failure of overburden layers and sill formation: Tectonophysics, v. 18, p. 311–354, doi:10.1016/0040-1951(73)90051-6.

Pollard, D.D., Muller, O.H., and Dockstader, D.R., 1975, The form and growth of fingered sheet intrusions: Geological Society of America Bulletin, v. 86, p. 351–363, doi:10.1130/0016-7606(1975)86<351:TFAGOF>2.0.CO;2.

Polteau, S., Mazzini, A., Galland, O., Planke, S., and Malthe-Sørenssen, A., 2008a, Saucer-shaped intrusions: Occurrences, emplacement and implications: Earth and Planetary Science Letters, v. 266, p. 195–204, doi:10.1016/j.epsl.2007.11.015.

Polteau, S., Ferré, E.C., Planke, S., Neumann, E.R., and Chevallier, L., 2008b, How are saucer-shaped sills emplaced? Constraints from the Golden Valley Sill, South Africa: Journal of Geophysical Research, v. 113, B12104, doi:10.1029/2008JB005620.

Rateau, R., Schofield, N., and Smith, M., 2013, The potential role of igneous intrusions on hydrocarbon migration: West of Shetland: Petroleum Geoscience, v. 19, p. 259–272.

Rickwood, P., 1990, The anatomy of a dyke and the determination of propagation and magma flow directions, *in* Parker, A.J., et al., eds., Mafic dykes and emplacement mechanisms: Rotterdam, Balkema, p. 81–100.

Rohrman, M., 2013, Intrusive large igneous provinces below sedimentary basins: An example from the Exmouth Plateau (NW Australia): Journal of Geophysical Research, v. 118, p. 4477–4487, doi:10.1002/jgrb.50298.

Rohrman, M., 2015, Delineating the Exmouth mantle plume (NW Australia) from denudation and magmatic addition estimates: Lithosphere, v. 7, p. 589–600, doi:10.1130/L445.1.

Rooney, T.O., Bastow, I.D., and Keir, D., 2011, Insights into extensional processes during magma assisted rifting: Evidence from aligned scoria cones: Journal of Volcanology and Geothermal Research, v. 201, p. 83–96, doi:10.1016/j.jvolgeores.2010.07.019.

Rooney, T.O., Hanan, B.B., Graham, D.W., Furman, T., Blichert-Toft, J., and Schilling, J.-G., 2012, Upper mantle pollution during Afar plume–continental rift interaction: Journal of Petrology, v. 53, p. 365–389, doi:10.1093/petrology/egr065.

Rubin, A.M., 1995, Propagation of magma-filled cracks: Annual Review of Earth and Planetary Sciences, v. 23, p. 287–336, doi:10.1146/annurev.ea.23.050195.001443.

Rui, G., Gongcheng, Z., Jinwei, Z., Xingbin, Z., Junbang, L., Dawei, Y., and Shuang, S., 2013, Fingered Intrusion of shallow saucer-shaped igneous sills: Insights from the Jiaojiang Sag, East China Sea: Acta Geologica Sinica, v. 87, p. 1306–1318, doi:10.1111/1755-6724.12130.

Saunders, A., Fitton, J., Kerr, A., Norry, M., and Kent, R., 1997, The North Atlantic igneous province, *in* Mahoney, J.J., and Coffin, M.F., eds., Large igneous provinces: Continental, oceanic, and planetary flood volcanism: American Geophysical Union Geophysical Monograph 100, p. 45–93, doi:10.1029/GM100p0045.

Scheiber-Enslin, S., Webb, S., and Eebbing, J., 2014, Geophysically plumbing the main Karoo Basin, South Africa: South African Journal of Geology, v. 117, p. 275–300, doi:10.2113/gssajg.117.2.275.

Schirnick, C., van den Bogaard, P., and Schmincke, H.-U., 1999, Cone sheet formation and intrusive growth of an oceanic island—The Miocene Tejeda complex on Gran Canaria (Canary Islands): Geology, v. 27, p. 207–210, doi:10.1130/0091-7613(1999)027<0207:CSFAIG>2.3.CO;2.

Schofield, A., Totterdell, J., and Australia, G., 2008, Distribution, timing and origin of magmatism in the Bight and Eucla Basins: Geoscience Australia, v. 24, p. 1–19.

Schofield, N., and Jolley, D.W., 2013, Development of intra-basaltic lava-field drainage systems within the Faroe-Shetland Basin: Petroleum Geoscience, v. 19, p. 273–288, doi:10.1144/petgeo2012-061.

Schofield, N., Stevenson, C., and Reston, T., 2010, Magma fingers and host rock fluidization in the emplacement of sills: Geology, v. 38, p. 63–66, doi:10.1130/G30142.1.

Schofield, N.J., Brown, D.J., Magee, C., and Stevenson, C.T., 2012a, Sill morphology and comparison of brittle and non-brittle emplacement mechanisms: Journal of the Geological Society [London], v. 169, p. 127–141, doi:10.1144/0016-76492011-078.

Schofield, N., Heaton, L., Holford, S.P., Archer, S.G., Jackson, C.A.L., and Jolley, D.W., 2012b, Seismic imaging of 'broken bridges': Linking seismic to outcrop-scale investigations of intrusive magma lobes: Journal of the Geological Society [London], v. 169, p. 421–426, doi:10.1144/0016-76492011-150.

Schofield, N., Alsop, I., Warren, J., Underhill, J.R., Lehné, R., Beer, W., and Lukas, V., 2014, Mobilizing salt: Magma-salt interactions: Geology, v. 42, p. 599–60, doi:10.1130/G35406.1.

Schofield, N., et al., 2015, Regional magma plumbing and emplacement mechanisms of the Faroe-Shetland Sill Complex: Implications for magma transport and petroleum systems within sedimentary basins: Basin Research, doi:10.1111/bre.12164.

Sigmundsson, F., et al., 2015, Segmented lateral dyke growth in a rifting event at Bárðarbunga volcanic system, Iceland: Nature, v. 517, p. 191–195, doi:10.1038/nature14111.

Siler, D.L., and Karson, J.A., 2009, Three-dimensional structure of inclined sheet swarms: Implications for crustal thickening and subsidence in the volcanic rift zones of Iceland: Journal of Volcanology and Geothermal Research, v. 188, p. 333–346, doi:10.1016/j.jvolgeores.2009.09.017.

Skogseid, J., Pedersen, T., Eldholm, O., and Larsen, B.T., 1992, Tectonism and magmatism during NE Atlantic continental break-up: The Vøring Margin, *in* Storey, B.C., et al., eds., Magmatism and the causes of continental break-up: Geological Society of London Special Publication 68, p. 305–320, doi:10.1144/GSL.SP.1992.068.01.19.

Smallwood, J.R., and Maresh, J., 2002, The properties, morphology and distribution of igneous sills: Modelling, borehole data and 3D seismic from the Faroe-Shetland area, *in* Jolley, D.W., and Bell, B.R., eds., The North Atlantic Igneous Province: Stratigraphy, tectonic, volcanic and magmatic processes: Geological Society of London Special Publication 197, p. 271–306, doi:10.1144/GSL.SP.2002.197.01.11.

Sparks, R.S.J., 2003, Forecasting volcanic eruptions: Earth and Planetary Science Letters, v. 210, p. 1–15, doi:10.1016/S0012-821X(03)00124-9.

Sparks, R., Biggs, J., and Neuberg, J., 2012, Monitoring volcanoes: Science, v. 335, no. 6074, p. 1310–1311, doi:10.1126/science.1219485.

Stevenson, C.T.E., Owens, W.H., Hutton, D.H.W., Hood, D.N., and Meighan, I.G., 2007, Laccolithic, as opposed to cauldron subsidence, emplacement of the Eastern Mourne pluton, N. Ireland: Evidence from anisotropy of magnetic susceptibility: Journal of the Geological Society [London], v. 164, p. 99–110, doi:10.1144/0016076492006-008.

Storey, B., and Kyle, P., 1997, An active mantle mechanism for Gondwana breakup: South African Journal of Geology, v. 100, p. 283–290.
Storey, M., Duncan, R.A., and Tegner, C., 2007, Timing and duration of volcanism in the North Atlantic Igneous Province: Implications for geodynamics and links to the Iceland hotspot: Chemical Geology, v. 241, p. 264–281, doi:10.1016/j.chemgeo.2007.01.016.
Sun, Q., Wu, S., Cartwright, J., Wang, S., Lu, Y., Chen, D., and Dong, D., 2014, Neogene igneous intrusions in the northern South China Sea: Evidence from high-resolution three dimensional seismic data: Marine and Petroleum Geology, v. 54, p. 83–95, doi:10.1016/j.marpetgeo.2014.02.014.
Svensen, H., Planke, S., Malthe-Sorenssen, A., Jamtveit, B., Myklebust, R., Rasmussen Eidem, T., and Rey, S.S., 2004, Release of methane from a volcanic basin as a mechanism for initial Eocene global warming: Nature, v. 429, no. 6991, p. 542–545, doi:10.1038/nature02566.
Svensen, H., Corfu, F., Polteau, S., Hammer, Ø., and Planke, S., 2012, Rapid magma emplacement in the Karoo Large Igneous Province: Earth and Planetary Science Letters, v. 325-326, p. 1–9, doi:10.1016/j.epsl.2012.01.015.
Svensen, H.H., Polteau, S., Cawthorn, G., and Planke, S., 2015, Sub-volcanic intrusions in the Karoo basin, South Africa: Advances in Volcanology, p. 1–14, doi:10.1007/11157_2014_7.
Symonds, P.A., Planke, S., Frey, O., and Skogseid, J., 1998, Volcanic evolution of the Western Australian continental margin and its implications for basin development, *in* Purcell, R.R., and Purcell, P.G., eds., The sedimentary basins of Western Australia: Proceedings of the PESA Symposium: Perth, Petroleum Exploration Society of Australia, p. 33–54.
Taisne, B., and Tait, S., 2011, Effect of solidification on a propagating dike: Journal of Geophysical Research, v. 116, B01206, doi:10.1029/2009JB007058.
Taisne, B., Tait, S., and Jaupart, C., 2011, Conditions for the arrest of a vertical propagating dyke: Bulletin of Volcanology, v. 73, p. 191–204, doi:10.1007/s00445-010-0440-1.
Tarling, D., and Hrouda, F., 1993, The magnetic anisotropy of rocks: London, Chapman and Hall, 218 p.
Tauxe, L., Gee, J., and Staudigel, H., 1998, Flow directions in dikes from anisotropy of magnetic susceptibility data: The bootstrap way: Journal of Geophysical Research, v. 103, no. B8, p. 17,775–17,790, doi:10.1029/98JB01077.
Thomson, K., 2007, Determining magma flow in sills, dykes and laccoliths and their implications for sill emplacement mechanisms: Bulletin of Volcanology, v. 70, p. 183–201, doi:10.1007/s00445-007-0131-8.
Thomson, K., and Hutton, D., 2004, Geometry and growth of sill complexes: Insights using 3D seismic from the North Rockall Trough: Bulletin of Volcanology, v. 66, p. 364–375, doi:10.1007/s00445-003-0320-z.
Thomson, K., and Schofield, N., 2008, Lithological and structural controls on the emplacement and morphology of sills in sedimentary basins, *in* Thomson, K., and Petford, N., eds., Structure and emplacement of high-level magmatic systems: Geological Society of London Special Publication 302, p. 31–44, doi:10.1144/SP302.3.
Tibaldi, A., 2015, Structure of volcano plumbing systems: A review of multi-parametric effects: Journal of Volcanology and Geothermal Research, v. 298, p. 85–135, doi:10.1016/j.jvolgeores.2015.03.023.
Trude, J., Cartwright, J., Davies, R.J., and Smallwood, J.R., 2003, New technique for dating igneous sills: Geology, v. 31, p. 813–816, doi:10.1130/G19559.1.
Valentine, G.A., and Gregg, T.K.P., 2008, Continental basaltic volcanoes—Processes and problems: Journal of Volcanology and Geothermal Research, v. 177, p. 857–873, doi:10.1016/j.jvolgeores.2008.01.050.
Valentine, G., and Krogh, K., 2006, Emplacement of shallow dikes and sills beneath a small basaltic volcanic center—The role of pre-existing structure (Paiute Ridge, southern Nevada, USA): Earth and Planetary Science Letters, v. 246, p. 217–230, doi:10.1016/j.epsl.2006.04.031.
van Wyk de Vries, B.W., Márquez, A., Herrera, R., Bruña, J.G., Llanes, P., and Delcamp, A., 2014, Craters of elevation revisited: Forced-folds, bulging and uplift of volcanoes: Bulletin of Volcanology, v. 76, p. 875–895, doi:10.1007/s00445-014-0875-x.
Wall, M., Cartwright, J., Davies, R., and McGrandle, A., 2010, 3D seismic imaging of a Tertiary dyke swarm in the southern North Sea, UK: Basin Research, v. 22, p. 181–194, doi:10.1111/j.1365-2117.2009.00416.x.
Weber, U., Kohn, B., Gleadow, A., and Nelson, D., 2005, Low temperature Phanerozoic history of the Northern Yilgarn Craton, Western Australia: Tectonophysics, v. 400, p. 127–151, doi:10.1016/j.tecto.2005.03.008.
Whaler, K., and Hautot, S., 2006, The electrical resistivity structure of the crust beneath the northern Main Ethiopian Rift, *in* Yirgu, G., et al., eds., The Afar Volcanic Province within the East African Rift System: Geological Society of London Special Publication 259, p. 293–305, doi:10.1144/GSL.SP.2006.259.01.22.
White, R., and McKenzie, D., 1989, Magmatism at rift zones: The generation of volcanic continental margins and flood basalts: Journal of Geophysical Research, v. 94, no. B6, p. 7685–7729, doi:10.1029/JB094iB06p07685.
White, R.S., et al., 2008, Lower-crustal intrusion on the North Atlantic continental margin: Nature, v. 452, no. 7186, p. 460–464, doi:10.1038/nature06687.
Widess, M., 1973, How thin is a thin bed?: Geophysics, v. 38, p. 1176–1180, doi:10.1190/1.1440403.
Wingate, M.T., Pirajno, F., and Morris, P.A., 2004, Warakurna large igneous province: A new Mesoproterozoic large igneous province in west-central Australia: Geology, v. 32, p. 105–108, doi:10.1130/G20171.1.
Wingate, M.T., Bodorkos, S., and Kirkland, C., 2008, 178113: Gabbro sill, Kurrajong bore: Geochronology Record 1013: Geological Survey of Western Australia, 7 p.
Wright, T.J., Ebinger, C., Biggs, J., Ayele, A., Yirgu, G., Keir, D., and Stork, A., 2006, Magma-maintained rift segmentation at continental rupture in the 2005 Afar dyking episode: Nature, v. 442, no. 7100, p. 291–294, doi:10.1038/nature04978.
Wright, T.J., et al., 2012, Geophysical constraints on the dynamics of spreading centres from rifting episodes on land: Nature Geoscience, v. 5, p. 242–250, doi:10.1038/ngeo1428.
Wyche, S., Pawley, M., Chen, S., Ivanic, T., Zibra, I., Van Kranendonk, M., Spaggiari, C., and Wingate, M., 2013, Geology of the northern Yilgarn Craton, *in* Wyche, S., et al., compilers, Proceedings, Youanmi and Southern Carnarvon seismic and magnetotelluric (MT) workshop: Geological Survey of Western Australia Record 2013/6, p. 33–65.
Zhao, F., Wu, S., Sun, Q., Huuse, M., Li, W., and Wang, Z., 2014, Submarine volcanic mounds in the Pearl River Mouth Basin, northern South China Sea: Marine Geology, v. 355, p. 162–172, doi:10.1016/j.margeo.2014.05.018.